Implications of prebiotic soup heterogeneity for nonenzymatic RNA replication and formation of primordial protocells

विद्या वाचस्पति की

उपाधि की अपेक्षाओं की आंशिक पूर्ति में प्रस्तुत शोध प्रबंध

A thesis submitted in partial fulfillment of the requirements of the degree of Doctor of Philosophy

द्वारा / By

गौरी मधुसूदन पतकी / Gauri Madhusudan Patki

पंजीकरण सं. / Registration No.: 20203721

शोध प्रबंध पर्यवेक्षक / Thesis Supervisor:

प्रो. सुधा राजामणी/ Prof. Sudha Rajamani

भारतीय विज्ञान शिक्षा एवं अनुसंधान संस्थान पुणे

INDIAN INSTITUTE OF SCIENCE EDUCATION AND RESEARCH PUNE

2025

CERTIFICATE

Certified that the work incorporated in the thesis entitled **"Implications of prebiotic soup heterogeneity for nonenzymatic RNA replication and formation of primordial protocells"** submitted by Gauri Madhusudan Patki was carried out by the candidate, under my supervision. The work presented here or any part of it has not been included in any other thesis submitted previously for the award of any degree or diploma from any other University or institution.

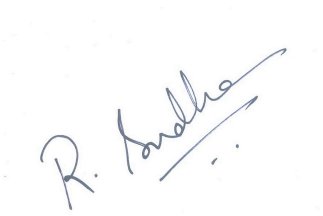

Prof. Sudha Rajamani

Date: 25.04.2025

DECLARATION

Name of Student: Gauri Madhusudan Patki

Reg. No.: 20203721
Thesis Supervisor: Prof. Sudha Rajamani

Department: Biology
Date of joining program: 02.01.2020

Date of Pre-Synopsis Seminar : 21.10.24

Title of Thesis : **Implications of prebiotic soup heterogeneity for nonenzymatic RNA replication and formation of primordial protocells**

I declare that this written submission represents my idea in my own words and where others' ideas have been included; I have adequately cited and referenced the original sources. I declare that I have acknowledged collaborative work and discussions wherever such work has been included. I also declare that I have adhered to all principles of academic honesty and integrity and have not misrepresented or fabricated or falsified any idea/data/fact/source in my submission. I understand that violation of the above will be cause for disciplinary action by the Institute and can also evoke penal action from the sources which have thus not been properly cited or from whom proper permission has not been taken when needed.

The work reported in this thesis is the original work done by me under the guidance of Prof. Sudha Rajamani.

Date: 25.04.2025

Gauri Madhusudan Patki

ACKNOWLWDGEMENTS

The journey of my doctoral degree has been a very enriching and transformative experience for me. Throughout this journey, I have received generous help, unwavering support and constant motivation from many wonderful people. I take this opportunity to thank every one of them.

First and foremost, I would like to express my profound gratitude to my thesis supervisor, Prof. Sudha Rajamani, for giving me the opportunity to work with her and introducing me to the field of astrobiology. She has been a wonderful mentor, who showed incredible patience during the difficult phase of my Ph.D., and supported me and kept me motivated all along. I thank her for giving me all the freedom to explore new ideas, think independently and become an independent researcher. Her consistent guidance and constructive feedback have played a pivotal role in helping me develop essential skills, including scientific writing and communication. I would like to acknowledge the members of my research advisory committee (RAC), Prof. Thomas Pucadyil, Dr. Nishad Matange and Dr. Tony Jia for assessing my progress and for giving me valuable inputs all along. I would like to extend my special thanks to Dr. Tony Jia for his invaluable comments, suggestions, and encouraging words on coacervate project. I would also like to thank Dr. Ramana Athreya for his help with statistical analysis.

I would like to thank all the past and present COoL lab members, who established and maintained a friendly and healthy work space. I thank Anupam, Chaitanya, Niraja, Manesh, Shikha, and Susovan and for being supportive seniors during the initial days of my PhD. I thank my colleagues Souradeep, Anuraag, Sahil, Raya, Udita, Abhishek, Daksh, Rashi, and all the past and present undergraduates for being wonderful labmates. I would like to extend special thanks to Vanthana Sridhar for her help with the initial standardization. Special thanks to lab meetings and journal clubs, where we explored different areas of scientific research, learnt about the use of various techniques and assays to build projects. I will genuinely miss all the fun during meetings and discussions over ‘chai’ sessions.

I would like to thank the Biology and Chemistry departments at IISER Pune for providing all the essential facilities and funding to pursue research. I would like acknowledge microscopy facility at IISER Pune. I would specially like to thank Vijay Vittal for his help in image acquisition. I would like to acknowledge all the administrative staff, technical and non-

technical staff, especially Sayalee, Piyush, Kalpesh, Mrinalini, Rupali, and Hari for all their support and help. I thank Department of Biotechnology (DBT), Government of India, for fellowship support.

As I bring these acknowledgements to a close, I would like to express my sincere gratitude to my friends and family. I am deeply grateful to my family, whose never ending support made all this possible. I thank my parents and my brother, Shriram, for being incredibly encouraging towards my goals. It is because of their understanding and accommodating nature, I was able to explore everything I wished to explore. I would also like to thank my in-laws and my husband, Om, for their unconditional love and support, which immensely helped me to focus on my work and meet all the academic deadlines. Finally, I would like to acknowledge all my friends. I thank Shruti, Vaidehi, Ankita, Anuraag, Atreyi, Arnab, Adesh, Kshitij, Mishika for always being there for me. A special thanks to Shivani and Namrata, who stood by me through thick and thin, and made the days at IISER Pune truly unforgettable.

TABLE OF CONTENTS

LIST OF FIGURES

LIST OF TABLES

SYNOPSIS

Chapters 1: Introduction

How 'life' emerged on Earth is one of the most intriguing scientific questions that continues to remain not fully answered. The fundamental unit of life, a cell, is a highly complex and well-organized machinery, which carries out metabolism and undergoes growth and division. Emergence of such an intricately designed structure from a pool of prebiotically plausible chemicals has fascinated chemists and biologists across the globe. To understand the emergence of life on prebiotic Earth, scientists came up with a definition of life, where life is defined as a self-sustaining chemical system capable of undergoing Darwinian evolution (Domagal-Goldman et al. 2016). Furthermore, as seen in modern biology, the three hallmarks of life are metabolism, replication and compartmentalization. Towards this, the formation of genetic polymer has been considered to be a pivotal step. In this context, RNA World hypothesis was put forward by Gilbert in 1986, which proposed that RNA would have served as a genetic material during the origin of life because of the competence of the RNA molecule to act as an informational polymer as well as a catalyst (Gilbert 1986). The foundation of an 'RNA World' is considered to have involved key steps including nonenzymatic synthesis of building blocks (such as nucleobases, nucleosides, nucleotides) from prebiotically plausible chemicals, nonenzymatic RNA oligomerization and its subsequent replication (Leslie E. 2004). The replication of RNA oligomers and the emergence of self-replicating RNA molecules prior to the evolution of protein machinery (to ensure faithful replication) appears seemingly challenging. Nevertheless, over the last few decades, nonenzymatic RNA replication has been characterized under various prebiotically pertinent conditions, using various starting reactants including chemically activated nucleotides, and for distinct sequences of short and long RNA molecules. Even though majority of these studies were carried out in purely buffered conditions, the prebiotically realistic scenario may have been far from simple, and would have comprised of a diverse pool of chemicals or 'co-solutes'. The effect of such chemical heterogeneity on the rate and fidelity of nonenzymatic RNA replication continues to be underexplored. Therefore, we first investigated how the heterogeneity of the prebiotic soup could affect the rates of various nonenzymatic RNA replication reactions.

In the process of life's origin, a second crucial step is thought to have been the encapsulation of the genetic material to form a primordial cell or 'protocell', which is thought to be an assembly of the genetic material encapsulated within a lipid membrane (Mansy et al. 2008;

Blain and Szostak 2014). The lipid membrane is hypothesized to have been made up of single chain amphiphiles (SCAs) due to their availability on the prebiotic Earth as a result of their endogenous synthesis and exogenous delivery. In this context, the role of SCAs in the formation of protocellular vesicles has been studied extensively (Apel et al. 2002; Sarkar et al. 2020). However, a recent study demonstrated the formation of coacervates, a type of liquid-liquid phase separation (LLPS), from SCAs (Zhou et al. 2022). Coacervates have an advantage over the membrane enclosed vesicle systems as model protocells in that they constitute an 'open' system, which can concentrate molecules, allow their ready exchange with the surrounding, and facilitate molecular diffusion and reactions within (Poudyal et al. 2018).

Notably, over the last decade, various coacervate systems, including polylysine/ATP, spermine/RNA, oligoarginine/RNA, polydiallyldimethylammonium chloride (PDAC)/RNA), are being explored as protocell models (Poudyal et al. 2018). However, the polymers used in the above systems are high molecular weight polymers, which is mainly why the prebiotic availability of many of them is debatable. Conversely, prebiotic soup is thought to contain a mixture of SCAs, especially short chain fatty acids and their derivatives (Monnard and Walde 2015; Sarkar et al. 2020). In this context, the role of amphiphilic chemical heterogeneity of the prebiotic soup, in the formation of compositionally diverse SCA-based LLPS systems, is a largely unexplored field. Therefore, we set out to design and characterize a prebiotically plausible mixed SCA-based LLPS system, as a robust protocell with implications for carrying out prebiotically relevant reactions.

Chapter 2: Purpose and rationale for the study

In the backdrop of the aforementioned context, we set out to explore the effect of prebiotic soup's chemical heterogeneity on; (1) template-directed nonenzymatic RNA replication, and (2) to construct and characterize a robust LLPS-based protocellular system composed of SCAs.

I. Template-directed nonenzymatic RNA replication: Nonenzymatic RNA replication reactions have been mainly studied using various 'activated nucleotides'. Particularly, a large body of work in this context has made use of imidazolide-based activation chemistry, to facilitate the reaction at laboratory timescales. Figure I depicts nucleoside-5′-monophosphates (5′-NMPs) that are chemically activated by adding various leaving groups to the 5′-phosphate of 5′-NMPs.

These make the molecules very reactive, and make the nonenzymatic replication reactions feasible in aqueous solutions and at moderate pH and temperature conditions.

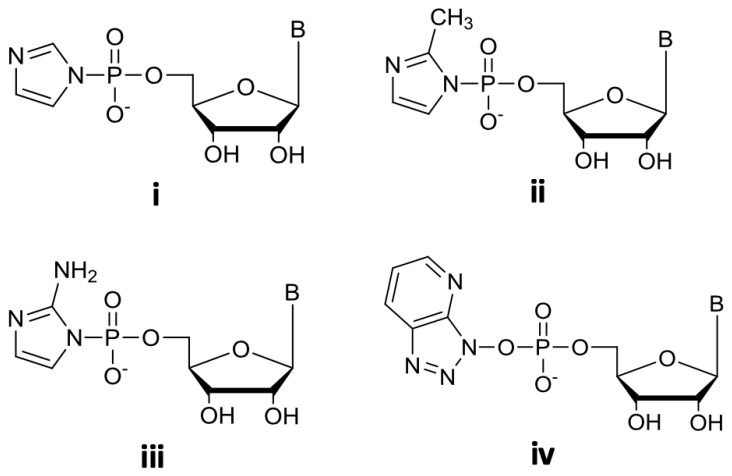

Figure I: Schematic showing various activated nucleotides employed to study nonenzymatic RNA replication. The leaving groups used to 'activate' the 5′-NMPs are imidazole (i), 2-methylimidazole (ii), 2-aminoimidazole (iii), oxyazabenzotriazole (iv). Figure reproduced from (Bapat 2018).

A typical reaction of template-directed nonenzymatic RNA replication reaction is studied by adding an activated nucleotide to a template-bound primer and doing a time course to quantify the rate of extension of the primer (Rajamani et al. 2010; Bapat and Rajamani 2015). In our study, we used imidazole-activated nucleotides (nucleoside-5′-phosphorimidazolides or 5′-ImpNs) to check for primer extension. Furthermore, to understand the effect of chemical complexity of prebiotic soup on RNA replication, we carried out the template-directed nonenzymatic replication of RNA in the presence of an equimolar mixture of all four 5′-NMPs (AMP, GMP, CMP, UMP) as co-solutes. This is because the activated nucleotides undergo spontaneous hydrolysis under aqueous conditions and result in the formation of 5′-NMPs. Also, the synthesis of 5′-NMPs under prebiotically plausible conditions has been demonstrated (Leslie E. 2004). Their presence in the reaction milieu could be problematic as they are devoid of a leaving group like ImpNs to facilitate an extension reaction. Furthermore, they possess the nucleobase, which can still interact with the templating base and potentially affect the rate of the reaction. This is specifically the reason why they are also known as 'spent' nucleotides. In this backdrop, we undertook this study to gain a systematic understanding of the effect of a mixture of all four spent nucleotides on the rate of primer extension in a nonenzymatic RNA replication.

II. To construct and characterize a robust LLPS-based protocellular system composed of SCAs: Towards characterizing a robust LLPS-based protocell system, we prepared a mixed amphiphile-based coacervate moiety and characterized its behaviour systematically. A recent study from 2022 demonstrated the transition of C-10 fatty acid (decanoic acid) vesicles into coacervates upon addition of dopamine (Zhou et al. 2022). Intrigued by the idea of vesicle to coacervate transition by SCAs, we wondered whether fatty acids having chain lengths shorter than decanoic acid could transition into coacervates. This is prebiotically a very pertinent consideration because exogenously delivered meteoritic samples have been demonstrated to contain fatty acids of up to only 12 carbon chain length (C-12), with a greater abundance of lower chain length hydrocarbons (Lai et al. 2019; Sarkar et al. 2020). Furthermore, Fischer-Tropsch type (FTT) synthesis, which is often considered as an endogenous route of fatty acid synthesis under primordial conditions, showed drastically reduced abundance of hydrocarbon species with increasing carbon chain length (McCollom et al. 1999; Rushdi and Simoneit 2001). Paradoxically, fatty acid vesicles composed of chain lengths shorter than decanoic acid, such as C-8 and C-9, have been minimally explored as protocellular systems when compared with longer chain fatty acids. This is mainly because of the following reasons; (i) critical vesicle concentration (CVC) of shorter chain fatty acids is few orders of magnitude higher than longer chain fatty acids (~150 mM for octanoic acid (C-8) as against ~1 mM for oleic acid (C-18)), (ii) the vesicles composed of short chain fatty acids are very dynamic than those of long chain fatty acids making them very sensitive to environmental perturbations, and (iii) short chain fatty acid vesicles tend to coagulate, which makes them unstable, all aspects that make these systems less attractive as protocell candidates. Furthermore, the previously reported SCA system can form droplets only at pH 7.5, and can remain stable only for a short while (1 hr) (Zhou et al. 2022). In this backdrop, we wondered whether the chemical heterogeneity of the prebiotic soup could enable the formation of a robust, compositionally heterogenous, mixed-amphiphile based coacervate systems from a shorter SCA, which, to the best of our knowledge, has not been reported earlier. Furthermore, we wanted to check the ability of these systems to sequester RNA and their capability to carry out a prebiotically important reaction like template-directed nonenzymatic RNA replication.

Chapter 3: Nonenzymatic RNA replication in a mixture of 'spent' nucleotides

We systematically looked at the effect of a mixture of spent nucleotides (5'-NMPs) as co-solutes on the rate of primer extension in a template-directed nonenzymatic RNA replication

reaction. For this, an RNA primer was annealed to an RNA template, and a 5′-NMP mixture comprising an equimolar mixture of all four spent nucleotides (5′-AMP, GMP, CMP, UMP) was added to make the basic reaction mixture. The reaction was then initiated by adding 5′-ImpN, which is complementary to the templating base, and the reaction was allowed to progress over a specific time course. The rate of the reaction was calculated by measuring the fraction of the extended primer at regular time intervals. In these reactions, the ratio of concentrations of imidazole-activated nucleotides to 5′-NMP mixture was kept as 1:5.

We set up four reactions with four different templates; all of these were exactly identical in sequence excepting for only one nucleotide, which was the templating base (U/C/G/A). It was observed that the rate of the reaction was significantly reduced in the presence of a mixture of spent nucleotides. This could have been because of two possibilities; (i) crowding effect coming from the five times excess of 5′-NMPs as compared to 5′-ImpN in a given reaction, (ii) direct interactions of the spent nucleotides with the templating base, hindering the access of the activated nucleotide to the templating base. To determine which possibility is correct, all the four reactions were carried out in the presence of the individual spent nucleotides, where the ratio of 5′-ImpN to 5′-NMP was kept as 1:5. If the reduction in the reaction rate observed earlier was because of crowding, all the reactions should show a similar reduction in the reaction rate. However, significant reduction in the rate was observed only in some reactions.

Specifically, the rates went down drastically for the reactions in which the added spent nucleotide was the Watson-Crick base-pairing partner (cognate spent nucleotide) of the templating base. For instance, when the templating base was U, and 5′-ImpA was added to extend the primer, the reaction containing 5′-AMP as a co-solute showed maximum reduction in the reaction rate. Further systematic experiments and statistical analyses alluded to a correlation between the base-pairing strength of the spent nucleotide with the templating base and the inhibition that was seen in the reaction. In this context, we also observed inhibition coming from certain spent nucleotides which were not the Watson-Crick base pairing partners (Wobble pairs) of the templating base. Additionally, inhibition coming from near neighbour interactions, potentially due to stacking of purine (spent) nucleotides on the primer's 3′ end, was also observed. This work underscored how prebiotic soup's chemical heterogeneity would have directly impinged on the rate of nonenzymatic RNA replication, with implication for evolution of sequence space of molecules in a putative RNA World.

Chapter 4: Characterizing a mixed single chain amphiphile-based coacervate entity as a robust protocell system

To understand whether prebiotically relevant short chain fatty acids other than decanoic acid could show transition from vesicles to coacervates, we characterized a nonanoic acid-based system (C-9) as a protocellular system, for reasons detailed in the above section. Furthermore, to the best of our knowledge, its role as a coacervate forming entity has not been explored to date. As previously demonstrated for the C-10 system, we used dopamine to look at the transition of nonanoic acid vesicles into coacervates (Zhou et al. 2022). Upon addition of dopamine to nonanoic acid vesicles, we observed an increase in the turbidity of the sample, which when observed under microscope showed the presence of spherical coacervate droplets. However, two problems were encountered with nonanoic acid/dopamine system; (i) it formed droplets only at pH 7, (ii) dopamine got readily oxidized into polydopamine, and thus, the system showed reduced droplets over time.

A robust protocellular system would be the one that withstands various prebiotically plausible selection pressures, including change in pH, temperature, presence of salts in the environment etc. In the context of pH, the absence of coacervate droplets at pHs higher than pH 7 can be attributed to the absence of vesicles in the first place. This is because fatty acids are known to form vesicles at pH that is equivalent to the apparent pKa of their carboxylic acid headgroup (Sarkar et al. 2020). This is 7 for nonanoic acid, and therefore, it forms vesicles at pH 7 (Apel et al. 2002). However, when the fatty acid is doped with its alcohol derivative, it can form vesicles across a broader pH range. In this context, it has been that when nonanoic acid was doped with nonanol, it results in the formation of vesicles under alkaline conditions (Apel et al. 2002). With this knowledge, we added dopamine to the vesicles composed of nonanoic acid (NA) and nonanol (NOH) system (having a ratio 10:1) and observed the presence of droplets from pH 7 to pH 9. This again emphasizes the advantage of compositionally diverse, mixed amphiphile-based coacervates over a single amphiphile-based ‘pure’ system.

Furthermore, in order to overcome the challenge of dopamine oxidation, we replaced dopamine with tyramine (Tyra). The new system, NA-NOH/Tyra showed the presence of droplets that persisted even at 8 days. Given this, we systematically characterized the NA-NOH/Tyra system, wherein, using spectroscopy and microscopy the concentrations of NA-NOH and Tyra were determined across which coacervate droplets could form. Using Laurdan GP value, the differences in the micropolarity of the resultant coacervates, formed across various

concentrations of NA-NOH and Tyra, were measured. Furthermore, the system was observed to form coacervates across a wide range of temperatures, ranging from 5 °C to 65 °C. Additionally, the coacervates were found to tolerate up to 20 mM $MgCl_2$ and up to 600 mM NaCl. In this manner, we characterized the NA-NOH/Tyra coacervates and found it to withstand various prebiotically relevant selection pressures.

As the next obvious step, the functional significance of these coacervates was evaluated. Towards this, we first looked at the sequestration of biomolecules like GFP and Cy3-labelled RNA in these moieties. GFP was found to be partitioning much more efficiently than RNA into the coacervates. However, sequestration of RNA was enhanced upon addition of cationic amino acids, which would have been present readily in the prebiotic soup as co-solutes. This result emphasized the role of prebiotic soup's chemical heterogeneity in the formation of functional LLPS-based protocellular compartments. Finally, the coacervates were observed to facilitate biomolecular diffusion as well as to carry out template-directed nonenzymatic RNA replication reaction, demonstrating the functional significance of these coacervates as a pertinent prebiotic model protocellular system.

References:

1. Apel CL, Deamer DW, Mautner MN (2002) Self-assembled vesicles of monocarboxylic acids and alcohols: conditions for stability and for the encapsulation of biopolymers. Biochimica et Biophysica Acta (BBA) - Biomembranes 1559:1–9. https://doi.org/10.1016/S0005-2736(01)00400-X

2. Bapat N (2018) Role of co-solutes in nonenzymatic RNA replication on prebiotic Earth. Thesis, Dept. of Biology

3. Bapat NV, Rajamani S (2015) Effect of Co-solutes on Template-Directed Nonenzymatic Replication of Nucleic Acids. J Mol Evol 81:72–80. https://doi.org/10.1007/s00239-015-9700-1

4. Blain JC, Szostak JW (2014) Progress Toward Synthetic Cells. Annu Rev Biochem 83:615–640. https://doi.org/10.1146/annurev-biochem-080411-124036

5. Domagal-Goldman SD, Wright KE, Domagal-Goldman SD, et al (2016) The Astrobiology Primer v2.0. Astrobiology 16:561–653. https://doi.org/10.1089/ast.2015.1460

6. Gilbert W (1986) Origin of life: The RNA world. Nature 319:618–618. https://doi.org/10.1038/319618a0

7. Lai JC-Y, Pearce BKD, Pudritz RE, Lee D (2019) Meteoritic abundances of fatty acids and potential reaction pathways in planetesimals. Icarus 319:685–700. https://doi.org/10.1016/j.icarus.2018.09.028

8. Leslie E. O (2004) Prebiotic Chemistry and the Origin of the RNA World. Critical Reviews in Biochemistry and Molecular Biology 39:99–123. https://doi.org/10.1080/10409230490460765

9. Mansy SS, Schrum JP, Krishnamurthy M, et al (2008) Template-directed synthesis of a genetic polymer in a model protocell. Nature 454:122–125. https://doi.org/10.1038/nature07018

10. McCollom TM, Ritter G, Simoneit BRT (1999) Lipid Synthesis Under Hydrothermal Conditions by Fischer- Tropsch-Type Reactions. Orig Life Evol Biosph 29:153–166. https://doi.org/10.1023/A:1006592502746

11. Monnard P-A, Walde P (2015) Current Ideas about Prebiological Compartmentalization. Life 5:1239–1263. https://doi.org/10.3390/life5021239

12. Poudyal RR, Pir Cakmak F, Keating CD, Bevilacqua PC (2018) Physical Principles and Extant Biology Reveal Roles for RNA-Containing Membraneless Compartments in Origins of Life Chemistry. Biochemistry 57:2509–2519. https://doi.org/10.1021/acs.biochem.8b00081

13. Rajamani S, Ichida JK, Antal T, et al (2010) Effect of Stalling after Mismatches on the Error Catastrophe in Nonenzymatic Nucleic Acid Replication. J Am Chem Soc 132:5880–5885. https://doi.org/10.1021/ja100780p

14. Rushdi AI, Simoneit BRT (2001) Lipid Formation by Aqueous Fischer-Tropsch-Type Synthesis over a Temperature Range of 100 to 400 °C. Orig Life Evol Biosph 31:103–118. https://doi.org/10.1023/A:1006702503954

15. Sarkar S, Das S, Dagar S, et al (2020) Prebiological Membranes and Their Role in the Emergence of Early Cellular Life. J Membrane Biol 253:589–608. https://doi.org/10.1007/s00232-020-00155-w

16. Zhou L, Koh JJ, Wu J, et al (2022) Fatty Acid-Based Coacervates as a Membrane-free Protocell Model. Bioconjugate Chem 33:444–451. https://doi.org/10.1021/acs.bioconjchem.1c00559

Chapter 1

INTRODUCTION

1.1.Origin of life: The transition from chemistry to biology

'How did life emerge on the prebiotic Earth?'; this is one of the most fundamental, intriguing and as yet unanswered questions in biology. It is contemplated by the origins of life (OoL) researchers that life would have emerged from the chemicals present in the prebiotic soup or primordial soup on the early Earth about 4 billion years ago (Leslie E. 2004; Blain and Szostak 2014). These chemicals in the prebiotic soup would have reacted with each other to form biologically relevant precursor molecules, such as amino acids, nucleobases, sugars, and fatty acids, which make the bulk of extant life biochemistry. However, the fundamental unit of modern life, i.e. a cell, is an extremely complex structure and for it to have emerged directly from inert chemicals would have been a very unlikely event. Thus, OoL researchers consider that modern unicellular organisms would have preceded by not one, but many simpler and more primitive forms of 'life' (Figure 1.1) (Smets and Barkay 2005).

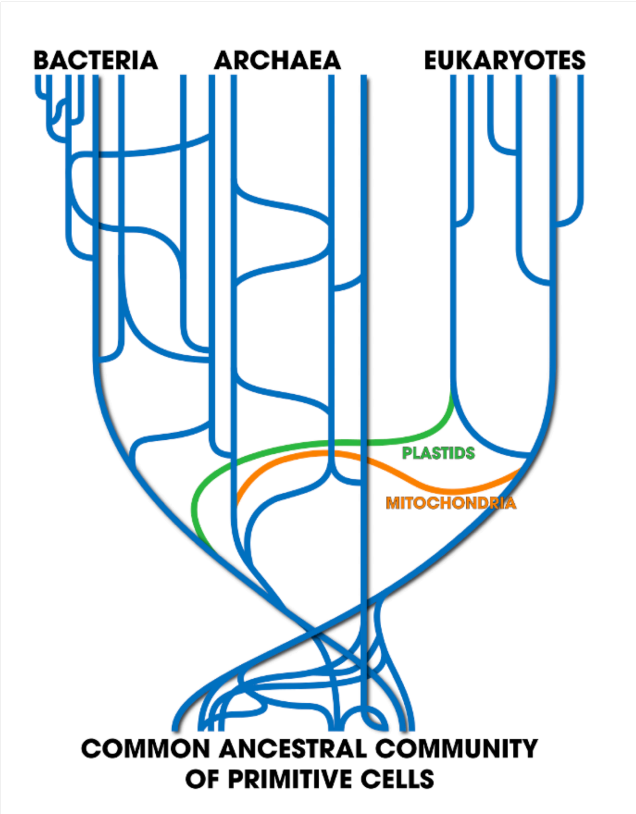

Figure 1.1: Common ancestral community of primitive cells. Modern life is thought to have evolved from a community of primordial cells, which are considered to have preceded the unicellular life during the course of evolution. Image reproduced from: Smets, B.F. and Barkay, T., 2005. Horizontal gene transfer: perspectives at a crossroads of scientific disciplines. *Nature Reviews Microbiology*, *3*(9), pp.675-678.

But what is life and how to define it?

Life is defined as "a self-sustaining chemical system capable of undergoing Darwinian evolution" (Domagal-Goldman et al. 2016). Based on this definition, one can start looking for chemical systems that can undergo Darwinian evolution. The primordial soup, as mentioned earlier, is thought to be chemically heterogenous, wherein simpler molecules would have reacted with each other to result in complex biomolecular precursors, such as sugars, nucleobases, amino acids, fatty acids, etc. (Leslie E. 2004; Pressman et al. 2015). These precursors are hypothesized to have further reacted with each other under prebiotically plausible conditions to form an ensemble of biomolecules, such as nucleotides and nucleic acid, peptides and lipids (Leslie E. 2004; Pressman et al. 2015; Frenkel-Pinter et al. 2020). However, how these biomolecules would have assembled to form one of the primordial forms of life is not fully clear. In other words, how the transition from chemistry to biology would have happened is unknown. In this context, scientists have put forward prebiotically plausible routes to explain the potential origin of life on the prebiotic Earth (Figure 1.2) (Krishnamurthy 2017). The more accepted ones include metabolism-first hypothesis, lipid world hypothesis, RNA world hypothesis and RNA-protein World hypothesis, which are detailed below.

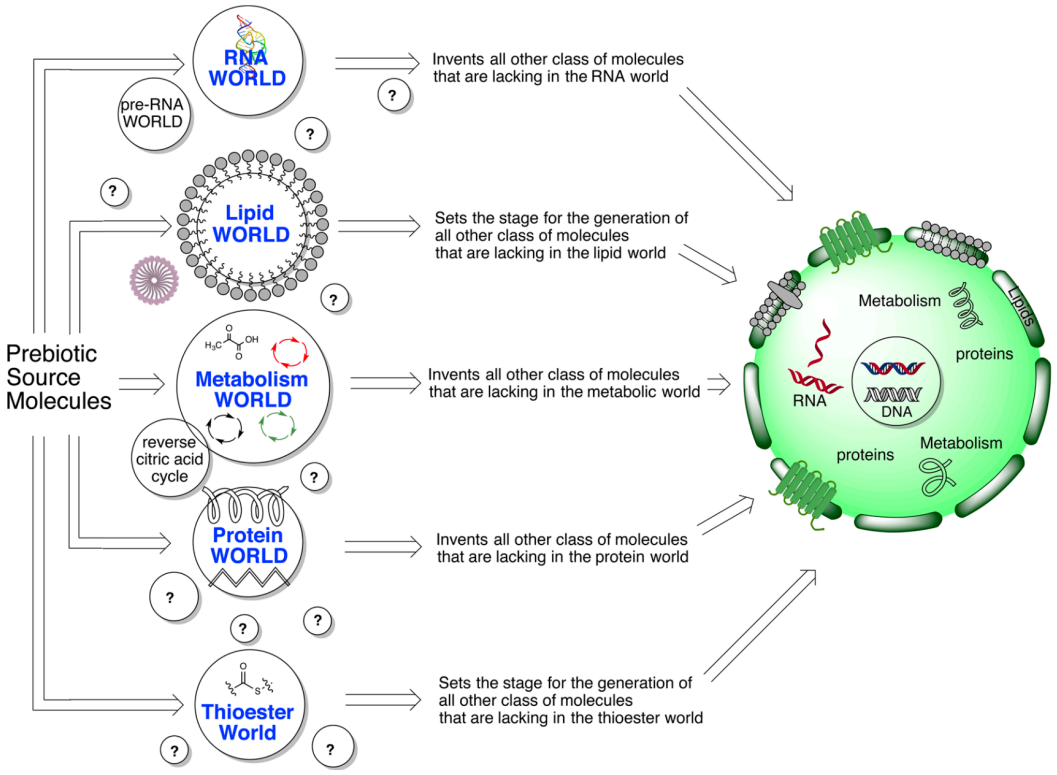

Figure 1.2. **The various worlds that potentially led to the transition from chemistry to biology.** Reproduced from Krishnamurthy, R., 2017. Giving rise to life: transition from prebiotic chemistry to protobiology. *Accounts of chemical research*, *50*(3), pp.455-459.

1.2. The hypotheses pertaining to various 'Worlds'

1.2.1. Metabolism-first hypothesis

The metabolism first hypothesis proposes that self-sustaining, autocatalytic, chemical reaction networks or protometabolic reaction networks, consisting of simple organic compounds, would have built the foundation for the origin of life on the prebiotic Earth (Morowitz et al. 2000). Such protometabolic cycles would have served as the precursors to progressively more complex metabolic pathways, which would have eventually led to the synthesis of genetic components (Wächtershäuser 1990). Furthermore, greater focus of metabolism-first hypothesis has remained on investigating autocatalytic cycles, which can form biomolecules in a sustained manner (Damiano and Luisi 2010). In this context, reductive citric acid cycle (rTCA) is considered to have given rise to a set of complex organic molecules with an input of water, CO_2 and chemical energy (Trefil et al. 2009). Additionally, autocatalytic formose reaction has been explored as a source of sugars on the early Earth (Leslie E. 2004).

Recently, glyoxylate was also demonstrated to form various molecules, including α-hydroxy acids, analogues of α-keto acids formed in rTCA, α-amino acids and pyrimidine nucleobases (Krishnamurthy and Liotta 2023). Notably, Iron-Sulfur World hypothesis is in support of the metabolism-first hypothesis, and proposes that these kind of protometabolic reactions may have been catalyzed by mineral surfaces rich in iron and sulfur, such as pyrite, in deep hydrothermal vent environments (Wächtershäuser 1988; Huber and Wächtershäuser 1997). Additionally, certain reactions of rTCA cycles were shown to be getting promoted by minerals containing Zn^{2+}, Cr^{3+} and Fe^{0} in an acidic solution (Muchowska et al. 2017). In all, the metabolism-first hypothesis focuses on the investigation of prebiotically plausible chemical reaction networks, which can yield biomolecules or their precursors.

1.2.2. Lipid World hypothesis

Modern cells are surrounded by a lipid bilayer membrane, which not only creates a protective barrier for the cellular contents, but also maintains the structural integrity of the cell, facilitates transport of molecules, and enables communication with the neighboring cells as well as with the surrounding environment. These membranes are mainly composed of three classes of lipids, phospholipids, sphingomyelins and sterols (Segré et al. 2001; Sohlenkamp and Geiger 2016; Harayama and Riezman 2018). Membranes composed of phospholipids have extremely low permeability for small polar molecules while prebiotic membranes are thought to have

comprised of simpler amphiphilic molecules, such as fatty acids that result in dynamic membranes (Sarkar et al. 2020). This dynamicity makes them more permeable to a variety of small molecules when compared to phospholipid membranes. This would have crucial for early membranes because sophisticated protein channels that facilitate diffusion of molecules across the membrane would have been lacking (Joyce and Szostak 2018; Sarkar et al. 2020).

In addition to fatty acids having the ability to spontaneously assemble into vesicles under appropriate conditions in aqueous solution (Gebicki and Hicks 1973; Deamer 1985; Morigaki and Walde 2007), they have been shown to readily form under prebiotically plausible conditions too (McCollom et al. 1999; Rushdi and Simoneit 2001). Given all this, fatty acid-based vesicles are proposed to have formed the primordial cells, which is termed as 'protocell', encapsulating genetic material in their lumen (Joyce and Szostak 2018). Isoprenoids and polycyclic aromatic hydrocarbons have also been considered as prebiotically plausible molecules, which assisted in the formation of prebiotic membranes. (Sarkar et al. 2020). In all, Lipid World hypothesis has predominantly focused on the potential role of prebiotically plausible amphiphiles in the formation of early compartments in the history of the origin of life.

Additionally, characterizing the role of lipids as co-solutes in prebiotically relevant reactions has gained much attention over the last decade. In this context, lipid environments were demonstrated to facilitate the formation of RNA-like polymers (Rajamani et al. 2008). Furthermore, when oligomerization of amino acid was investigated in the presence of lipids under wet-dry cycling conditions, emergence of a new molecular species, N-acyl amino acid (NAA), was observed, which was also observed to form vesicles (Joshi et al. 2021). Moreover, they were shown to act as substrates to react with other amino acids in the surroundings to form lipopeptides (Joshi et al. 2022). These studies highlight how interactions between prebiotically plausible molecular systems could have driven chemical evolution on the early Earth.

1.2.3. RNA World hypothesis

Modern cell is a highly complex assembly where different biomolecules- proteins, lipids, RNA, and DNA- perform specialized functions, such as metabolism, replication, growth, and division, in a well-coordinated manner. Among these biomolecules, proteins play a vital role in regulating numerous key cellular processes, including transport of molecules across the cell, signal transduction, enzyme catalysis, regulation of metabolic pathways. Furthermore, they

play an essential role in governing the crucial steps involved in central dogma, such as DNA replication, transcription and translation. Through these processes, they ensure faithful replication of the genetic material while catalyzing their own synthesis. Despite their versatility in performing various sub-cellular functions, proteins are considered too complex to have existed during the life's origin without a genetic molecule to code for the variety. This raises a fundamental question, which came first, the genetic material or the protein?

This conundrum was addressed by an comprehensive model proposed for the origin of life, called the RNA World hypothesis (Gilbert 1986). This term was first coined by Gilbert in 1986, where he proposed that RNA would have served as the genetic material for the early life forms before the emergence of DNA and proteins. This is chiefly because of two reasons- first, RNA can act as an informational polymer, and second, it can also catalyze chemical reactions as ribozymes in the absence of proteins. The experimental observation that the catalytic core of the ribosome in contemporary cells comprises of RNA, supports the idea that RNA would have preceded DNA and proteins in early life forms (Robertson and Joyce 2012). This brings up a few important questions about how RNA could have come about on the prebiotic Earth.

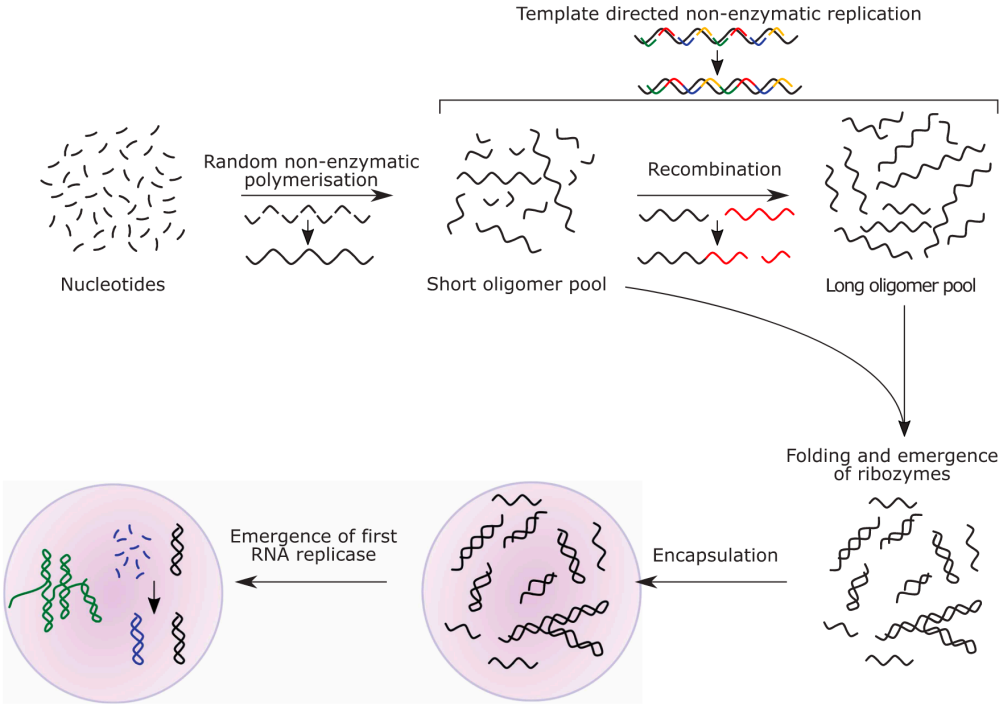

Figure 1.3: Plausible steps involved in the establishment of the putative RNA World. Reproduced from Le Vay, K. and Mutschler, H., 2019. The difficult case of an RNA-only origin of life. *Emerging Topics in Life Sciences*, *3*(5), pp.469-475.

According to the scheme shown in Figure 1.3, ribonucleotides would have undergone nonenzymatic oligomerization to form RNA oligomers, which are thought to have undergone nonenzymatic replication to produce more copies of themselves. Furthermore, some RNA molecules, capable of folding upon themselves, may potentially have led to the emergence of first ribozymes capable of self-replication. In this context, experimental demonstration of prebiotic nucleotide synthesis, nonenzymatic RNA oligomerization, template-directed nonenzymatic replication and ribozyme catalysis, strongly support the putative RNA World hypothesis. Among all the aforementioned hypotheses for the origin of life, the RNA world hypothesis, not surprisingly, is the most widely accepted one in the field of origins of life.

1.3 Potential prerequisites for the establishment of the proposed RNA World on the prebiotic Earth

1.3.1. Nucleotide synthesis:

Miller-Urey experiment, which demonstrated the abiotic synthesis of amino acids, was the pioneering milestone in demonstrating that the building blocks of life could have been formed abiotically from the chemicals present on the early Earth (Miller 1953). This suggests that the synthesis of nucleotides on the prebiotic Earth may have likely occurred through similar abiotic processes, in contrast to enzyme-driven nucleotide synthesis observed in modern biology. However, unlike amino acids, nucleotides are composed of three components, a ribose sugar, a nucleobase and one or more phosphate group/s. In the context of prebiotic synthesis of sugars, Butlerow's formose reaction established a foundational work. The formose reaction involves formaldehyde as the starting reactant, which upon polymerization under slightly alkaline conditions and in the presence of catalysts (such as Pb^{2+} and Ti^{+}), first forms glycolaldehyde and then glyceraldehyde, and thereafter form a mixture of sugars where the yield of ribose is low (Leslie E. 2004). However, when monophosphates of glycolaldehyde and glyceraldehyde were used for the reaction by Eschenmoser, ribose-2,4-diphosphate was formed as the major product (Leslie E. 2004).

In regards to the prebiotic synthesis of nucleobases, when Juan Oro and coworkers refluxed ammonium cyanide in aqueous solution, they obtained adenine as a result of cyanide polymerization, which was the first demonstration of prebiotic synthesis of a nucleobase (Oró and Kimball 1961; Leslie E. 2004). Furthermore, when HCN was used as a starting reactant, its polymerization not only yielded adenine, but small amounts of guanine were also detected

(Miyakawa et al. 2002b, a; Leslie E. 2004). HCN undergoes polymerization to form a tetramer, which undergoes further polymerization to form a dark solid that releases molecules such as adenine, guanine and a whole bunch of other uncharacterized entities (Leslie E. 2004). Although a prebiotically plausible route to the synthesis of adenine was demonstrated, scientists also consider that the exogenous delivery of adenine would have made it available on the prebiotic Earth, since carbonaceous chondrites were found to contain substantial amounts of adenine (Miyakawa, 2000; Orgel 2004).

In the context of prebiotic pyrimidine synthesis, reaction of cyanoacetylene or cyanoacetaldehyde with cyanate, cyanogen or urea have been shown to lead to the formation of cytosine in good amounts (Ferris et al. 1968, 1974; Robertson and Miller 1995; Leslie E. 2004). Furthermore, prebiotically plausible route to the formation of uracil is proposed to be the hydrolysis of cytosine (Leslie E. 2004). While the prebiotic synthesis of nucleobases is now mostly established, the question that arises is how did prebiotic chemistry advanced from nucleobases to the formation of nucleosides and nucleotides, the building blocks of the genetic polymers?

Towards the synthesis of nucleoside from the nucleobase and ribose, when hypoxanthine, a molecule closely resembling guanine, was heated along with D-ribose, β-D-inosine (nucleoside of hypoxanthine) was formed. However, when similar reaction was carried out with adenine instead of hypoxanthine, adenosine was formed only as a minor product. Additionally, similar reaction between ribose and cytidine or uracil did not readily yield the pyrimidine nucleosides. Instead, a reaction between cyanamide, cyanoacetylene, and ribose yielded α-cytidine (Fuller et al. 1972; Leslie E. 2004). Interestingly, when ribose was substituted by ribose-5-phosphate in the aforementioned reaction, α-cytidine-5-monophosphate was obtained (Sanchez and Orgel 1970). Furthermore, nucleoside phosphorylation was shown by mobilization of phosphate from minerals in urea-based solvents (Burcar et al. 2016). Additionally, phosphorylation of nucleosides was also demonstrated by using a prebiotically plausible phosphorylating agent, diamidophosphate (DAP) (Gibard et al. 2018). More recently, formation of activated pyrimidine nucleotides was demonstrated by an alternate reaction sequence involving arabinose amino-oxazoline and anhydronucleoside intermediates that bypassed the requirement of having free ribose and nucleobase, since selective ribose synthesis is difficult and addition of pyrimidines to ribose does not occur at all (Powner et al. 2009).

1.3.2. Nucleotide oligomerization

Chemically linking the nucleotides to form oligomers would have been the next crucial step in the establishment of the proposed RNA World. In contemporary biology, nucleotide polymerization is facilitated by enzymes which utilize high-energy activated monomers, such as nucleoside triphosphates and aminoacyl t-RNAs. In the context of prebiotically plausible oligomerization, the processes by which nucleotides would have undergone oligomerization without the assistance of an enzyme have been the focus of most investigations. In general, the process of oligomerization is a condensation reaction, requiring the removal of a water molecule, which makes it an uphill reaction in aqueous solution (Leslie E. 2004). The free energy barrier for the formation of a phosphodiester bond at 25°C and at pH 7 is 5.3 kcal mol^{-1}. Furthermore, the rate of phosphodiester bond formation of nucleoside-5'-triphosphates or NTPs was found to be 5.4×10^{-7} per hour (Bartel and Szostak 1993), which is seemingly very low.

In contrast to NTPs, where pyrophosphate acts as the leaving group, forming a phosphodiester bond between two nucleoside-5'-monophosphates (NMPs) requires that a hydroxyl (-OH) on the phosphate act as the leaving group. However, -OH is known to be a poor leaving group for the reaction to occur, especially at moderate temperatures, pH and aqueous conditions. Given this, it is often replaced by better leaving groups, such as imidazole which is used the form of nucleoside-5'-phosphorimidazolide ((ImpN) derivatives of the monomer (Lohrmann 1977). This replacement of the hydroxyl group with imidazole speeds up the condensation reaction. In this context, oligomerization of such ImpNs has been studied extensively to delineate the underlying first principles of nonenzymatic templated replication (Lohrmann and Orgel 1973; Blain and Szostak 2014; Puthenvedu et al. 2015, 2018; Majerfeld et al. 2016). It has been found to be catalyzed by divalent ions, such as Zn^{2+}, Pb^{2+}, Co^{2+}, to name a few (Sawai and Orgel 1975; Sawai 1976). However, these reactions typically produce a mixture of phosphodiester linkages, such as 2′-5′, 3′-5′, and 5′-5′.

Additionally, nonenzymatic oligomerization in bulk solution is inefficient as a result of the large diffusional mobility of the monomers, resulting in less proximity between the monomers for the reaction to occur. In this context, prebiotically plausible ways were studied to increase the local concentration of monomers, and consequently provide the proximity effects for the reaction to proceed more efficiently. Towards this, adsorbing surfaces, such as clay and minerals, were found to catalyze oligomerization. In this regard, montmorillonite clay was investigated extensively and was found to form long oligomers (up to 40-mers) (Zagorevskii

et al. 2006). Additionally, studies reported that the clay-catalyzed oligomerization favored the formation of homochiral dimers over heterochiral ones, and 3′-5′ linkages over 2′-5′ ones (Urata et al. 2008).

Furthermore, eutectic phases have also been proposed as a potential means to concentrate molecules on the early Earth (in brine channels). In this context, when a mixture of ImpNs and divalent cations was incubated at -18°C for several days, oligomers of length ranging from 7 to 10 were observed (Kanavarioti et al. 2001). These environments could also have helped reduce the hydrolysis rates due to low temperatures. Apart from ImpNs, oligomerization of cyclic nucleotides (cNMPs), which are shown to be prebiotically plausible and intrinsically activated (Lohrmann and Orgel 1971; Saladino et al. 2009) has also been explored. The reactions with cNMPs were found to form oligomers ranging from trimers to 25-mers, depending on the reaction conditions (Verlander et al. 1973; Verlander and Orgel 1974; Costanzo et al. 2009, 2016; Dagar et al. 2020).

Besides studying clay adsorbing surfaces and eutectic phases as plausible mechanisms for concentrating molecules, researchers have investigated the role of 'wet-dry cycles' or 'dehydration-rehydration cycles', which, as a result of day-night variations or seasonal fluctuations, are thought to have been prevalent on the early Earth just as they are today (Damer and Deamer 2015). Specifically, wet-dry cycles were facilitated in the presence of vesicles. First, during the drying phase, the lipid vesicles collapse and form a multilamellar matrix of alternate hydrophilic and hydrophobic regions. The nucleotide monomers are suggested to get trapped in the hydrophilic part of this matrix. Second, dehydration results in reduced water activity, which along with elevated temperatures of drying, can facilitate condensation reaction between the monomers. Furthermore, rehydration facilitates blebbing out of the collapsed membrane into vesicles while encapsulating the solutes (including the newly formed oligomers) that are trapped within the multilamellar matrix. (Damer and Deamer 2015).

Early experiments in this context were used to study the nonenzymatic oligomerization of non-activated nucleotides (NMPs) and amino acids. As mentioned earlier, NMPs lack a good leaving group for oligomerization to occur in bulk aqueous solution at moderate temperature and pH. Notably, with this reaction set-up, RNA-like oligomers ranging from 25 to 75 nucleotides were observed (Rajamani et al. 2008), which could be readily encapsulated into a vesicle during rehydration, setting the stage for the emergence of protocell-like entities. In all, prebiotically plausible routes to the synthesis of RNA oligomers on the early Earth were

demonstrated by various groups. This raises further question, would there have been any prebiotically plausible mechanism for the replication of genetic material in the absence of enzymes?

1.3.3. Template-directed replication of RNA

RNA oligomers that would have formed on the prebiotic Earth would have transferred their genetic information by means of replication, albeit in a nonenzymatic manner. Modern biology uses sophisticated enzymatic machinery to carry out replication. For instance, a highly evolved DNA polymerase has different subunits to take care of different functions required for replication, such that helicase unwinds the two strands of the DNA duplex, ß-clamps hold the primer and the template together, and the polymerase subunit performs the function of addition of nucleotides against the templating bases. However, it is fundamental to think how replication would have occurred in the absence of enzymes, since life is considered to have begun with the onset of replication. As mentioned earlier (section 1.3.2), chemically linking two nucleotides is an uphill reaction in aqueous solutions and at moderate temperatures and pHs. Therefore, nucleotide monomers were chemically activated by adding a good leaving group on to the 5'-phosphate of the nucleotide. In this backdrop, various ways of nonenzymatic template-directed replication have been studied (Figure 1.4), which are alluded to in the subsequent sections.

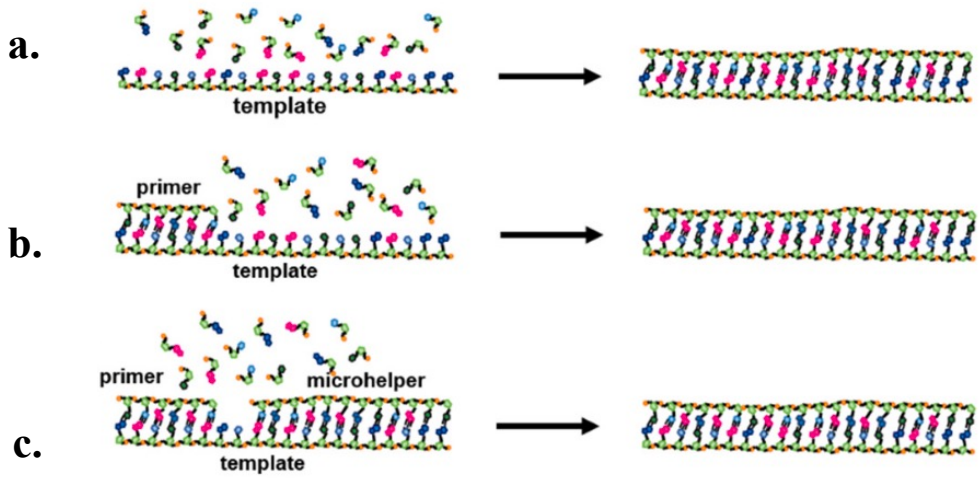

Figure 1.4: Illustration depicting the types of nonenzymatic RNA replication. (a) Template-directed oligomerization, (b) template-directed primer extension, and (c) template-directed primer extension in the presence of a downstream microhelper. Figure adapted from Kaddour, H. and Sahai, N., 2014. Synergism and mutualism in non-enzymatic RNA polymerization. *Life*, *4*(4), pp.598-620.

1.3.3.1. Template-directed oligomerization

In template-directed oligomerization reactions, template RNA oligomer directs polymerization to occur between the activated monomers. The underlying principle behind these reactions is that the template brings the free monomers in close proximity through base-pairing interactions, which can facilitate attack of 2′ or 3′- nucleophile of one nucleotide on the 5'-phosphate of the next, leading to phosphodiester bond formation (Sulston et al. 1968, 1969; Leslie E. 2004). Furthermore, replacement of the 2′- or 3′- nucleophile from hydroxyl group to amino group on the nucleotide monomers increased the rate of reaction between the two nucleotides (Zielinski and Orgel 1985, 1987). Additionally, replacing the imidazole group by methylimidazole group on the 5′- phosphate of the nucleotide (2-MeImpNs) was shown to increase the rate of the reaction (Inoue and Orgel 1981).

1.3.3.2. Template-directed primer extension

In template-directed primer extension reactions, pre-formed RNA oligomers are considered to have acted as primers and templates. A pre-formed RNA oligomer, base-paired with a template RNA, is allowed to react with activated nucleotides. In this process, the nucleotide first base pairs with the templating base and stabilized by near neighbouring interactions. This is followed by the nucleophilic attack of the primer's nucleophilic group on the 5′- phosphate of the base-paired activated nucleotide. While looking for the mechanism, it was found that the 2-MeImpNs react with each other, and forms an imidazolium bridged dinucleotide, which then binds to the templating base. Subsequent attack of the 2′ or 3′- nucleophile of the primer results in displacement of one of the activated nucleotide, leading to primer extension (Walton and Szostak 2016; Zhang et al. 2017).

Primer extension reactions were first studied using an RNA hairpin, where the shorter arm served as a primer, and the longer arm that base paired with the primer, served as a template. In this study, 2-MeImp was used as activated nucleotides, and it was found that the copying of C templating base was more efficient than A. This was potentially because of the more efficient base-pairing of the cognate G nucleotides with the templating base C, when compared to that of U nucleotides against templating base A (Wu and Orgel 1992c, b, a). Jack Szostak's group and Clemens Richert's group made significant contributions to advance the understanding of template-directed primer extension reactions.

In this context, replacement of the 2′ or 3′- OH group of the primer and the incoming nucleotide by NH_2 group, was found to increase the rate of the reaction (Mansy et al. 2008; Schrum et al. 2009; O'Flaherty et al. 2019). Furthermore, nucleotides containing 1-hydroxy-7-azabenzotriazole (HOAt) as the leaving group were also found to enhance the rates of the reaction (Stütz et al. 2007). Moreover, when primer extension was carried out in the presence of a microhelper strand, a short oligomeric strand that base-pairs with the template downstream of the primer, the rate of the primer extension reaction was observed to be accelerated (Vogel et al. 2005). Thus, besides acting as primers, some oligomers could have aided the replication of other sequences by acting as microhelpers. Additionally, some short RNA oligomers could have formed longer strands by a process called as 'ligation', which is detailed in the subsequent section.

1.3.3.3. Template-directed ligation of oligomers

In template-directed ligation reactions, two oligomers, complementary in sequence to the templating bases undergo ligation reaction to form longer oligomers. These reactions are interesting, because extension that has been observed in reactions involving activated mononucleotides is 25 nucleotides (O'Flaherty et al. 2019), however, replication of the entire RNA templating sequence to form oligomers of the length of a ribozyme in a prebiotically plausible manner has remained a challenge. In these reactions, a condensing agent, 1-ethyl-3-(3-dimethylaminopropyl) carbodiimide (EDC)) was first employed to bring about the condensation reaction to facilitate the ligation reaction between the two dimers or trimers, resulting in tetramers or hexamers, respectively (Leslie E. 2004).

The activation of oligomers using imidazole was found to be less efficient in the case of ligation reactions of oligomers than that in the case of monomers (Ninio and Orgel 1978). Furthermore, ligation reactions are also fascinating, as they have the potential to overcome the difficulties posed by single nucleotide extension reactions such as copying of sequences having secondary structures or A/U rich regions, or accomplishing completion of the copying till the very last nucleotide (Zhou et al. 2020). A recent study carried out ligation reactions using 3'- amino terminated oligonucleotides, which showed not only the efficient template copying through multistep ligation reactions, but also the assembly of long template strands using RNA tetramers (Zhou et al. 2020).

Subsequently, from the resultant diverse pool of RNA sequences that resulted in a putative RNA World, some RNAs, capable of folding upon themselves, would have evolved into functional ribozymes. An RNA ligase ribozyme (class I RNA ligase) capable of ligating RNA strands, was experimentally evolved from a random pool of ~10^{15} RNA oligomers (Bartel and Szostak 1993). The ligase was capable of catalyzing 3′-5′ phosphodiester bond formation at a rate 10^7 times faster than an uncatalyzed reaction Furthermore, self-replicating ribozymes (R3C ribozyme) were evolved, which could ligate daughter strands to form the ribozyme itself (Rogers and Joyce 2001; Paul and Joyce 2002). Apart from ligases, ribozymes having polymerase activity that could incorporate single nucleotides against the template were also evolved. In this context, ribozymes extending the primer by 6 nucleotides (a variant of class I ligase) (Ekland and Bartel 1996), 14 nucleotides (round 18 (R18) ribozyme) (Johnston et al. 2001) and 20 nucleotides (B6.61 ribozyme, a further evolved variant of R18 ribozyme) (Zaher and Unrau 2007) were developed.

Furthermore, ribozyme having a more general polymerase activity was evolved, which was capable of synthesizing up to 95 nucleotides long RNA (tC19 ribozyme) (Wochner et al. 2011). All these aforementioned studies establish the potential for the availability of ribozymes that were endowed with diverse functional capabilities. Nonetheless, ribozyme functioning also meant the need for a specific ribozyme to be in close proximity with its substrate, allowing for effective catalysis and prevention of information degradation due to parasitic sequence (Schrum et al. 2010; Das et al. 2024a). For this, compartmentalization has been argued as a crucial step, along with it being imperative for Darwinian evolution to gain traction. Also, compartmentalization of the self-replicating ribozyme could have led to the formation of a functional protocell capable of Darwinian evolution.

1.4. Protocell: The enigma of life

A protocell is a compartmentalization-centric hypothetical concept, typically described as a membrane-bound assembly that contains genetic material and protometabolic networks, which is capable of undergoing Darwinian evolution (Ruiz-Mirazo et al. 2014; Monnard and Walde 2015; Sarkar et al. 2020). The idea of a protocell is shown in figure 1.5.

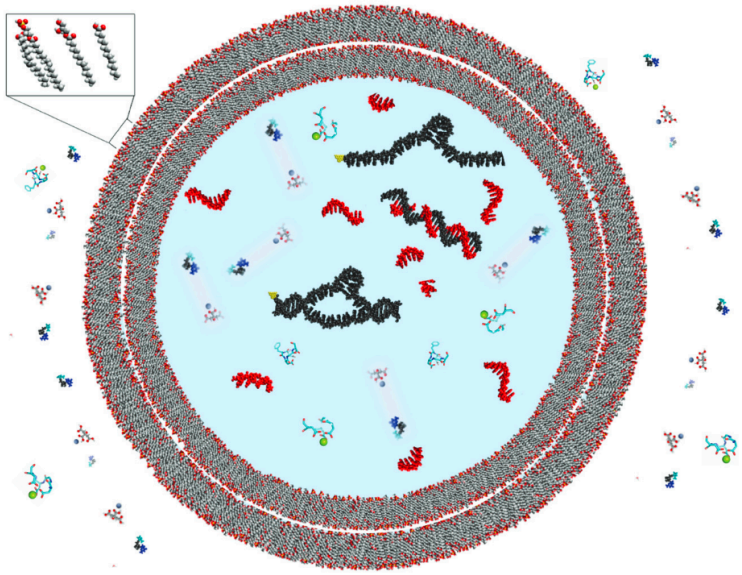

Figure 1.5: Idea of a protocell. Image reproduced from Joyce, G.F. and Szostak, J.W., 2018. Protocells and RNA self-replication. *Cold Spring Harbor Perspectives in Biology*, *10*(9), p.a034801.

In this context, researchers have extensively studied the strategies for prebiotically plausible compartmentalization, since they are thought to have protected the internal components by establishing a boundary that separates the inside from the outside (Joyce and Szostak 2018). Furthermore, by enclosing molecules within, protocells would have increased their local concentration, while also safeguarding the protocellular contents from the intrusion of parasites (Joyce and Szostak 2018). In these and other ways, the protocellular compartments are thought to have played a crucial role in kickstarting Darwinian evolution in these systems, setting the stage for the emergence of early forms of cellular life. Towards this, predominantly, two types of compartmentalization strategies are proposed as model protocells- vesicles, and, more recently, compartments formed by liquid-liquid phase-separation (LLPS).

1.4.1. Vesicular compartments

As mentioned earlier, prebiotically plausible membranes are thought to have formed of single chain amphiphiles (SCAs) in contrast to phospholipid-based membranes found in extant biology (Sarkar et al. 2020). Specifically, the fatty acid vesicle membranes are thought to have been composed of short chain fatty acids, their alcohol and glycerol derivatives. Fatty acids form vesicles when the pH of the solution is near the pKa of the carboxylate headgroup (Figure 1.6) (Sarkar et al. 2020). At pH near the pKa, nearly half of the fatty acid molecules are deprotonated, while the other half are protonated. Thus, hydrophobic interactions between the

acyl chains of the fatty acids drive the fatty acid molecules to cluster together while the hydrogen bonding interactions between the head groups give a pseudo-diacyl like structure (similar to that seen in phospholipids), conferring stability to the resulting membrane assembly.

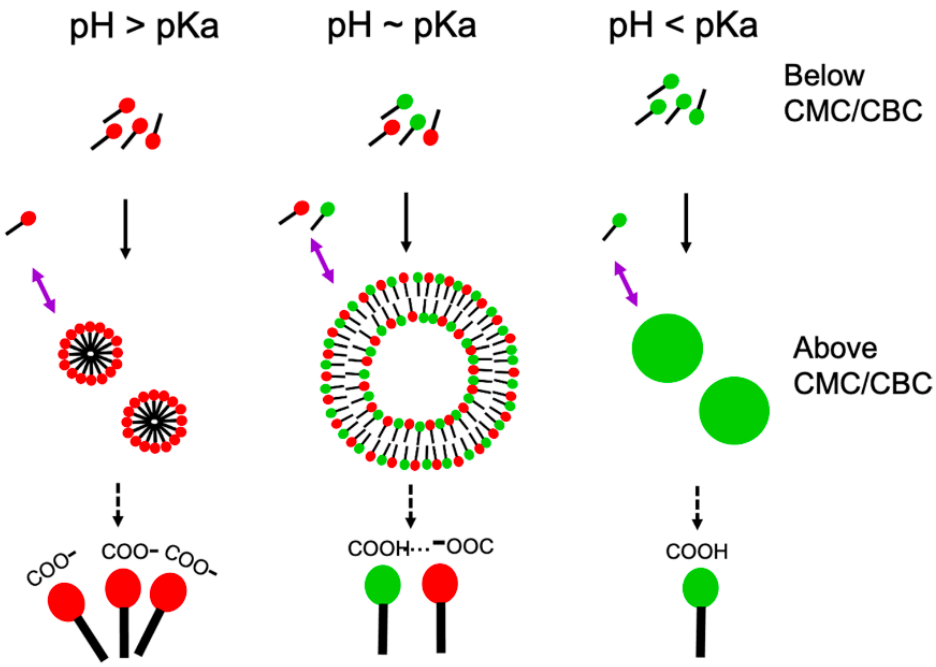

Figure 1.6: Various self-assemblies of fatty acids in aqueous solution as a function of pH. At a pH of the surrounding equivalent to the apparent pKa of the carboxylate headgroup of fatty acids and above the critical bilayer concentration (CBC), fatty acids form bilayers and vesicles. At a pH greater than the carboxylate headgroup and above the critical micellar concentration (CMC), fatty acid molecules assemble into micelles. At a pH lower than the pKa of carboxylate headgroup, fatty acid molecules form oil droplets. Figure reproduced from Sarkar, S., Das, S., Dagar, S., Joshi, M.P., Mungi, C.V., Sawant, A.A., Patki, G.M. and Rajamani, S., 2020. Prebiological membranes and their role in the emergence of early cellular life. *The Journal of Membrane Biology*, *253*, pp.589-608.

However, these fatty acid vesicles remain stable only across a narrow pH range. Nevertheless, the idea that doping fatty acids with their prebiotically plausible alcohol and/or glycerol derivatives was found to substantially increase the stability of these membranes across a broad range of pH (Apel et al. 2002; Sarkar et al. 2020). In this context, a good body of research has gone into characterizing various fatty acid membrane systems. Furthermore, template-directed nonenzymatic replication has also been successfully demonstrated to be occurring inside the lumen of the fatty acid-based vesicles (Mansy et al. 2008; O'Flaherty et al. 2019).

Although fatty acid vesicles are an extremely interesting protocellular model, the fatty acid bilayer acts as a barrier for the diffusion of large polar molecules and hence they are considered

as ‘closed’ systems (Poudyal et al. 2018). This could have presented a challenge for the efficient exchange of nutrients and wastes across the bilayer, especially because sophisticated membrane protein channels would have been absent. As a result, researchers started to look for ‘open’ protocellular systems. In this context, LLPS systems have been explored as model protocells, especially over the last decade.

1.4.2. Compartments formed by LLPS

In 1930s, Alexander Oparin proposed the idea of formation of ‘coacervates’ as a result of liquid-liquid phase-separation of organic molecules, hypothesizing that this could have served as the first step towards the origin of life on the prebiotic Earth (Harrow 1938). Pertinently, it is such coacervation is thought to have resulted in the formation of first protocells, which would have kickstarted life on prebiotic Earth. But why would LLPS have formed the first protocells? It is their characteristic features detailed below that makes them an excellent system to be studied as a protocell model.

1.4.2.1. Characteristic features of Liquid-liquid phase-separated systems

a. **A mechanism to concentrate molecules:** As mentioned earlier, life is considered to have emerged in a dilute pool of chemicals, called primordial soup, wherein chemical reactions relevant to the origin of life are thought have occurred. However, since the pool is likely to have been dilute, certain prebiotically plausible mechanisms would have been required to concentrate the chemical molecules for the reactions to take place. In this context, LLPS is relevant as it allows for a range of molecules to get concentrated within (Poudyal et al. 2018).
b. **Ready diffusion of molecules:** One of the most important characteristics is their ability to allow for the exchange of molecules with the surroundings. Furthermore, they can facilitate molecular diffusion within the compartment as well. This property allows chemical reactions such as ribozyme catalysis, to occur readily within these compartments (Poudyal et al. 2018).
c. **Enhancement of reaction rates:** Due to the increased concentration of reactant molecules within the compartments, the rate of prebiotically plausible reactions in coacervates has been found to be higher than that in the bulk solution (Poudyal et al. 2018).

d. **Relevance to modern biology:** A modern cell contains many liquid-liquid phase-separated compartments, including nucleolus, P-bodies, stress granules, Cajal bodies. The constituents of these LLPS compartments predominantly include proteins and nucleic acids, which can facilitate multivalent interactions with other protein/RNA molecules in the surroundings. Furthermore, they can concentrate biomolecules and facilitate reactions between them (Keating 2012).

Thus, the aforementioned properties of coacervates make them a very pertinent system to be explored as protocell models. However, what causes organic molecules to undergo LLPS in the first place? Furthermore, can all molecules undergo phase separation? The following section answers these questions by delineating the molecular mechanism and types of LLPS.

1.4.2.2. Types of LLPS

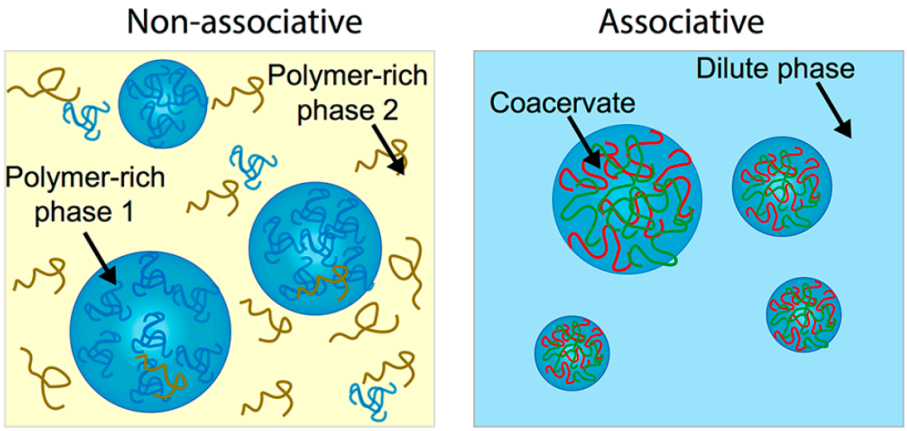

Figure 1.7: Types of LLPS. Figure reproduced from Poudyal, R.R., Pir Cakmak, F., Keating, C.D. and Bevilacqua, P.C., 2018. Physical principles and extant biology reveal roles for RNA-containing membraneless compartments in origins of life chemistry. *Biochemistry*, *57*(17), pp.2509-2519.

As shown in Figure 1.7, two types of LLPS systems exist, non-associative (segregative) and associative (Poudyal et al. 2018). When two polymers are mixed in a solution above a certain concentration, they can repel each other resulting in the formation of two separate phases, each rich in the individual polymer. This type of phase separation is termed as 'non-associative' or 'segregative' LLPS. Aqueous Two-Phase Systems (ATPS), like PEG-Dextran, is an example of segregative type of phase separation. On the other hand, when two polymers have attractive interactions between them, they come together and phase separate from the rest of the bulk solvent. Such phase separation is called as 'associative' LLPS.

Specifically, when the interacting molecules are oppositely charged, the associative phase separation is called as 'coacervation'. For example, when cationic polylysine is mixed with an anionic molecule like ATP above certain threshold concentrations, they phase separate from the bulk solution where the coacervate phase is rich in both the molecules. More often than not, the molecules which undergo phase separation are polymers having high molecular weight and/or multivalency, which ensures multiple interactions with other molecules in the surrounding. Thus, when such molecules come together above a certain threshold concentration, they spontaneously phase separate. This property makes LLPS a prebiotically plausible mechanism for the formation of protocells. In this context, how does one explore LLPS experimentally?

1.4.2.3. Experimental approaches to study LLPS

To study LLPS, the liquid-like nature of LLPS is tested by various parameters and techniques. For instance, when a phase separated mixture of two oppositely charged polyelectrolytes is placed on a glass slide, and visualized under a microscope, spherical entities, often termed as 'droplets', appear that are of various sizes. Thus, the first simple test to call a system a liquid-liquid phase-separated system, is to look for their spherical nature.

a. **Spherical nature:** It is the surface tension, a property that specifically applies to liquids, which makes the phase separated compartments appear in a spherical form. Thus, it is necessary to first check the appearance of spherical particles (droplets) under microscope (Hyman et al. 2014).
b. **Molecular diffusion:** In liquids, molecules are constantly undergoing random motion, a phenomenon called as Brownian motion. Now, if the phase-separated compartment shows liquid-like properties, it would also allow for random movement of molecules within itself and also between the compartment and the surrounding. This can be quantified by a technique called 'fluorescence recovery after photobleaching' or FRAP (Hyman et al. 2014; Alberti et al. 2019). Here, a fluorescently tagged molecule is first encapsulated into the droplets, and then a small area within the droplet (or sometimes a whole droplet) is bleached by using high power lasers in a confocal microscope set-up. If the compartment allows molecular diffusion within itself, then the bleached area will recover fluorescence as a result of the diffusion of unbleached fluorescent molecules from the rest of the droplet into the bleached spot. When a small area within the droplet is bleached, it is called as partial FRAP,

whereas, when the entire droplet is bleached, it is called as full FRAP. Thus, characterization of a novel LLPS system, often involves examining the recovery of fluorescence in droplets having encapsulated a fluorescently tagged biomolecule (RNA/protein).

c. **Coalescence:** Coalescence refers to the merging of two or more phase separated droplets to form a single large droplet (Alberti et al. 2019). Surface tension, a property which works to reduce the surface area of the liquid, is what drives coalescence. The surface of a single large droplet is more when compared to that of two small droplets. This process ensures reduction in the overall energy of the system. Furthermore, concentration gradients of solutes across various droplets are also thought to drive coalescence to favor equal distribution of solutes within the droplets. In all, the underlying properties of liquids is what mainly drives coalescence.

1.4.2.4. Prebiotically plausible reactions in LLPS systems

The interior of LLPS droplets enables macromolecular crowding, which results in enhanced concentration of the solute molecules within the droplet when compared to the bulk solution (Keating 2012; Hyman et al. 2014). To study a particular LLPS system as a protocell model, one of the major emphases is given on the ability of the system to sequester molecule and carry out prebiotically relevant reactions. Particularly, emphasis has been on RNA-based molecules, to carry out reactions pertinent to the RNA World hypothesis. In this context, a notable enhancement in the concentration of RNA relative to the bulk solution (~10,000 fold), was observed within the droplets composed of polyamines and nucleotides (Frankel et al. 2016). Furthermore, it was found that longer RNAs sequester better than the shorter ones (Drobot et al. 2018). Similar trend was observed with peptides as well (Aumiller et al. 2016).

To carry out reactions such as template-directed RNA replication and ribozyme catalysis, divalent cations are used as they play a crucial role. Towards this, a coacervate system composed of polyamine/nucleotides was found to show a remarkable increase in the concentration of encapsulated Mg^{2+} (~300 fold) and nucleotides (~1500 fold) (Frankel et al. 2016). Besides the aforementioned molecules, a prebiotically relevant metabolite, porphyrin, was shown to be getting sequestered into a coacervate system composed of polylysine and ATP (Koga et al. 2011). Partitioning of solutes into the droplets occurs as a result of interaction of the solutes with the components of the droplets. In this context, the type of interactions that are at play are electrostatic, π-π stacking, van der Waal's and hydrophobic interactions (Ghosh et al. 2021).

Polylysine/ATP coacervates, for instance, showed preferential partitioning of anionic solutes over cationic ones. This is mainly due to the favorable electrostatic interactions between the anionic solutes with the cationic component of coacervates, i.e. polylysine (Koga et al. 2011). Likewise, coacervates containing polyU RNA as one of the components were shown to sequester polyA RNA molecules better than polyU RNA (Poudyal et al. 2018). Moreover, in the PEG/dextran ATPS, denatured proteins partitioned into the PEG rich phase, while the native proteins partitioned into the dextran rich phase (Dominak et al. 2010). Interestingly, such events would have created different protocell populations with compositionally distinct components, thereby, encapsulating chemically diverse molecules. This scenario has been argued to be crucial for systems chemistry type reactions (Ashkenasy et al. 2017, 2023).

Since solutes were found to be concentrated more by orders of magnitude in the LLPS compartments when compared to the bulk solution, it is imperative to ask whether these compartments could also facilitate reactions within them. In this context, template-directed nonenzymatic replication reaction and ribozyme catalysis have been demonstrated in LLPS-based protocells (Poudyal et al. 2018, 2019). Specifically, the yield of the product varied with the composition of coacervates, suggesting an additional significance of the coacervate's chemical composition on the reaction rates (Poudyal et al. 2019). Furthermore, when ribozyme catalysis was carried out in PEG/dextran ATPS, the reaction rate was found to be enhanced by ~70 fold (Strulson et al. 2012; Poudyal et al. 2018). This increase in the reaction rate was attributed to the enhanced concentration and folding of ribozyme in the dextran rich phase.

Interestingly, the polylysine/nucleotide coacervates were shown to compartmentalize and facilitate reactions pertinent to metabolism such as those involving hexokinase and glucose-6-phosphatase (Koga et al. 2011). Moreover, in the context of metabolic reactions, the polyarginine/anionic metabolite coacervate system was found to be facilitating reactions such as the conversion of malonate to 3-carboxymalate and the nonenzymatic oxidation of NADH (Smokers et al. 2022). In all, as proposed by Alexander Oparin back in the 1930s, LLPS systems composed of organic polymers could indeed have acted as model protocells by concentrating prebiotically relevant molecules in the prebiotic soup, and thereby enhancing the rates of prebiotically relevant reactions.

Apart from forming prebiotically relevant compartments, research on LLPS has strong overlaps with bottom-up synthetic biology research that, aims to build life-like systems from simplistic chemical components (Das et al. 2024a). In this context, one of the main goals is to construct

artificial cells that mimic certain cellular functions. Artificial cells not only help understand how living systems could have arisen from non-living matter, but they also offer promising applications in the field of biotechnology and medicine, bridging the gap between fundamental research and its real-world applications. In this context, we investigated a mixed amphiphile-based LLPS system (Chapter 4) that can form under prebiotically plausible conditions, sequester biomolecules, and facilitate chemical reactions, highlighting its potential as a model protocell. However, its capability to function as an artificial cell remains to be explored. Future studies could focus on examining how physicochemical properties affect reaction rates within these compartments, as well as on tuning the physicochemical properties that could enable the development of such LLPS-based drug delivery systems.

Although LLPS-based compartments show intriguing properties, such as molecular sequestration and facilitation of chemical reactions with enhanced reaction rates, they have some fundamental drawbacks. A major drawback is their inherent property to undergo coalescence or form crystals over time (Spruijt 2023). To circumvent this problem, researchers have begun to investigate the properties and applications of 'hybrid protocells', where, lipid bilayers are being used to surround the LLPS droplets, resulting in agglomerates that could embody the advantages inherent in the two parent systems (Dora Tang et al. 2014; Lu et al. 2023; Das et al. 2024b). A design like this has the potential to facilitate macromolecular crowding and enhancement of reaction rates, while the presence of bilayer could avert coalescence of coacervate droplets preventing the loss of their individuality.

1.5. References

1. Alberti S, Gladfelter A, Mittag T (2019) Considerations and Challenges in Studying Liquid-Liquid Phase Separation and Biomolecular Condensates. Cell 176:419–434. https://doi.org/10.1016/j.cell.2018.12.035

2. Apel CL, Deamer DW, Mautner MN (2002) Self-assembled vesicles of monocarboxylic acids and alcohols: conditions for stability and for the encapsulation of biopolymers. Biochimica et Biophysica Acta (BBA) - Biomembranes 1559:1–9. https://doi.org/10.1016/S0005-2736(01)00400-X

3. Ashkenasy G, Kauffman S, Lancet D, et al (2023) Collectively autocatalytic sets. CR-PHYS-SC 4:. https://doi.org/10.1016/j.xcrp.2023.101594

4. Ashkenasy G, M. Hermans T, Otto S, F. Taylor A (2017) Systems chemistry. Chemical Society Reviews 46:2543–2554. https://doi.org/10.1039/C7CS00117G

5. Aumiller WM, Pir Cakmak F, Davis BW, Keating CD (2016) RNA-Based Coacervates as a Model for Membraneless Organelles: Formation, Properties, and Interfacial Liposome Assembly. Langmuir 32:10042–10053. https://doi.org/10.1021/acs.langmuir.6b02499

6. Bartel DP, Szostak JW (1993) Isolation of New Ribozymes from a Large Pool of Random Sequences. Science 261:1411–1418. https://doi.org/10.1126/science.7690155

7. Blain JC, Szostak JW (2014) Progress Toward Synthetic Cells. Annu Rev Biochem 83:615–640. https://doi.org/10.1146/annurev-biochem-080411-124036

8. Burcar B, Pasek M, Gull M, et al (2016) Darwin's Warm Little Pond: A One-Pot Reaction for Prebiotic Phosphorylation and the Mobilization of Phosphate from Minerals in a Urea-Based Solvent. Angewandte Chemie International Edition 55:13249–13253. https://doi.org/10.1002/anie.201606239

9. Costanzo G, Pino S, Ciciriello F, Mauro ED (2009) Generation of Long RNA Chains in Water *. Journal of Biological Chemistry 284:33206–33216. https://doi.org/10.1074/jbc.M109.041905

10. Costanzo G, Pino S, Timperio AM, et al (2016) Non-Enzymatic Oligomerization of 3', 5' Cyclic AMP. PLOS ONE 11:e0165723. https://doi.org/10.1371/journal.pone.0165723

11. Dagar S, Sarkar S, Rajamani S (2020) Geochemical influences on nonenzymatic oligomerization of prebiotically relevant cyclic nucleotides. RNA 26:756–769. https://doi.org/10.1261/rna.074302.119

12. Damer B, Deamer D (2015) Coupled Phases and Combinatorial Selection in Fluctuating Hydrothermal Pools: A Scenario to Guide Experimental Approaches to the Origin of Cellular Life. Life 5:872–887. https://doi.org/10.3390/life5010872

13. Damiano L, Luisi PL (2010) Towards an Autopoietic Redefinition of Life. Orig Life Evol Biosph 40:145–149. https://doi.org/10.1007/s11084-010-9193-2

14. Das S, Patki GM, Sridhar V, et al (2024a) Compartmentalization as a ubiquitous feature of life: from origins of life to biomimetics. Eur Phys J Spec Top. https://doi.org/10.1140/epjs/s11734-024-01203-5

15. Das S, Patki GM, Sridhar V, et al (2024b) Compartmentalization as a ubiquitous feature of life: from origins of life to biomimetics. Eur Phys J Spec Top. https://doi.org/10.1140/epjs/s11734-024-01203-5

16. Deamer DW (1985) Boundary structures are formed by organic components of the Murchison carbonaceous chondrite. Nature 317:792–794. https://doi.org/10.1038/317792a0

17. Domagal-Goldman SD, Wright KE, Domagal-Goldman SD, et al (2016) The Astrobiology Primer v2.0. Astrobiology 16:561–653. https://doi.org/10.1089/ast.2015.1460

18. Dominak LM, Gundermann EL, Keating CD (2010) Microcompartmentation in Artificial Cells: pH-Induced Conformational Changes Alter Protein Localization. Langmuir 26:5697–5705. https://doi.org/10.1021/la903800e

19. Dora Tang T-Y, Rohaida Che Hak C, Thompson AJ, et al (2014) Fatty acid membrane assembly on coacervate microdroplets as a step towards a hybrid protocell model. Nature Chem 6:527–533. https://doi.org/10.1038/nchem.1921

20. Drobot B, Iglesias-Artola JM, Le Vay K, et al (2018) Compartmentalised RNA catalysis in membrane-free coacervate protocells. Nat Commun 9:3643. https://doi.org/10.1038/s41467-018-06072-w

21. Ekland EH, Bartel DP (1996) RNA-catalysed RNA polymerization using nucleoside triphosphates. Nature 382:373–376. https://doi.org/10.1038/382373a0

22. Ferris JP, Sanchez RA, Orgel LE (1968) Studies in prebiotic synthesis: III. Synthesis of pyrimidines from cyanoacetylene and cyanate. Journal of Molecular Biology 33:693–704. https://doi.org/10.1016/0022-2836(68)90314-8

23. Ferris JP, Zamek OS, Altbuch AM, Freiman H (1974) Chemial evolution. J Mol Evol 3:301–309. https://doi.org/10.1007/BF01796045

24. Frankel EA, Bevilacqua PC, Keating CD (2016) Polyamine/Nucleotide Coacervates Provide Strong Compartmentalization of Mg^{2+} , Nucleotides, and RNA. Langmuir 32:2041–2049. https://doi.org/10.1021/acs.langmuir.5b04462

25. Frenkel-Pinter M, Samanta M, Ashkenasy G, Leman LJ (2020) Prebiotic Peptides: Molecular Hubs in the Origin of Life. Chem Rev 120:4707–4765. https://doi.org/10.1021/acs.chemrev.9b00664

26. Fuller WD, Sanchez RA, Orgel LE (1972) Studies in prebiotic synthesis. VII. J Mol Evol 1:249–257. https://doi.org/10.1007/BF01660244

27. Gebicki JM, Hicks M (1973) Ufasomes are Stable Particles surrounded by Unsaturated Fatty Acid Membranes. Nature 243:232–234. https://doi.org/10.1038/243232a0

28. Ghosh B, Bose R, Tang T-YD (2021) Can coacervation unify disparate hypotheses in the origin of cellular life? Current Opinion in Colloid & Interface Science 52:101415. https://doi.org/10.1016/j.cocis.2020.101415

29. Gibard C, Bhowmik S, Karki M, et al (2018) Phosphorylation, Oligomerization and Self-assembly in Water Under Potential Prebiotic Conditions. Nat Chem 10:212–217. https://doi.org/10.1038/nchem.2878

30. Gilbert W (1986) Origin of life: The RNA world. Nature 319:618–618. https://doi.org/10.1038/319618a0

31. Harayama T, Riezman H (2018) Understanding the diversity of membrane lipid composition. Nat Rev Mol Cell Biol 19:281–296. https://doi.org/10.1038/nrm.2017.138

32. Harrow B (1938) The Origin of Life: The Origin of Life. By A. I. Oparin. Translated by Sergius Morgulis. Macmillan, 1938. Science 88:58–58. https://doi.org/10.1126/science.88.2272.58.a

33. Huber C, Wächtershäuser G (1997) Activated Acetic Acid by Carbon Fixation on (Fe,Ni)S Under Primordial Conditions. Science 276:245–247. https://doi.org/10.1126/science.276.5310.245

34. Hyman AA, Weber CA, Jülicher F (2014) Liquid-Liquid Phase Separation in Biology. Annu Rev Cell Dev Biol 30:39–58. https://doi.org/10.1146/annurev-cellbio-100913-013325

35. Inoue T, Orgel LE (1981) Substituent control of the poly(C)-directed oligomerization of guanosine 5'-phosphoroimidazolide. J Am Chem Soc 103:7666–7667. https://doi.org/10.1021/ja00415a051

36. Johnston WK, Unrau PJ, Lawrence MS, et al (2001) RNA-Catalyzed RNA Polymerization: Accurate and General RNA-Templated Primer Extension. Science 292:1319–1325. https://doi.org/10.1126/science.1060786

37. Joshi MP, Sawant AA, Rajamani S (2021) Spontaneous emergence of membrane-forming protoamphiphiles from a lipid–amino acid mixture under wet–dry cycles. Chem Sci 12:2970–2978. https://doi.org/10.1039/D0SC05650B

38. Joshi MP, Uday A, Rajamani S (2022) Elucidating N-acyl amino acids as a model protoamphiphilic system. Commun Chem 5:147. https://doi.org/10.1038/s42004-022-00762-9

39. Joyce GF, Szostak JW (2018) Protocells and RNA Self-Replication. Cold Spring Harb Perspect Biol 10:a034801. https://doi.org/10.1101/cshperspect.a034801

40. Kanavarioti A, Monnard PA, Deamer DW (2001) Eutectic phases in ice facilitate nonenzymatic nucleic acid synthesis. Astrobiology 1:271–281. https://doi.org/10.1089/15311070152757465

41. Keating CD (2012) Aqueous Phase Separation as a Possible Route to Compartmentalization of Biological Molecules. Acc Chem Res 45:2114–2124. https://doi.org/10.1021/ar200294y

42. Koga S, Williams DS, Perriman AW, Mann S (2011) Peptide–nucleotide microdroplets as a step towards a membrane-free protocell model. Nature Chem 3:720–724. https://doi.org/10.1038/nchem.1110

43. Krishnamurthy R (2017) Giving Rise to Life: Transition from Prebiotic Chemistry to Protobiology. Acc Chem Res 50:455–459. https://doi.org/10.1021/acs.accounts.6b00470

44. Krishnamurthy R, Liotta CL (2023) The potential of glyoxylate as a prebiotic source molecule and a reactant in protometabolic pathways—The glyoxylose reaction. Chem 9:784–797. https://doi.org/10.1016/j.chempr.2023.03.007

45. Leslie E. O (2004) Prebiotic Chemistry and the Origin of the RNA World. Critical Reviews in Biochemistry and Molecular Biology 39:99–123. https://doi.org/10.1080/10409230490460765

46. Lohrmann R (1977) Formation of nucleoside 5′-phosphoramidates under potentially prebiological conditions. J Mol Evol 10:137–154. https://doi.org/10.1007/BF01751807

47. Lohrmann R, Orgel LE (1973) Prebiotic Activation Processes. Nature 244:418–420. https://doi.org/10.1038/244418a0

48. Lohrmann R, Orgel LE (1971) Urea-Inorganic Phosphate Mixtures as Prebiotic Phosphorylating Agents. Science 171:490–494. https://doi.org/10.1126/science.171.3970.490

49. Lu T, Javed S, Bonfio C, Spruijt E (2023) Interfacing Coacervates with Membranes: From Artificial Organelles and Hybrid Protocells to Intracellular Delivery. Small Methods 7:2300294. https://doi.org/10.1002/smtd.202300294

50. Majerfeld I, Puthenvedu D, Yarus M (2016) Cross-backbone templating; ribodinucleotides made on poly(C). RNA 22:397–407. https://doi.org/10.1261/rna.054866.115

51. Mansy SS, Schrum JP, Krishnamurthy M, et al (2008) Template-directed synthesis of a genetic polymer in a model protocell. Nature 454:122–125. https://doi.org/10.1038/nature07018

52. McCollom TM, Ritter G, Simoneit BRT (1999) Lipid Synthesis Under Hydrothermal Conditions by Fischer- Tropsch-Type Reactions. Orig Life Evol Biosph 29:153–166. https://doi.org/10.1023/A:1006592502746

53. Miller SL (1953) A Production of Amino Acids Under Possible Primitive Earth Conditions. Science 117:528–529. https://doi.org/10.1126/science.117.3046.528

54. Miyakawa S, Cleaves HJ, Miller SL (2002a) The Cold Origin of Life: B. Implications Based on Pyrimidines and Purines Produced From Frozen Ammonium Cyanide Solutions. Orig Life Evol Biosph 32:209–218. https://doi.org/10.1023/A:1019514022822

55. Miyakawa S, James Cleaves H, Miller SL (2002b) The Cold Origin of Life: A. Implications Based On The Hydrolytic Stabilities Of Hydrogen Cyanide And Formamide. Orig Life Evol Biosph 32:195–208. https://doi.org/10.1023/A:1016514305984

56. Monnard P-A, Walde P (2015) Current Ideas about Prebiological Compartmentalization. Life 5:1239–1263. https://doi.org/10.3390/life5021239

57. Morigaki K, Walde P (2007) Fatty acid vesicles. Current Opinion in Colloid & Interface Science 12:75–80. https://doi.org/10.1016/j.cocis.2007.05.005

58. Morowitz HJ, Kostelnik JD, Yang J, Cody GD (2000) The origin of intermediary metabolism. Proceedings of the National Academy of Sciences 97:7704–7708. https://doi.org/10.1073/pnas.110153997

59. Muchowska KB, Varma SJ, Chevallot-Beroux E, et al (2017) Metals promote sequences of the reverse Krebs cycle. Nat Ecol Evol 1:1716–1721. https://doi.org/10.1038/s41559-017-0311-7

60. Ninio J, Orgel LE (1978) Heteropolynucleotides as templates for non-enzymatic polymerizations. J Mol Evol 12:91–99. https://doi.org/10.1007/BF01733260

61. O'Flaherty DK, Zhou L, Szostak JW (2019) Nonenzymatic Template-Directed Synthesis of Mixed-Sequence 3′-NP-DNA up to 25 Nucleotides Long Inside Model Protocells. J Am Chem Soc 141:10481–10488. https://doi.org/10.1021/jacs.9b04858

62. Oró J, Kimball AP (1961) Synthesis of purines under possible primitive earth conditions. I. Adenine from hydrogen cyanide. Archives of Biochemistry and Biophysics 94:217–227. https://doi.org/10.1016/0003-9861(61)90033-9

63. Paul N, Joyce GF (2002) A self-replicating ligase ribozyme. Proceedings of the National Academy of Sciences 99:12733–12740. https://doi.org/10.1073/pnas.202471099

64. Poudyal RR, Guth-Metzler RM, Veenis AJ, et al (2019) Template-directed RNA polymerization and enhanced ribozyme catalysis inside membraneless compartments formed by coacervates. Nat Commun 10:490. https://doi.org/10.1038/s41467-019-08353-4

65. Poudyal RR, Pir Cakmak F, Keating CD, Bevilacqua PC (2018) Physical Principles and Extant Biology Reveal Roles for RNA-Containing Membraneless Compartments in Origins of Life Chemistry. Biochemistry 57:2509–2519. https://doi.org/10.1021/acs.biochem.8b00081

66. Powner MW, Gerland B, Sutherland JD (2009) Synthesis of activated pyrimidine ribonucleotides in prebiotically plausible conditions. Nature 459:239–242. https://doi.org/10.1038/nature08013

67. Pressman A, Blanco C, Chen IA (2015) The RNA World as a Model System to Study the Origin of Life. Current Biology 25:R953–R963. https://doi.org/10.1016/j.cub.2015.06.016

68. Puthenvedu D, Janas T, Majerfeld I, et al (2015) Poly(U) RNA-templated synthesis of AppA. RNA 21:1818–1825. https://doi.org/10.1261/rna.052696.115

69. Puthenvedu D, Majerfeld I, Yarus M (2018) Non-Watson–Crick RNA synthesis suited to origin functions. RNA 24:90–97. https://doi.org/10.1261/rna.063974.117

70. Rajamani S, Vlassov A, Benner S, et al (2008) Lipid-assisted Synthesis of RNA-like Polymers from Mononucleotides. Orig Life Evol Biosph 38:57–74. https://doi.org/10.1007/s11084-007-9113-2

71. Robertson MP, Joyce GF (2012) The origins of the RNA world. Cold Spring Harb Perspect Biol 4:a003608. https://doi.org/10.1101/cshperspect.a003608

72. Robertson MP, Miller SL (1995) An efficient prebiotic synthesis of cytosine and uracil. Nature 375:772–774. https://doi.org/10.1038/375772a0

73. Rogers J, Joyce GF (2001) The effect of cytidine on the structure and function of an RNA ligase ribozyme. RNA 7:395–404. https://doi.org/10.1017/S135583820100228X

74. Ruiz-Mirazo K, Briones C, de la Escosura A (2014) Prebiotic Systems Chemistry: New Perspectives for the Origins of Life. Chem Rev 114:285–366. https://doi.org/10.1021/cr2004844

75. Rushdi AI, Simoneit BRT (2001) Lipid Formation by Aqueous Fischer-Tropsch-Type Synthesis over a Temperature Range of 100 to 400 °C. Orig Life Evol Biosph 31:103–118. https://doi.org/10.1023/A:1006702503954

76. Saladino R, Crestini C, Ciciriello F, et al (2009) From formamide to RNA: the roles of formamide and water in the evolution of chemical information. Research in Microbiology 160:441–448. https://doi.org/10.1016/j.resmic.2009.06.001

77. Sanchez RA, Orgel LE (1970) Studies in prebiotic synthesis: V. Synthesis and photoanomerization of pyrimidine nucleosides. Journal of Molecular Biology 47:531–543. https://doi.org/10.1016/0022-2836(70)90320-7

78. Sarkar S, Das S, Dagar S, et al (2020) Prebiological Membranes and Their Role in the Emergence of Early Cellular Life. J Membrane Biol 253:589–608. https://doi.org/10.1007/s00232-020-00155-w

79. Sawai H (1976) Catalysis of internucleotide bond formation by divalent metal ions. J Am Chem Soc 98:7037–7039. https://doi.org/10.1021/ja00438a050

80. Sawai H, Orgel LE (1975) Oligonucleotide synthesis catalyzed by the zinc(2+) ion. J Am Chem Soc 97:3532–3533. https://doi.org/10.1021/ja00845a050

81. Schrum JP, Ricardo A, Krishnamurthy M, et al (2009) Efficient and Rapid Template-Directed Nucleic Acid Copying Using 2′-Amino-2′,3′-dideoxyribonucleoside−5′-Phosphorimidazolide Monomers. J Am Chem Soc 131:14560–14570. https://doi.org/10.1021/ja906557v

82. Schrum JP, Zhu TF, Szostak JW (2010) The origins of cellular life. Cold Spring Harb Perspect Biol 2:a002212. https://doi.org/10.1101/cshperspect.a002212

83. Segré D, Ben-Eli D, Deamer DW, Lancet D (2001) The Lipid World. Orig Life Evol Biosph 31:119–145. https://doi.org/10.1023/A:1006746807104

84. Smets BF, Barkay T (2005) Horizontal gene transfer: perspectives at a crossroads of scientific disciplines. Nature Reviews Microbiology 3:675–678. https://doi.org/10.1038/nrmicro1253

85. Smokers IBA, van Haren MHI, Lu T, Spruijt E (2022) Complex Coacervation and Compartmentalized Conversion of Prebiotically Relevant Metabolites**. ChemSystemsChem 4:e202200004. https://doi.org/10.1002/syst.202200004

86. Sohlenkamp C, Geiger O (2016) Bacterial membrane lipids: diversity in structures and pathways. FEMS Microbiol Rev 40:133–159. https://doi.org/10.1093/femsre/fuv008

87. Spruijt E (2023) Open questions on liquid–liquid phase separation. Commun Chem 6:23. https://doi.org/10.1038/s42004-023-00823-7

88. Strulson CA, Molden RC, Keating CD, Bevilacqua PC (2012) RNA catalysis through compartmentalization. Nature Chem 4:941–946. https://doi.org/10.1038/nchem.1466

89. Stütz JAR, Kervio E, Deck C, Richert C (2007) Chemical Primer Extension: Individual Steps of Spontaneous Replication. Chemistry & Biodiversity 4:784–802. https://doi.org/10.1002/cbdv.200790064

90. Sulston J, Lohrmann R, Orgel LE, et al (1969) Non-enzymic oligonucleotide synthesis on a polycytidylate template. Journal of Molecular Biology 40:227–234. https://doi.org/10.1016/0022-2836(69)90471-9

91. Sulston J, Lohrmann R, Orgel LE, Miles HT (1968) Nonenzymatic synthesis of oligoadenylates on a polyuridylic acid template. Proceedings of the National Academy of Sciences 59:726–733. https://doi.org/10.1073/pnas.59.3.726

92. Trefil J, Morowitz H, Smith E (2009) The Origin of Life. Am Sci 97:206. https://doi.org/10.1511/2009.78.206

93. Urata H, Fujimori M, Aono C, et al (2008) Regio- and diastereo-selectivity of montmorillonite-catalyzed oligomerization of racemic adenosine 5'-phosphorimidazolide. Nucleosides Nucleotides Nucleic Acids 27:421–430. https://doi.org/10.1080/15257770801954955

94. Verlander MS, Lohrmann R, Orgel LE (1973) Catalysts for the self-polymerization of adenosine cyclic 2′,3′-phosphate. J Mol Evol 2:303–316. https://doi.org/10.1007/BF01654098

95. Verlander MS, Orgel LE (1974) Analysis of high molecular weight material from the polymerization of adenosine cyclic 2′, 3′-phosphate. J Mol Evol 3:115–120. https://doi.org/10.1007/BF01796557

96. Vogel SR, Deck C, Richert C (2005) Accelerating chemical replication steps of RNA involving activated ribonucleotides and downstream-binding elements. Chem Commun 4922–4924. https://doi.org/10.1039/B510775J

97. Wächtershäuser G (1990) Evolution of the first metabolic cycles. Proceedings of the National Academy of Sciences 87:200–204. https://doi.org/10.1073/pnas.87.1.200

98. Wächtershäuser G (1988) Before enzymes and templates: theory of surface metabolism. Microbiol Rev 52:452–484. https://doi.org/10.1128/mr.52.4.452-484.1988

99. Walton T, Szostak JW (2016) A Highly Reactive Imidazolium-Bridged Dinucleotide Intermediate in Nonenzymatic RNA Primer Extension. J Am Chem Soc 138:11996–12002. https://doi.org/10.1021/jacs.6b07977

100. Wochner A, Attwater J, Coulson A, Holliger P (2011) Ribozyme-Catalyzed Transcription of an Active Ribozyme. Science 332:209–212. https://doi.org/10.1126/science.1200752

101. Wu T, Orgel LE (1992a) Nonenzymatic template-directed synthesis on hairpin oligonucleotides. 3. Incorporation of adenosine and uridine residues. J Am Chem Soc 114:7963–7969. https://doi.org/10.1021/ja00047a001

102. Wu T, Orgel LE (1992b) Nonenzymic template-directed synthesis on hairpin oligonucleotides. 2. Templates containing cytidine and guanosine residues. J Am Chem Soc 114:5496–5501. https://doi.org/10.1021/ja00040a002

103. Wu T, Orgel LE (1992c) Nonenzymic template-directed synthesis on oligodeoxycytidylate sequences in hairpin oligonucleotides. J Am Chem Soc 114:317–322. https://doi.org/10.1021/ja00027a040

104. Zagorevskii DV, Aldersley MF, Ferris JP (2006) MALDI analysis of oligonucleotides directly from montmorillonite. The official journal of The American Society for Mass Spectrometry 17:1265–1270. https://doi.org/10.1016/j.jasms.2006.05.012

105. Zaher HS, Unrau PJ (2007) Selection of an improved RNA polymerase ribozyme with superior extension and fidelity. RNA 13:1017–1026. https://doi.org/10.1261/rna.548807

106. Zhang W, Tam CP, Walton T, et al (2017) Insight into the mechanism of nonenzymatic RNA primer extension from the structure of an RNA-GpppG complex. Proceedings of the National Academy of Sciences 114:7659–7664. https://doi.org/10.1073/pnas.1704006114

107. Zhou L, O'Flaherty DK, Szostak JW (2020) Template-Directed Copying of RNA by Non-enzymatic Ligation. Angewandte Chemie International Edition 59:15682–15687. https://doi.org/10.1002/anie.202004934

108. Zielinski WS, Orgel LE (1987) Oligoaminudeoside phosphoramidates. Oligomeilzation of dimers of 3′-amino-3′-deoxy-nucleotides (GC and CG) in aqueous solution. Nucleic Acids Research 15:1699–1715. https://doi.org/10.1093/nar/15.4.1699

109. Zielinski WS, Orgel LE (1985) Oligomerization of activated derivatives of 3′-amino-3′-deoxyguanosine on poly(C) and poly(dC) templates. Nucleic Acids Research 13:2469–2484. https://doi.org/10.1093/nar/13.7.2469

Chapter 2

PURPOSE AND RATIONALE FOR THE STUDY

2.1.Exploring the implications of heterogeneity of prebiotic soup on prebiotic reactions

Prebiotic soup or primordial soup is thought to have constituted a wide variety of chemicals. Thus, all the potential processes that are proposed to have kickstarted life on the prebiotic Earth, including nonenzymatic RNA oligomerization and replication, ribozyme catalysis, metabolic reactions and compartmentalization, would have occurred in a chemically heterogenous environment as depicted in Figure 2.1 (Bapat 2018). However, the effect of the prebiotic soup's complexity on these processes has remained largely unexplored.

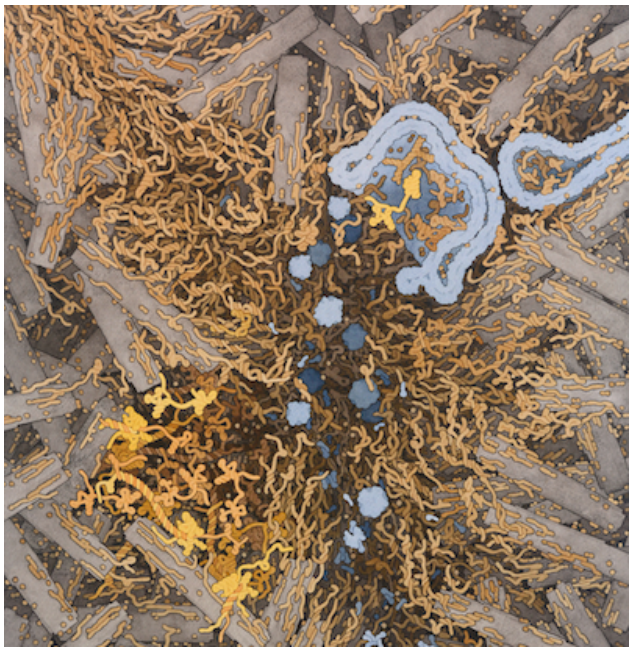

Figure 2.1. Abiogenesis. The illustration depicts the emergence and encapsulation of functional ribozymes (bright yellow strands) from a pool of RNA oligomers of varying lengths (shown in tan). Furthermore, it depicts the idea of compartmentalization, where membrane forming entities enter at the bottom of the picture and assemble into membranes, compartmentalizing the genetic material. Figure reproduced from RCSB Protein Data Bank. doi: 10.2210/rcsb_pdb/goodsell-gallery-034.

2.1.1. Implications of prebiotic soup's heterogeneity for nonenzymatic template-directed RNA replication

Nonenzymatic RNA replication is considered to have been a crucial step during the course of the origin of life. Even though these reactions have been explored extensively; they were mainly carried out in lab-controlled buffered conditions. In this backdrop, a recent study explored the role of co-solutes on nonenzymatic RNA replication, which demonstrated the effect of co-solutes on nonenzymatic template-directed RNA replication (Bapat and Rajamani

2015). The study used two co-solutes- PEG and DLPC vesicles. PEG was used as a proxy for facilitating macromolecular crowding that might have been possible in certain niches on the early Earth, as macromolecular crowding is known to significantly alter reaction rates. Additionally, phospholipid vesicles were used because they were likely present in the prebiotic environment as a relevant co-solute that result in higher order membrane structures.

Interestingly, it was observed that in the presence of the aforementioned co-solutes, the rate of incorporation of purine nucleotides against pyrimidine templating bases was reduced significantly. As the effect was found to be more pronounced in purines than pyrimidines, it was hypothesized to be stemming from the better stacking efficiency of purines than pyrimidines, which is thought to be have resulted in the lesser availability of purine monomers for the reaction to occur. This study, which was the first to look at the effect of co-solutes on nonenzymatic RNA replication, motivated us to further explore the prebiotically plausible chemical space and understand the effect of potential co-solutes on nonenzymatic RNA replication.

In this backdrop, we decided to study the effect of 'spent' nucleotides on nonenzymatic RNA replication. Nonenzymatic RNA replication is often studied using imidazole-activated nucleotides, which are chemically unstable, and thus, quickly undergo hydrolysis to form NMPs. The NMPs are called as 'spent' nucleotides that can still base-pair with the templating bases but cannot extend the primer on their own due to the lack of a good leaving group (Deck et al. 2011). Moreover, due to their base-pairing capacity, they are shown to inhibit the access of the incoming activated nucleotides to the templating bases (Deck et al. 2011). The NMPs are thought to have been present in the prebiotic soup as a result of their synthesis or hydrolysis of the activated nucleotides, making them potential co-solutes for the prebiotic reactions (Leslie E. 2004).

In modern biology, enzymes incorporate the correct nucleotide against a templating base from a mixture of all the four nucleotides. Thus, in the absence of any sophisticated enzymatic machinery, it is imperative to ask how the presence of a mixture of all the four spent nucleotides (AMP, GMP, CMP, UMP) as co-solutes, would have affected the process of nonenzymatic RNA replication. In this context, we found that the rate of the reaction is pronouncedly affected with the addition of the mixture of spent nucleotides, signifying the effect of co-solutes on nonenzymatic RNA replication. The detailed results of this study are discussed in Chapter 3.

2.1.2. Implications of prebiotic soup's heterogeneity for the formation of robust LLPS-based compartments

Prebiotic soup is thought to have had variable pHs and temperatures in addition to high concentrations of salts. Therefore, those protocellular compartments that would have remained stable across these conditions would have had a better chance to thrive than the others that were not inherently suited to do so. In the context of understanding the stability of model protocells under various prebiotically plausible selection pressures, fatty acid-based vesicular protocell systems have been much more explored than LLPS-based protocellular systems.

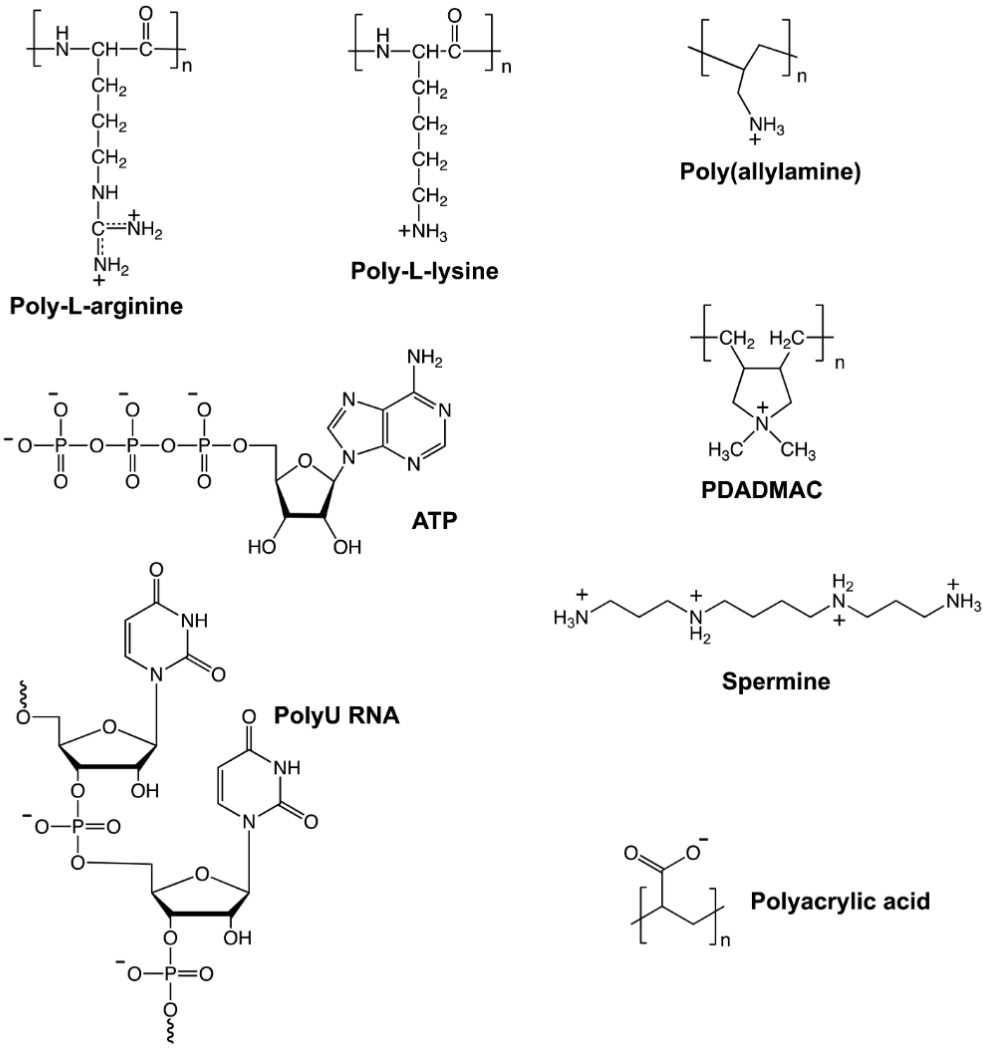

Figure 2.2. Molecules explored for studying the associative LLPS. Figure reproduced from Figure reproduced from Poudyal, R.R., Pir Cakmak, F., Keating, C.D. and Bevilacqua, P.C., 2018. Physical principles and extant biology reveal roles for RNA-containing membraneless compartments in origins of life chemistry. *Biochemistry*, *57*(17), pp.2509-2519.

Additionally, the prebiotic availability of a majority of polymers used to study LLPS-based protocellular systems (Poudyal et al. 2018) is questionable, especially the associative type that are shown in Figure 2.2. Thus, it is imperative to explore simpler and more prebiotically relevant LLPS-based protocellular systems, which can tolerate the aforementioned prebiotically pertinent selection pressures.

In this context, a recent study developed a simpler LLPS-based protocellular system composed of a short chain fatty acid, decanoic acid (Zhou et al. 2022). The work showed that decanoic acid vesicles can transition into coacervates upon the addition of a small molecule, dopamine. Furthermore, the coacervates were shown to partition a variety of dyes. However, the partitioning of the anionic dye was poorer when compared to cationic and hydrophobic dyes, suggesting that the interior of the coacervates may be hydrophobic and/or anionic. Thus, the partitioning of RNA into these coacervates could be a challenge. Moreover, the coacervate droplets could form only at pH 7.5 and did not remain stable for more than 1 hr.

The idea of utilizing short chain fatty acids to make coacervates is extremely intriguing as they are thought to have been readily available on the early Earth (McCollom et al. 1999; Rushdi and Simoneit 2001). Nevertheless, vesicles composed of short chain fatty acids are much less studied than those made of long chain fatty acids as protocellular systems, including for important thermodynamic constraints. In this light, we were motivated to study other short chain fatty acids other than decanoic acid, to see if they can form coacervates. Interestingly, we observed these systems to be forming coacervates. Amongst these, we characterized the one composed of nonanoic acid (C9-fatty acid), since it has been minimally explored as vesicles and, to the best of our knowledge, not explored as a constituent of coacervates.

Next, we wondered how the chemical heterogeneity of the prebiotic soup could impinge on the robustness of the coacervates. For this, we prepared a compositionally heterogenous mixed amphiphile-based coacervate system, as the prebiotic soup is thought to have contained a mixture of amphiphiles, especially the shorter chain length ones. It was found that the mixed amphiphile-based coacervates were stable across a broader range of pHs when compared to the pure nonanoic acid-based coacervates. Furthermore, it was found that this mixed amphiphile-based coacervate system could remain stable under various prebiotically plausible selection pressures, including various pHs, temperatures and salt concentrations. These coacervates were found to not only allow molecular diffusion, but were also capable of carrying out

nonenzymatic template-directed replication reaction within their interior. The data pertaining to the characterization of all the above aspects have been detailed in Chapters 4 and 5.

2.2.References:

1. Bapat N (2018) Role of co-solutes in nonenzymatic RNA replication on prebiotic Earth. Thesis, Dept. of Biology

2. Bapat NV, Rajamani S (2015) Effect of Co-solutes on Template-Directed Nonenzymatic Replication of Nucleic Acids. J Mol Evol 81:72–80. https://doi.org/10.1007/s00239-015-9700-1

3. Deck C, Jauker M, Richert C (2011) Efficient enzyme-free copying of all four nucleobases templated by immobilized RNA. Nature Chem 3:603–608. https://doi.org/10.1038/nchem.1086

4. Leslie E. O (2004) Prebiotic Chemistry and the Origin of the RNA World. Critical Reviews in Biochemistry and Molecular Biology 39:99–123. https://doi.org/10.1080/10409230490460765

5. McCollom TM, Ritter G, Simoneit BRT (1999) Lipid Synthesis Under Hydrothermal Conditions by Fischer- Tropsch-Type Reactions. Orig Life Evol Biosph 29:153–166. https://doi.org/10.1023/A:1006592502746

6. Poudyal RR, Pir Cakmak F, Keating CD, Bevilacqua PC (2018) Physical Principles and Extant Biology Reveal Roles for RNA-Containing Membraneless Compartments in Origins of Life Chemistry. Biochemistry 57:2509–2519. https://doi.org/10.1021/acs.biochem.8b00081

7. Rushdi AI, Simoneit BRT (2001) Lipid Formation by Aqueous Fischer-Tropsch-Type Synthesis over a Temperature Range of 100 to 400 °C. Orig Life Evol Biosph 31:103–118. https://doi.org/10.1023/A:1006702503954

8. Zhou L, Koh JJ, Wu J, et al (2022) Fatty Acid-Based Coacervates as a Membrane-free Protocell Model. Bioconjugate Chem 33:444–451. https://doi.org/10.1021/acs.bioconjchem.1c00559

Chapter 3

NONENZYMATIC RNA REPLICATION IN A MIXTURE OF 'SPENT' NUCLEOTIDES

Adapted from: *FEBS letters*, *597*(24), 3125-3134.

3.1. Introduction

The RNA World hypothesis endeavours to provide an explication for the emergence, replication and evolution of genetic material in the absence of enzymes during life's origins (Gilbert 1986; Szostak 2012; Robertson and Joyce 2012). However, the efficiency of such nonenzymatic replication processes remains deficient. This contention about the efficiency is especially driven by two critical steps of replication (in addition to strand separation): selection of the correct nucleotide for incorporation against a templating base and the proofreading mechanism that corrects for an incorrect incorporation. In the cellular milieu, these two steps are stringently facilitated by enzymes during enzymatic replication process. Thus, the error rates associated with enzymatic processes remain very low, ensuring faithful replication in extant biology (Loeb and Kunkel 1982). Conversely, high error rates have been associated with nonenzymatic replication (Leu et al. 2013).

Although nonenzymatic replication raises concerns about the fidelity of replication, it has been shown that stalling after incorporation of a mismatched base pair could have intrinsically prevented 'error catastrophe' (Rajamani et al. 2010). Therefore, correct base pairing, which impinges on the appropriate stereochemistry of the extension terminus, is in itself a critical factor for determining fidelity of nonenzymatic replication (Blain and Szostak 2014). Generally, nonenzymatic template-directed replication reactions have been studied by characterizing the primer extension process, using activated or nonactivated nucleoside monophosphates (Prabahar and Ferris 1996; Leslie E. 2004; Kervio et al. 2016; Bapat and Rajamani 2018; Dagar et al. 2023). In a typical reaction, the template first forms a duplex with the primer, which is then followed by a nucleophilic attack of the 3' end of the primer onto the incoming nucleotide, resulting in the extension of the primer by one nucleotide at a time (Walton et al. 2019). Activated nucleotides bear a good leaving group, which makes the process of nonenzymatic primer extension feasible under ambient aqueous conditions, without invoking high temperatures or external catalysts (Leslie E. 2004).

These activated moieties, however, are extremely unstable and prone to getting hydrolyzed into the corresponding nucleoside 5′-monophosphates (NMPs). The NMPs thus formed, also called as 'spent' monomers, cannot extend the primer on their own under the aforementioned reaction conditions. However, the spent monomers possess an intact base pairing moiety, which allows them to continue to base pair with the templating base (Deck et al. 2011). This affinity of the spent monomers for the templating base can hinder the access of the activated nucleotides to

the templating site, consequently altering the reaction kinetics of subsequent primer extensions (Deck et al. 2011; Kervio et al. 2014). Thus, in addition to governing the fidelity of nonenzymatic replication, base pairing also factors importantly in potentially inhibiting the reaction in these aforesaid scenarios. Pertinently, NMPs would have been present as co-solutes in the prebiotic soup, thereby underscoring the importance of systematically characterizing their inhibitory potential in prebiotic reactions.

In the context of co-solutes, it has been previously reported that molecules such as lipids and polyethylene glycol (PEG) tend to reduce reaction rates (Bapat and Rajamani 2015). Specifically, they have been shown to affect the rate of incorporation of imidazole-activated purine nucleotides against pyrimidine templating bases, in template-directed replication reactions. In these reactions, PEG was used as a nonspecific co-solute and a proxy for macromolecular crowders in the prebiotic soup as macromolecular crowding is known to affect several reaction rates (Ellis 2001; Kilburn et al. 2013; Desai et al. 2014; Nakano et al. 2014)l.

Because prebiotic soup would have been a conglomerate of co-solutes, and as some co-solutes have been shown to affect the rate of enzyme free reactions, we set out to systematically assess the effect of a mixture of NMPs as co-solutes on nonenzymatic replication reactions. To the best of our knowledge, previous studies have looked at the inhibitory effect of only a single species of NMP on the primer extension process, at a given time. This was determined primarily by calculating the dissociation (and inhibitory) constants of the binding between the nonactivated nucleotide and the template in different sequence contexts (Deck et al. 2011; Kervio et al. 2014). Moreover, a comprehensive study looking at the effect of a mixture of all four spent nucleotides on templated-replication in an all-RNA system involving ribonucleotides, RNA primer, albeit amino-terminal and RNA templates is lacking.

To address this aforesaid lacuna, we investigated how the presence of a mixture of AMP, GMP, CMP and UMP (mixture of NMPs) would affect reaction rates, as they all would have been simultaneously present in a heterogenous prebiotic soup. This gains importance when accounting for the fact that a sophisticated replicating protein machinery was not present then. Therefore, the interference from these co-solutes due to their base pairing ability with the template would have directly influenced the reaction rates and their outcomes (Kervio et al. 2014; Izgu et al. 2015). Furthermore, a combination of intermolecular interactions, such as stacking, hydrogen bonding and secondary electrostatic interactions, is postulated to play a

crucial role in determining the binding strength of a nucleotide to its templating base (Kervio et al. 2014).

Such a complex interplay of interactions between the nucleotide and the template makes it all the more important to characterize how the presence of a mixture of all the four spent nucleotides would have affected the rate of the reaction, given that each of them would have different binding strengths with the template, and thus different inhibitory potentials. All of this essentially raises two primary questions: (i) How would a mixture of NMPs affect nonenzymatic replication rates? (ii) How much would have the contribution of the individual components of the mixture been, towards this process? Given the aforementioned reasons, we set out to understand the effect of a mixture of spent nucleotides on nonenzymatic templated-replication reactions in an all-RNA context. For this, we used a previously standardized reaction set up (Tables 2.1 and 2.2; Methods and Materials (Bapat and Rajamani 2015). We observed that a 1 : 1 : 1 : 1 mixture of the four spent nucleotides (the NMP mixture) reduced the templated-replication rate significantly.

Primarily, we observed that the spent nucleotides that prominently base pair with the templating base were the ones that were mainly responsible for the effects that were observed. Furthermore, we observed predisposition of some reactions to inhibition, due to contribution from near-neighbour interactions and wobble base pairing that came from the spent nucleotides. Lastly, we conclude that the predominant factor responsible for reducing the reaction rate in the mixture is the spent nucleotide that is the Watson–Crick base pairing partner of the templating base. In all, undertaking this study is pertinent to discerning how template-directed nonenzymatic replication of RNA in a putative RNA World would have realistically panned out in the presence of a mixture of spent monomers in the vicinity. Moreover, this knowledge will have ramifications for characterizing prebiotically plausible mechanisms of ‘rescuing’ these replication reactions from ‘parasitic monomers’.

3.2. Materials and Methods

3.2.1. Materials

Nucleoside-50-phosphorimidazolides (ImpNs) were purchased from GLSynthesis Inc. The RNA primer terminated with 3′-amino-2′,3′-dideoxynucleotide (Amino G primer) was acquired from Keck laboratory, Yale, USA, and was gel purified before use. RNA templates were purchased from Sigma-Aldrich (Bangalore) and were used without any further purification. Sequences of the primer and template are mentioned in Table 1. Disodium salts of nucleoside-5′-monophosphates (5'-NMPdss) were purchased from Sigma-Aldrich (Bangalore). All other reagents were purchased from Sigma-Aldrich and were of analytical grade.

3.2.2. Methods

3.2.2.1. Reaction set-up and time points

1.3 μM of respective template and 0.325 μM amino terminal primer (sequences as specified in the main text) were mixed and heated at 90 °C for 5 min, after which the mixture was allowed to cool approximately for a minute. Tris (pH 7) and NaCl were added at final concentrations of 100 and 200 mM, respectively. Nucleoside 5′-monophosphates were added in the form of a mixture of all the four NMPs or individually at a final concentration of either 50 or 12.5 mM, depending on the reaction. A stock of 5′-ImpN was made fresh and added to the reaction mixture at a final concentration of 10 mM. Final reaction volume was set to 10 μL. One microliter of the reaction mixture was withdrawn at respective time points, put in TBE buffer containing 8 mM urea, and was frozen immediately at -35 °C. Zero time point is withdrawn right after mixing the freshly made 5′-ImpN with the reaction mixture.

3.2.2.2. Reference lane

As used in the previous study, respective control reactions are incubated separately for 1 h and 1 μL of it is processed and loaded on the gel like the rest of the time points. These reactions are done separately and are only for the purpose of using for the reference positioning of the N and N + 1 bands.

3.2.2.3. Quantification of the reaction

The amino primer bears Cyanine 3 (Cy3) fluorophore label at its 5′ end for its detection on the gel. Before loading the aforementioned time points on the gel, 15 times excess of an unlabeled competitive RNA, which is exactly identical in sequence with the amino primer, was added to the time points. The mixture was heated at 90 °C for 5 min, so as to separate template from the labelled primer. The individual time points were run on 20% urea PAGE. The gel was visualised by exploiting the Cy3 fluorescence at the 5′- terminal of the amino primer, which ensures detection of only primer bands. The extended primer (N + 1) and the unextended primer (N) resolved into two separate bands on 20% denaturing PAGE, intensity of which was measured on ImageQuant L. Fraction of the extended product was calculated by following formula.

$$Fraction\ N+1 = \frac{Intensity\ of\ extended\ primer}{Intensity\ of\ extended\ primer + Intensity\ of\ unextended\ primer}$$

… (Equation 1)

3.2.2.4. Statistical analysis

For all the statistical analysis, GraphPad Prism 9 was used. For a comparison between two reactions, Student's unpaired two-tailed t-test was used. For a simultaneous comparison between individual reactions with control, Dunnett's test was used. One-way ANOVA was used for multiple comparisons. For any given comparison between reaction populations, changes were considered statistically significant only for P-values < 0.05.

3.3. Results

3.3.1. Effect of spent nucleotide mixture on the reaction rate of template-directed RNA replication

We carried out nonenzymatic replication reactions as mentioned in Table 3.1 with each reaction being assigned a reaction symbol as indicated in the table. The details of the primer template sequences and the activated imidazolides used in the reactions have been detailed in Table 3.2.

Table 3.1: Reactions

Sr. No.	**Reaction**	**Reaction Symbol**	**Incoming Imidazole-activated nucleotide**	**Templating Base**	**Co-solute Mixture (NMPs)**
1	A across U	A_U	10 mM ImpA	U	Final 50 mM of **AMP**+GMP+CMP+UMP
2	G across C	G_C	10 mM ImpG	C	Final 50 mM of AMP+**GMP**+CMP+UMP
3	C across G	C_G	10 mM ImpC	G	Final 50 mM of AMP+GMP+**CMP**+UMP
4	U across A	U_A	40 mM* ImpU	A	Final 50 mM of AMP+GMP+CMP+**UMP**

Nucleotides indicated in bold in the last column of Table 1 denote the cognate spent nucleotides in the NMP mixture, which corresponds to the respective templating bases.

*Since U_A is an extremely slow reaction, the concentration of the activated nucleotide used in this reaction is 4 times greater as compared to that in other reaction (Rajamani et al. 2010; Bapat and Rajamani 2015).

Table 3.2: Sequences of Primer and Template

Primer	Template	Templating Base	Incoming activated nucleotide
(Cy3) 5′ GG GAU UAA UAC GAC UCA CUG-NH_2	5′ AGU GAU CU**A** CAG UGA GUC GUA UUA AUC CC	A	ImpU
	5′ AGU GAU CU**G** CAG UGA GUC GUA UUA AUC CC	G	ImpC
	5′ AGU GAU CU**C** CAG UGA GUC GUA UUA AUC CC	C	ImpG
	5′ AGU GAU CU**U** CAG UGA GUC GUA UUA AUC CC	U	ImpA

Single letter notation of nucleotides indicated in bold in the second column of Table 3.2 denote the templating base.

In a typical reaction, a mixture of all the four spent nucleotides were added at a total concentration of 50 mM to the reaction mixture (where the individual nucleotide's concentration is 12.5 mM). We hypothesized a reduction in the rates of all the four reactions in such a scenario because of two primary possibilities: (i) due to general crowding that is facilitated in these reactions by the presence of spent nucleotides as it could potentially affect the availability of the incoming activated nucleotide across the templating base (as was seen in an earlier study (Bapat and Rajamani 2015)) or (ii) occurrence of specific (Watson-Crick) and/or nonspecific (non-Watson-Crick) interactions between the spent monomers and the templating base and other near-neighbour bases, all of which could retard the addition of the incoming nucleotide.

For any given reaction (Table 3.1), the mixture of spent nucleotides would have one NMP that would be the Watson-Crick base pairing partner of the templating base (indicated in bold), and it would henceforth be referred to as the 'cognate spent monomer' for the sake of brevity. Conversely, the rest of three spent monomers in the NMP mixture are the non-Watson-Crick base pairing partners of the templating base, which would henceforth be referred to as the 'noncognate spent monomer'. When the mixture of spent monomers was added as co-solutes in the replication reaction, a significant drop in the initial reaction rates was observed for A_U,

G_C and C_G reactions (Fig. 3.1(i) C-(iii) C). However, reaction U_A appeared to remain unaffected (Fig. 3.1(iv) C). It is pertinent to note that such an effect could be observed because of the higher ratio of ImpU:NMP mixture used in U_A reaction (4:5 of ImpU to NMP mixture) when compared to other reactions (where it is 1:5 of ImpN to NMP mixture). When the U_A reaction was carried out in the presence of 200 mM NMP mixture (i.e., at 1:5 ratio), a significant reduction in the reaction rate was observed (Figure 3.12).

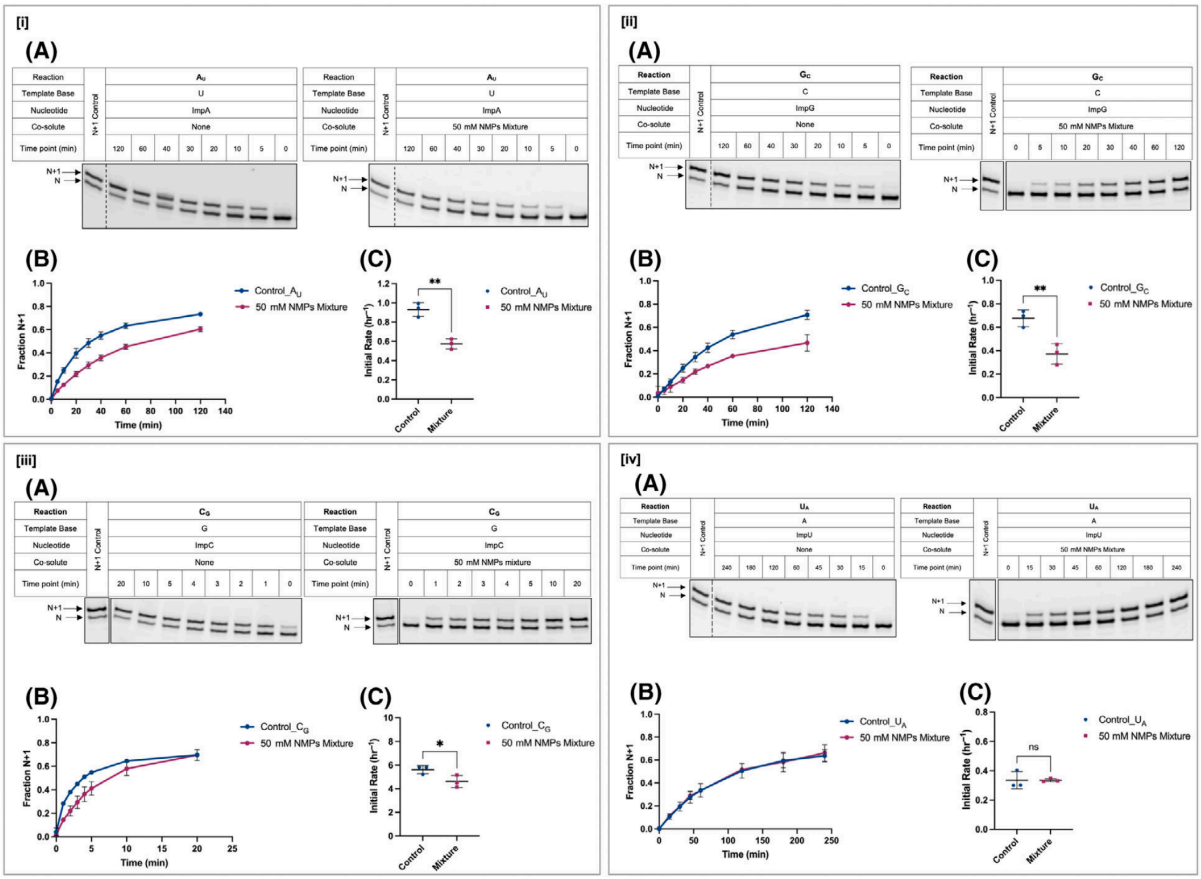

Figure 3.1: **Effect of mixture of spent nucleotides on the rate of nonenzymatic template-directed reaction.** Panels indicate **[i]** A_U reaction; **[ii]** G_C reaction; **[iii]** C_G reaction; **[iv]** U_A reaction, respectively. Subpanels indicate **A.** 20% denaturing gels of the relevant reaction in the absence (control) of co-solutes (left) and in the presence of 50 mM NMPs mixture (right). Each gel image has a reference lane to represent the positions of the N and N+1 bands (Methods). Dotted line separates the reference lane from the adjacent lanes on the same gel. The reference lane is shown as a separate box when the sample was loaded a little away from the reaction of interest in the same gel (Full gel images have been included in Figure 3.6-3.12). **B.** Comparison of reaction progress between the control reaction and that with 50 mM NMPs mixture for the reaction detailed in a given panel; **C.** Effect of presence of 50 mM NMPs mixture (as co-solutes) on the initial reaction rate. For every reaction, the initial rate is calculated by fitting a linear curve to the first few time points before the reaction plateaus (methods and Figure 3.2-3.5). It is important to note that the values for initial rates are different for four different control reactions. Error bars represent standard deviation. N=3.

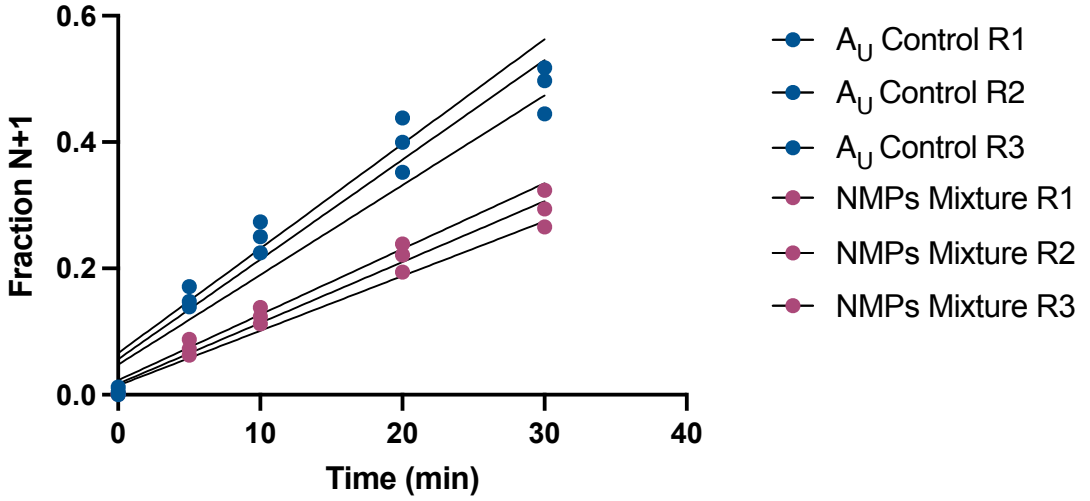

Figure 3.2: **Linear fits for three replicates of initial rate calculations of A_U control reaction and that of the 50 mM NMPs Mixture.**

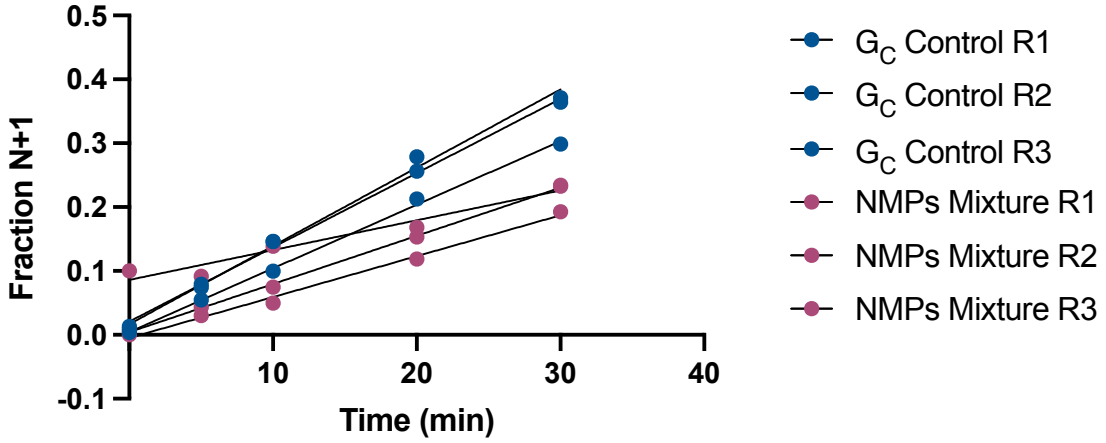

Figure 3.3: **Linear fits for three replicates of initial rate calculations of G_c control reaction and that of the 50 mM NMPs Mixture.**

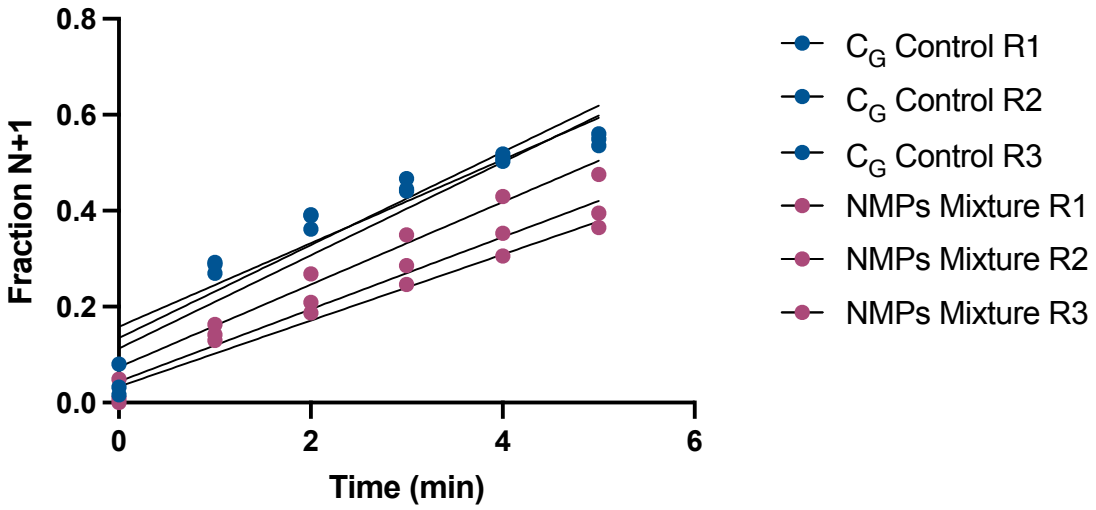

Figure 3.4: **Linear fits for three replicates of initial rate calculations of C_G control reaction and that of the 50 mM NMPs Mixture.**

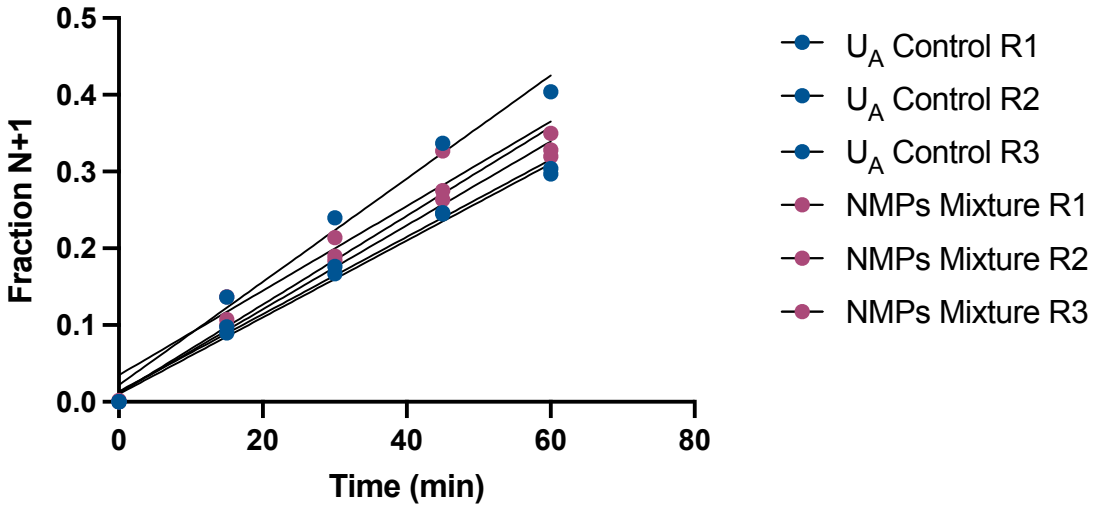

Figure 3.5: **Linear fits for three replicates of initial rate calculations of U_A control reaction and that of the 50 mM NMPs Mixture.**

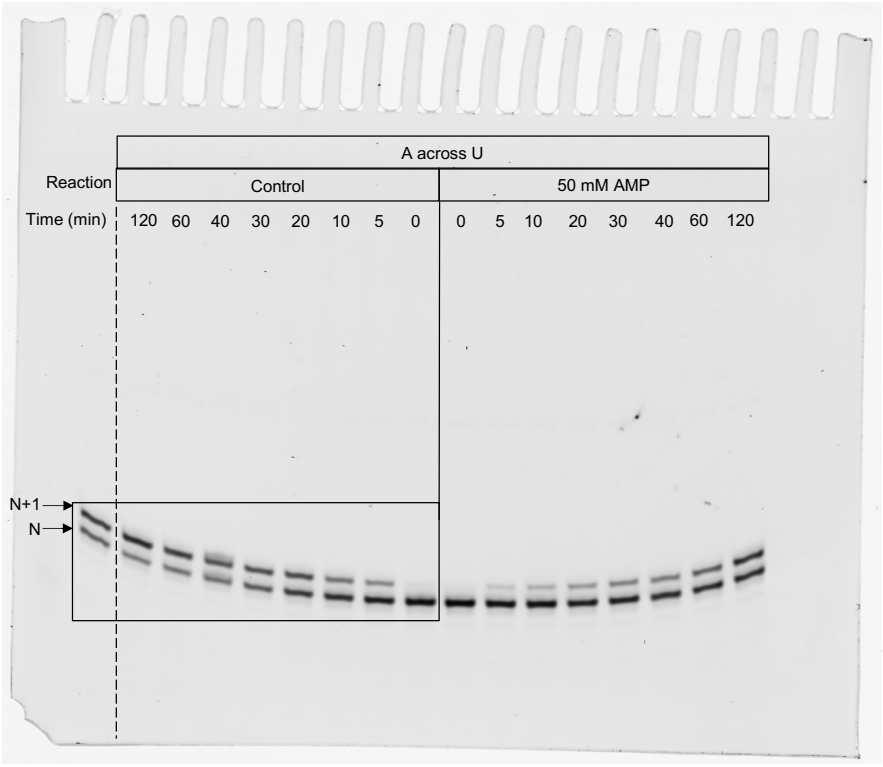

Figure 3.6: **Box represents the cropped part of A_U reaction shown in Figure 3.1(i)A.**

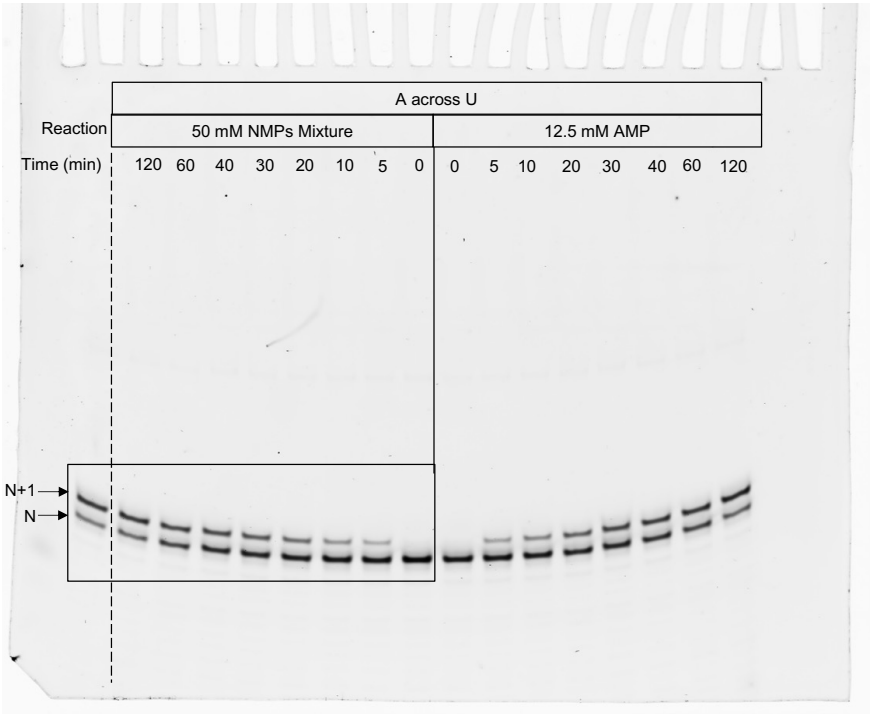

Figure 3.7: **Box represents the cropped part of A_U reaction shown in Figure 3.1(i)A.**

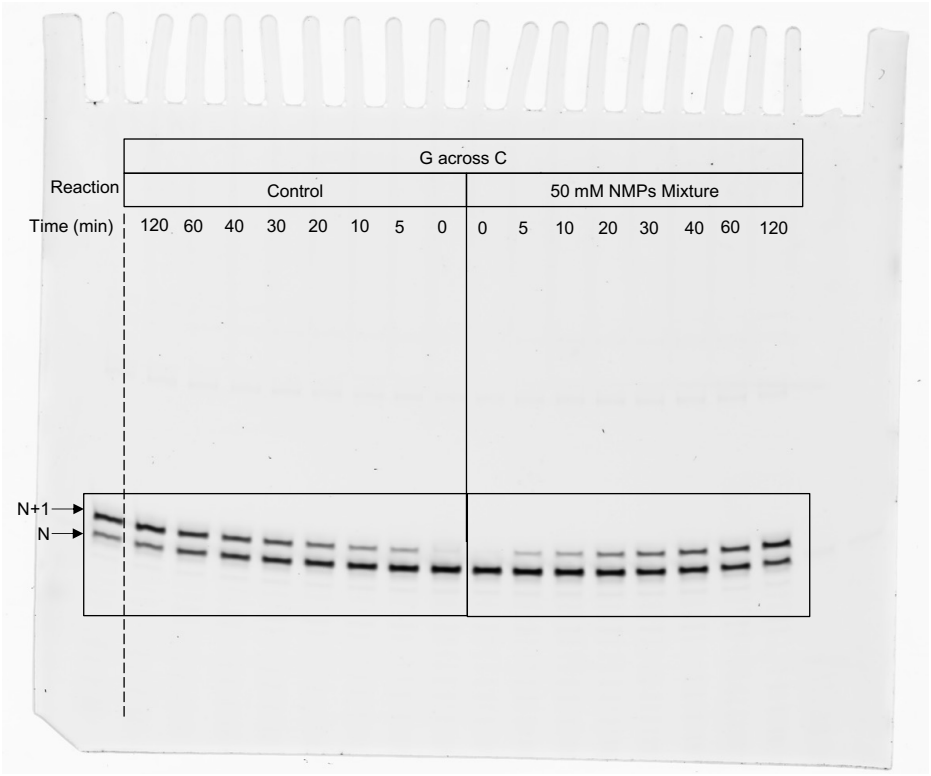

Figure 3.8: **Boxes represent the cropped part of G_C reaction shown in Figure 3.1(ii)A.**

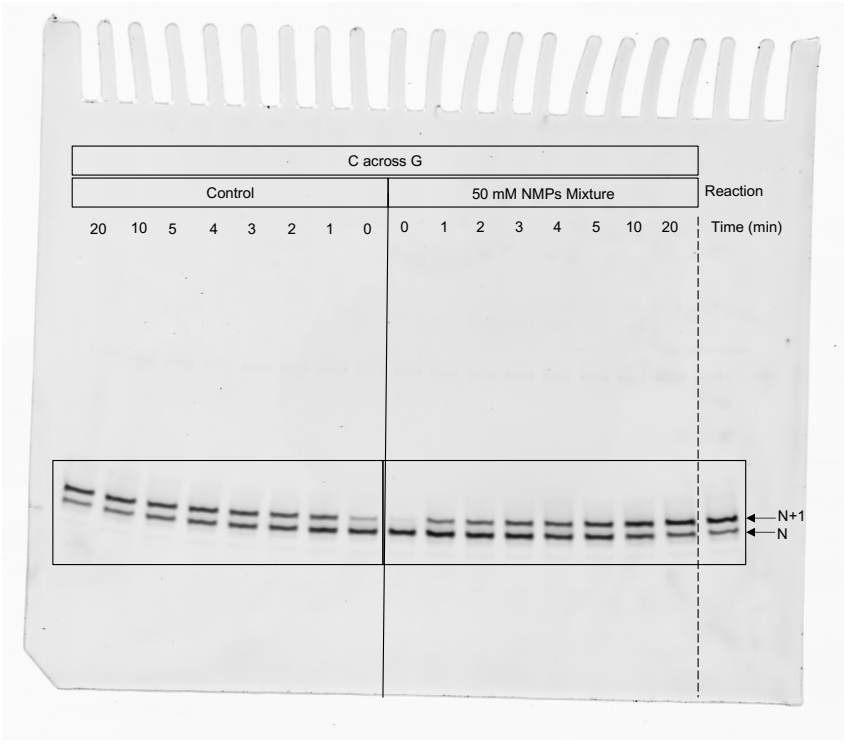

Figure 3.9: **Boxes represent the cropped part of C_G reaction shown in Figure 3.1(iii)A.**

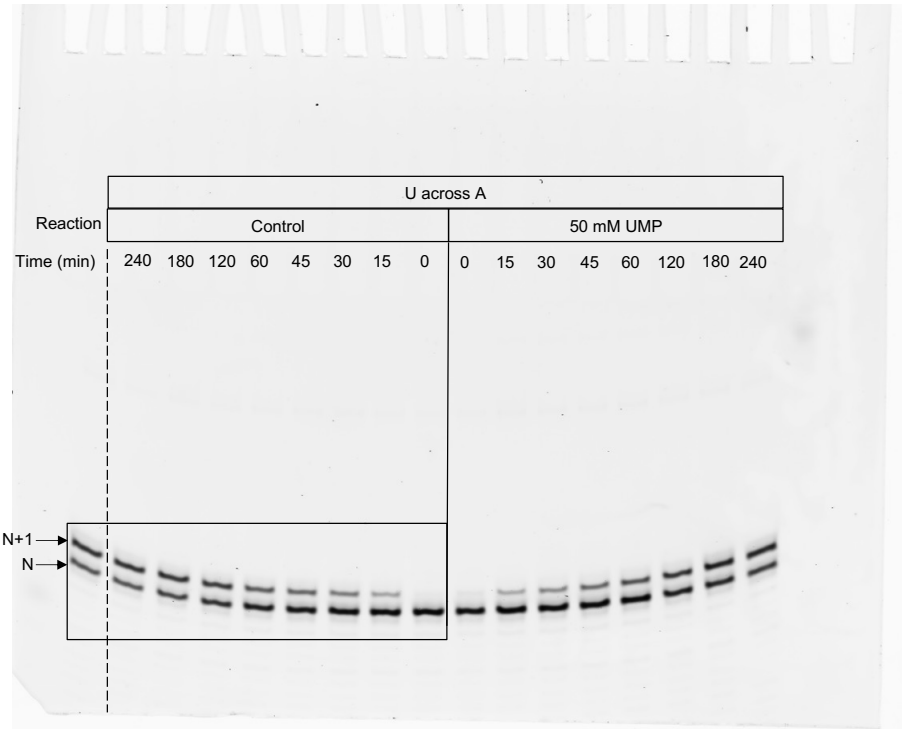

Figure 3.10: **Box represents the cropped part of U_A reaction shown in Figure 3.1(iv)A.**

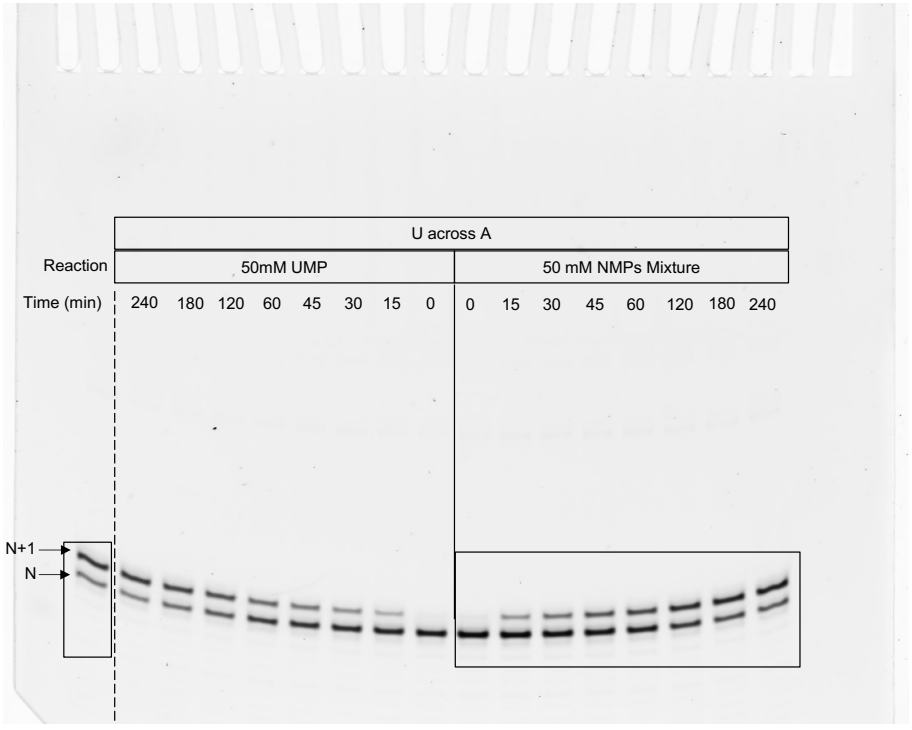

Figure 3.11: **Box represents the cropped part of U_A reaction shown in Figure 3.1(iv)A.**

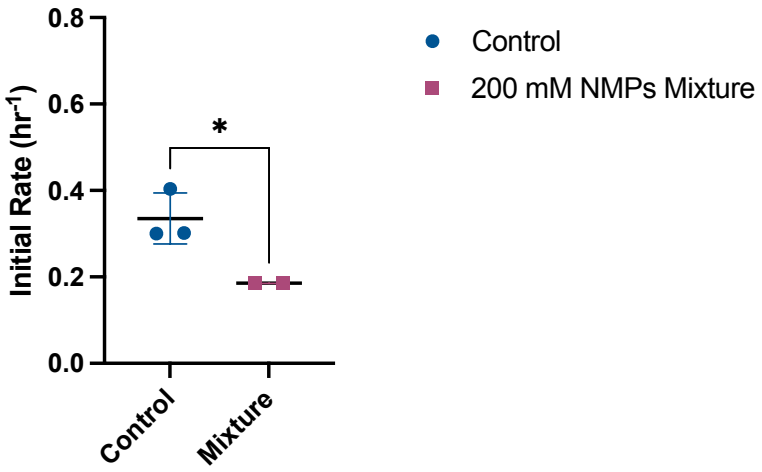

Figure 3.12: **Effect of 200 mM NMPs mixture on the initial rate of U_A reaction.** Error bars represent standard deviation. N=3 for control, N=2 for 200 mM NMPs mixture.

Nevertheless, the result obtained with the 4:5 ratio corroborated a previous observation wherein even 10 equivalents of dTMP showed only a modest reduction in the T across A reaction in the context of DNA (Kervio et al. 2014). In the same study, Richert and coworkers also quantified the binding strengths of the dNMPs to the corresponding Watson-Crick base pairing partners in the DNA template. This varied across the different templating bases, ranging from 10 to 280 mM. This prompted us to ask how much would the individual spent nucleotides in our RNA-based reactions (containing the NMP mixture) actually affect the reaction rates when added individually at a final concentration of 50 mM in each of the above reactions. This would be important for understanding whether the reduction is a result of a collective inhibitory effect of all the spent monomers in the reaction or is mainly coming only from specific monomers. Therefore, to delineate the contribution of the individual nucleotides to the reaction rate reduction (especially as was observed in the presence of the NMP mixture), we next carried out all the reactions in the presence of individual spent monomers.

3.3.2. Inhibition of nonenzymatic RNA replication by individual spent nucleotides

In the context of understanding the role of individual spent monomers as co-solutes in templated-replication reactions, it is reasonable to assume that the stronger the interaction between the spent monomer and the templating base, the more would be its ability to compete with the incoming activated nucleotide for the templating base. Consequently, the contribution of the cognate spent monomer in reducing the reaction rate would be greater when compared to others in the mixture. Indeed, it was clearly observed that the cognate spent monomer affects

the rate of the reaction to a significantly greater extent than the non-cognate ones (Fig. 3.13A-C; Fig. 3.14-3.17).

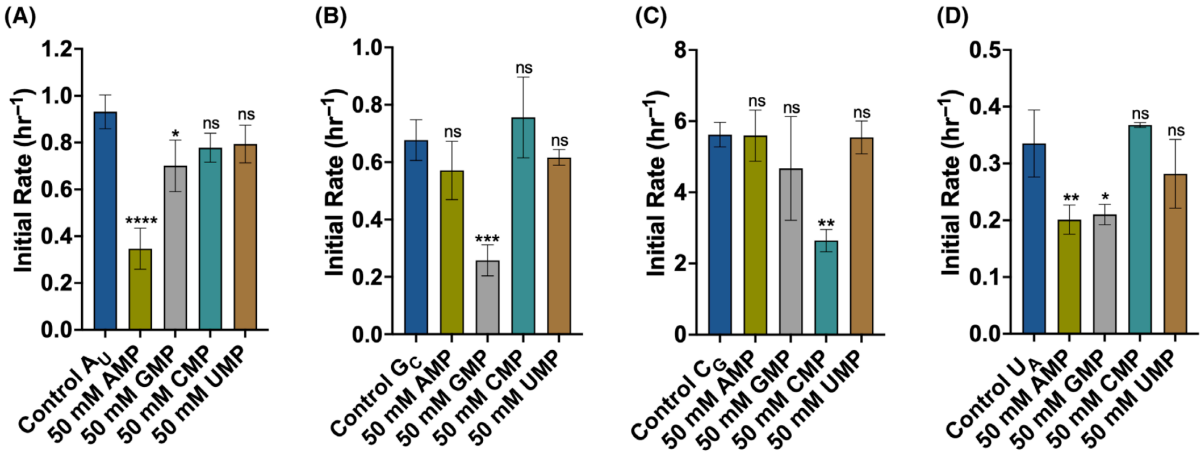

Figure 3.13: Effect of individual spent monomers on nonenzymatic template-directed replication reactions: **[A]** A_U reaction; **[B]** G_C reaction; **[C]** C_G reaction; **[D]** U_A reaction. The cognate spent monomers, AMP, GMP, and CMP in A, B and C, respectively, affect the progress of the reactions the most. These are indicated by green-, grey- and teal-coloured bars, respectively. In U_A reaction, the cognate spent monomer, UMP, did not show any effect on reaction rate (brown). Statistical analysis was done using Dunnett's test, where means of all the reactions are compared to that of the control. Error bars represent standard deviation. N=3.

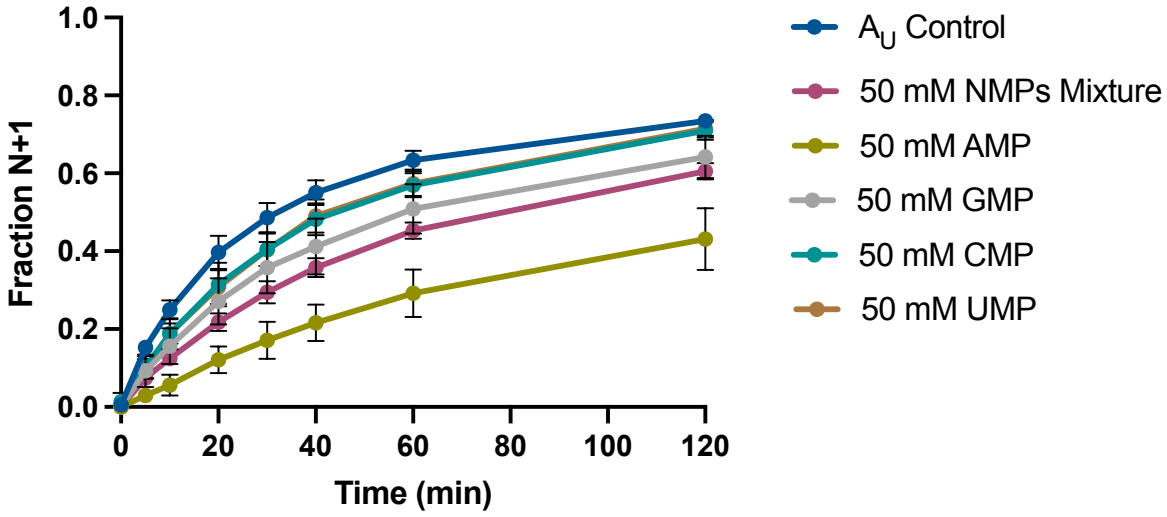

Figure 3.14: **Reaction progress of A_U reaction in the presence of various co-solutes.**

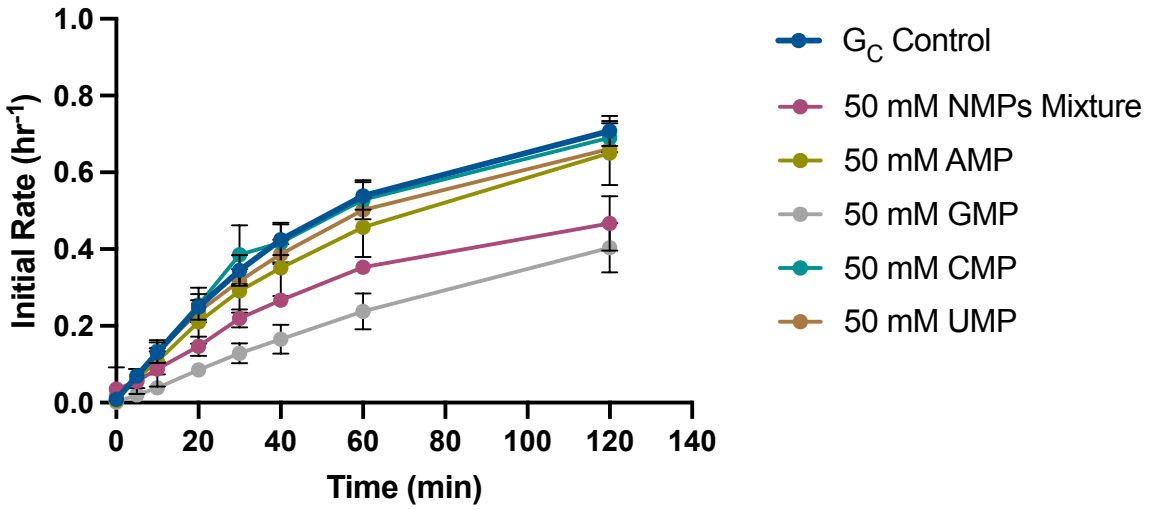

Figure 3.15: **Reaction progress of G_C reaction in the presence of various co-solutes.**

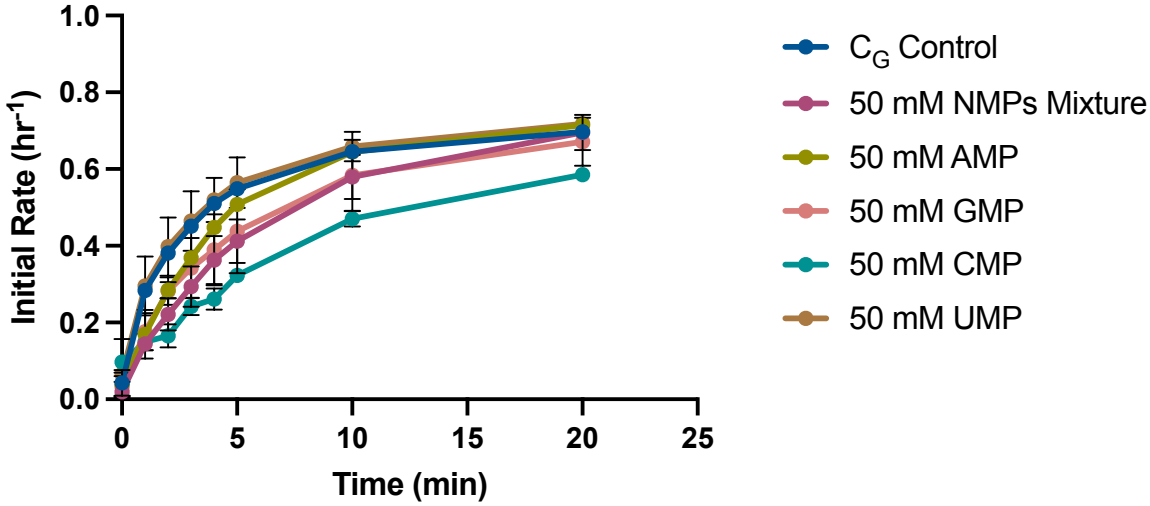

Figure 3.16: **Reaction progress of C_G reaction in the presence of various co-solutes.**

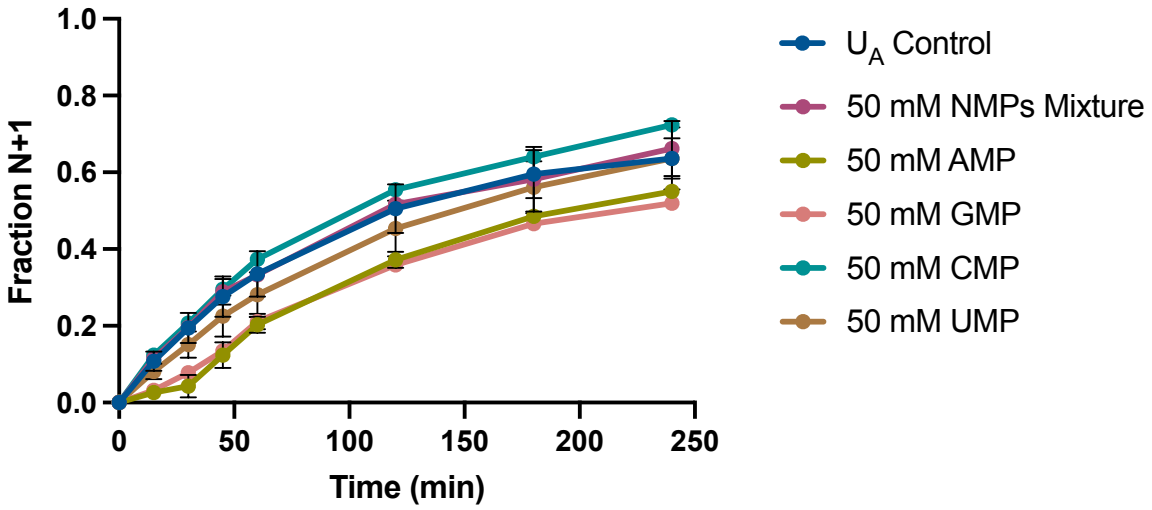

Figure 3.17: **Reaction progress of U_A reaction in the presence of various co-solutes.**

This set of data suggested that the rate reduction that we observed in the reactions detailed in Fig. 3.1 could chiefly be because of the specific interactions of the cognate spent monomers with the templating base. This, in turn, could be causing hindrance in the interactions between the incoming activated nucleotide and the templating base. However, this scenario is not as straightforward as the aforementioned scenario indicates. Although the most significant decrease was seen in the case of the cognate spent monomer, two more cases showed remarkable effect too.

First, there was a significant decrease in the reaction rate in the presence of GMP as a co-solute in the A_U reaction (Fig. 3.13A). It was evident from this rate reduction that GMP, a well-known wobble of U (Izgu et al. 2015), does indeed compete with ImpA in the reaction, thereby significantly affecting the rate of this templated-replication reaction. Second, a statistically significant reduction in the U_A reaction rate was observed, when purines were present as co-solutes (Fig. 3.13D). This effect could be attributed to the 3′- terminal guanine residue of the primer, as it can provide near-neighbour stacking interactions especially for the incoming purine nucleotides.

Pertinently, Fig. 3.13 shows that in isolation, the cognate spent monomer reduces the reaction rate even more when compared to the mixture (Fig. 3.13A–C vs Fig. 3.1(i) C–(iii) C). However, this observation could be attributed to the higher concentration of the cognate spent monomers that was used in the individual reactions, when compared to what was used in the mixtures. Since the mixture contains 1:1:1:1 ratio of all the four spent monomers, the concentration of the individual nucleotides in these scenarios is 12.5 mM. Given this, we thought it was

imperative to also understand whether the 12.5 mM concentration of the cognate spent monomer would also affect the rate by itself to the same extent, and how this compares to when it is present in the mixture (of NMPs). If this indeed turns out to be the case, it would be clear that the cognate spent monomer that was present in the mixture was predominantly responsible for inhibiting the reaction in the mixed spent nucleotides experiments.

3.3.3. Cognate spent nucleotide chiefly affects the nonenzymatic replication reaction

When 12.5 mM concentration of the cognate spent monomer was used in the reaction, we still observed a significant drop in the initial rate of the reactions when compared to the respective control reactions (Fig. 3.18, Fig. 3.19-3.21). We further compared the reaction rates involving 50- and 12.5 mM cognate spent monomers, versus the 50 mM NMP mixture containing reactions (Fig. 4A–C). For this, we performed one-way ANOVA (multiple comparisons) to compare the means of each of the above (rates involving 50 mM cognate spent monomer, 12.5 mM cognate spent monomer, and 50 mM NMP mixture) in A_U, G_C and C_G reactions. Since there was no effect of the cognate spent monomer on the reaction rate in case of U_A (Fig. 2D), we excluded the same from further analyses. In rest of the three cases, we observed a statistically nonsignificant difference in the reaction rates between 50 mM NMPs mixture and 12.5 mM cognate spent monomer (Fig. 3.22A–C). From this, it can be deciphered that the reduction that is being seen in the mixture is predominantly being governed by the cognate spent monomer even in the mixed NMP containing reactions.

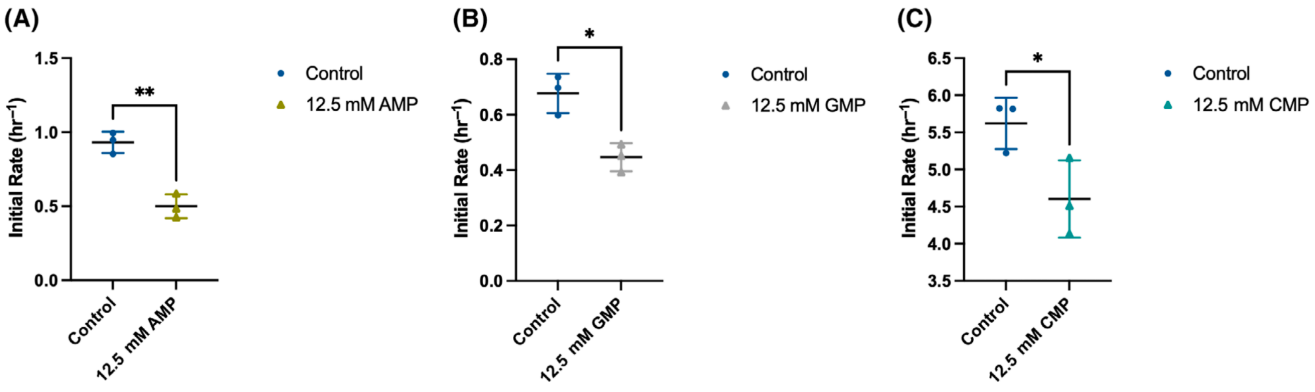

Figure 3.18: **Effect of 12.5 mM cognate spent monomer**: **[A]** A_U reaction; **[B]** G_C reaction; **[C]** C_G reaction. Statistical analysis was done using Student's unpaired two-tailed t-test. The linear fits for these are shown in Figure 3.19-. Error bars represent standard deviation. N=3.

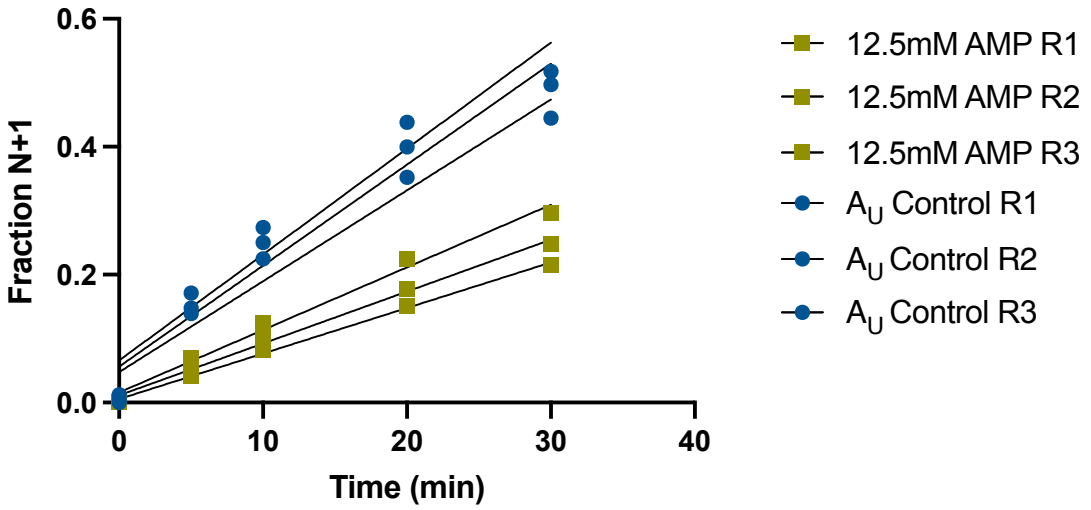

Figure 3.19: **Linear fits for three replicates for initial rate calculations of A_U control reaction and that of the 12.5 mM NMPs Mixture.**

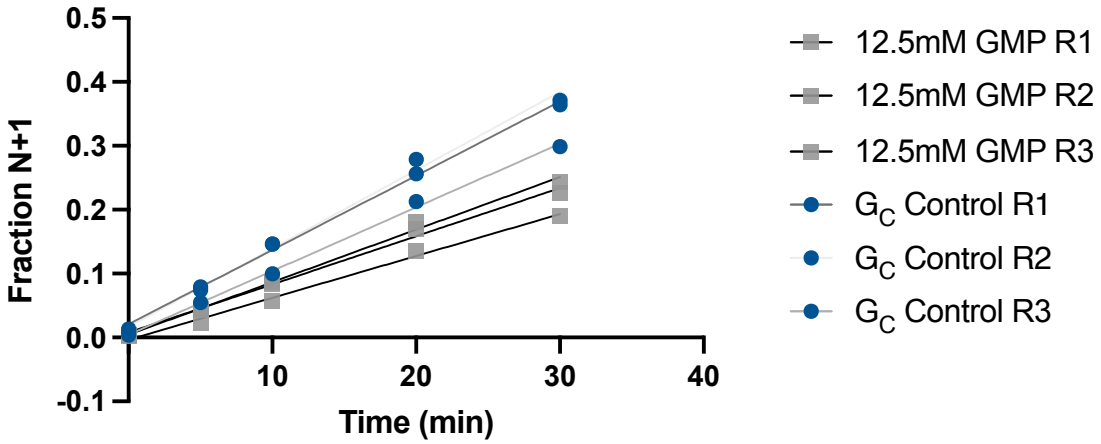

Figure 3.20: **Linear fits for three replicates of initial rate calculations of G_C control reaction and that of the12.5 mM NMPs Mixture.**

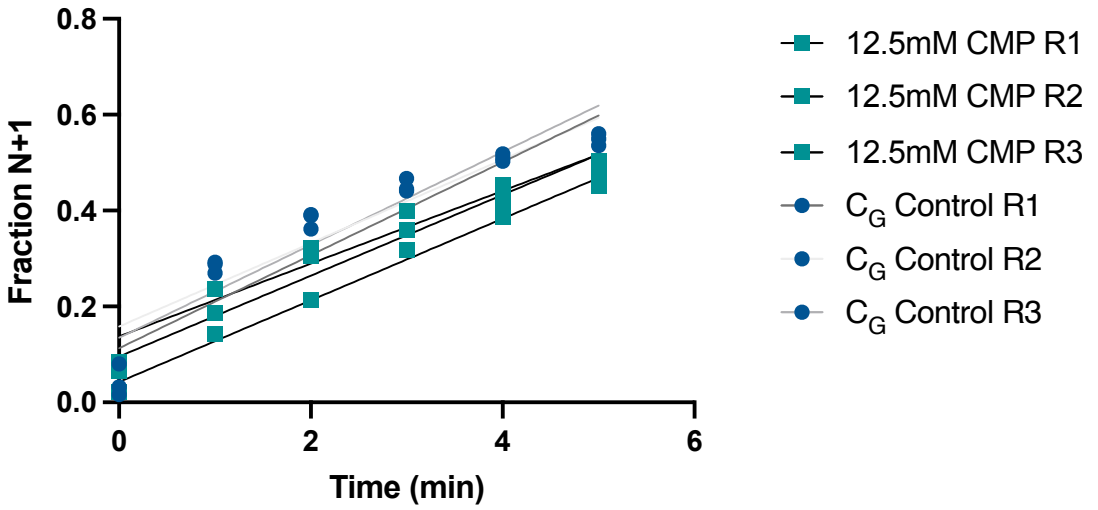

Figure 3.21: **Linear fits for three replicates of initial rate calculations of C_G control reaction and that of the 12.5 mM NMPs Mixture.**

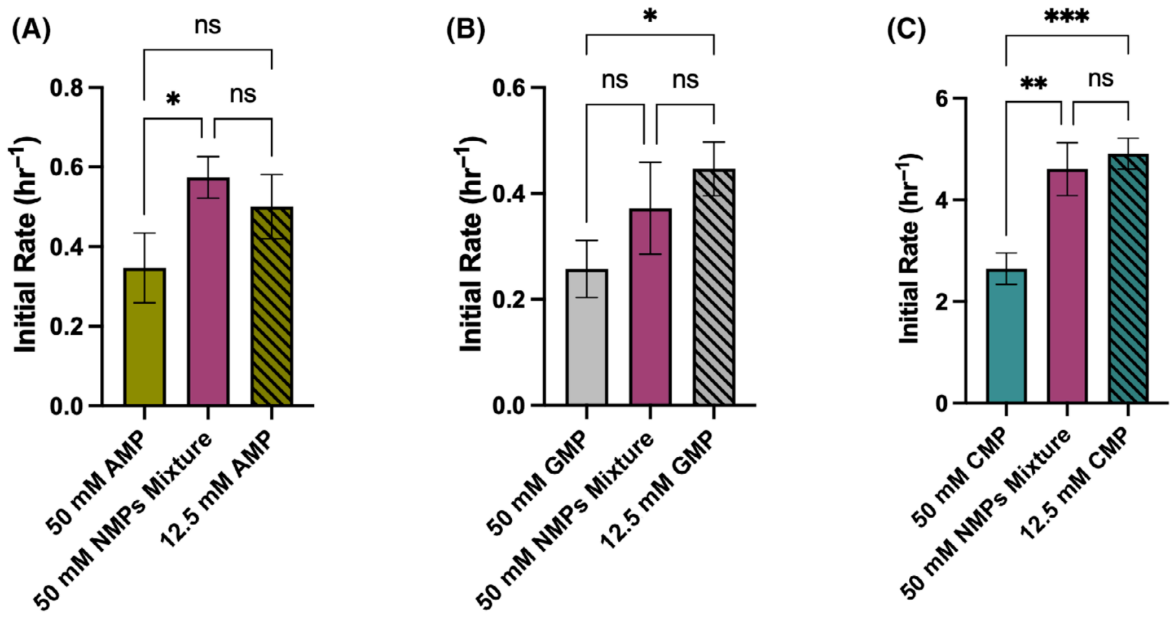

Figure 3.22: Identification of the determining factor for rate reduction: **[A]** A_U reaction; **[B]** G_C reaction; **[C]** C_G reaction. There is no statistically significant difference between initial rates of reactions containing 50mM NMP mixture and 12.5 mM respective cognate spent monomer in all the three reactions, suggesting that the reduction that was observed in the case of mixed NMPs would have predominantly been brought about by the cognate spent nucleotide in the mixture. Statistical analysis was done using one-way ANOVA (multiple comparisons). Error bars represent standard deviation. N=3

3.4. Discussion

Extant biology relies on transmission of genetic information, a process that is co-ordinated by a highly sophisticated enzyme machinery. This allows to distinguish between nucleotides and despite the presence of all four nucleotides (co-solutes) in the cellular milieu, faithful replication is still ensured with minimal errors. However, given the prebiotic heterogeneity and the absence of a complex enzymatic machinery, it becomes crucial to delineate how co-solutes in the prebiotic soup would have affected the rate of nonenzymatic templated-replication; one of the crucial milestones in a putative RNA World. In this context, we chose to look at spent nucleotides as co-solutes because of their availability in the prebiotic soup, their spontaneous formation as by-products from activated nucleotides and their base pairing potential with the templating base.

Also, we chose to study 'RNA-based' reactions, which is the fundamental basis for the RNA World hypothesis. We addressed the effect of heterogeneity by checking the effect of a mixture of all four spent nucleotides on templated-replication. Upon the addition of 50 mM NMP mixture to a given nonenzymatic template-directed replication reaction, the rate of the reaction significantly dropped. A_U showed 46.4% reduction in the initial rate while G_C showed 45.1% reduction and C_G showed a comparatively lesser reduction at 20.6% (Fig. 3.23).

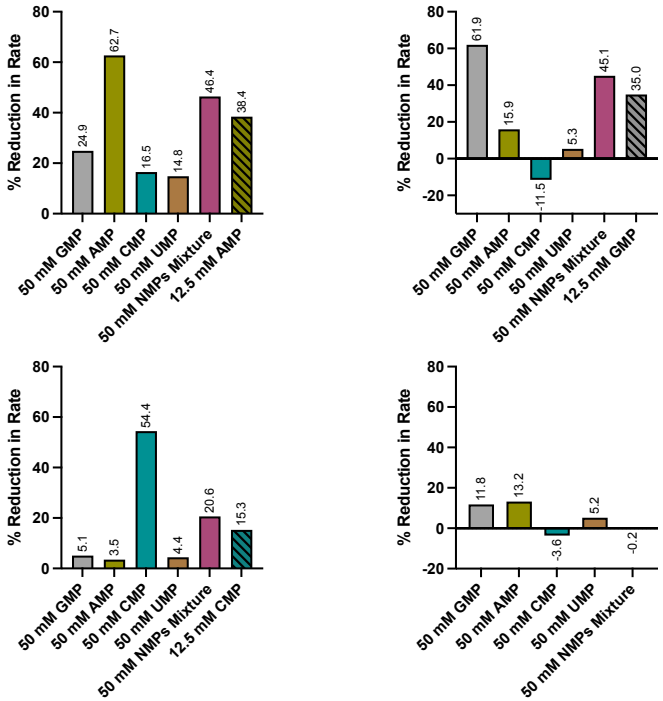

Figure 3.23: **Percentage reduction in the initial rate of A_U (A), G_C (B), C_G(C), U_A (D) reactions in the presence of various co-solutes (based on rates obtained for three reaction replicates, as indicated in above**

figures). The negative values that are observed in G_C and U_A reactions fall within the error range of the respective controls (Figure 3.13B, 3.13D and 3.1(iv)C), and do not affect the interpretation of the results.

We observed that the rates of G_C, C_G and U_A control reactions were slightly lesser when compared to an earlier study (Bapat and Rajamani 2015). To address this, we systematically checked the hydrolysis profiles of all the ImpN monomers on HPLC (Table 3.3). ImpNs were dissolved in ultrapure water (pH-7±0.05). Their concentrations were determined and equal amounts were loaded on to the HPLC (Infinity Series 1260HPLC, Agilent Technologies). The activated and non-activated molecules were separated on DNAPac PA 200 column (Thermo Scientific). A previously standardized method was used to separate activated nucleotide from the non-activated spent monomer (Dagar et al. 2020).

We observed hydrolysis in ImpG, ImpC and ImpU monomers. We attribute the difference observed in the rates of control reactions when compared to the earlier study to this hydrolysis (as a result of which, the effective concentration of ImpN that went into the reaction was modestly lower than 10 mM). Despite this observation, it is important to take into consideration that the concentration of the hydrolyzed species was much lesser when compared to that of the co-solute that was externally added to the reactions, suggesting that the reduction in the rate would have been predominantly driven by the added co-solute. Although A_U, G_C and C_G got affected, the effect seen in the case of U_A, was negligible. It is also relevant to note that for an unambiguous comparison across various reaction sets, we wanted to keep the concentration of the co-solutes same across all the reactions (50 mM), and thus, we did not change it for U_A despite the relatively higher concentration of ImpU that was used in the control reaction.

Table 3.3: Hydrolysis profiles of ImpNs at different time points.

Stock	**% Species at t=0**		**% Species at t=x**		
	ImpN	**NMP**	**x (min)#**	**ImpN**	**NMP**
ImpA	96.6	3.4	30	88.0	12.0
ImpG	77.7	22.3*	30	68.4	31.6
ImpC	86.7	13.3*	5	85.3	14.7
ImpU	72.1	27.9*	60	72.0	28.0

* Although there is some hydrolysis observed in ImpG, ImpC and ImpU, it is pertinent to note that only 2.2mM, 1.3mM and 11.16mM of hydrolysed GMP, CMP, and UMP, respectively, made it in to our reactions from these

ImpN stocks (Table 3.4). This concentration is much lesser when compared to the concentration of the co-solutes that were added externally to the reaction mixtures.

[#] This t reflects the reaction timelines used for the calculation of the initial reaction rates for the various reactions studied.

Table 3.4: Concentrations of NMPs from hydrolysed ImpNs in the reactions based on the hydrolysis profiles in Table 3.3.

Reaction	**ImpN**	**Concentration of ImpN used in the reaction**	**Concentration of hydrolyzed NMP at t=0**	**Concentration of hydrolyzed NMP at endpoint time considered for rate calculations (t=x)**
A_U	ImpA	10 mM	0.34 mM	1.2 mM
G_C	ImpG	10 mM	2.23 mM	3.16 mM
C_G	ImpC	10 mM	1.33 mM	1.47 mM
U_A	ImpU	40 mM	11.16 mM	11.2 mM

In the U_A reaction, the presence of UMP did not show any effect on the reaction rate. This could be because of the extremely poor potential of binding of UMP to the complementary templating base, such that the presence of it in excess was still inconsequential (Izgu et al. 2015). However, this same U_A reaction was observed to get affected by the presence of purines as co-solutes. This effect stems from the fact that interactions other than direct base pairing are also deemed crucial in determining reaction rates. These include near-neighbour interactions such as stacking of the incoming nucleotide with one of the bases in the primer, or with a downstream helper strand (Vogel et al. 2005; Hagenbuch et al. 2005). In our study, we found that the slowest reaction U_A was affected significantly by spent purine nucleotides, which could be because of the potential of the terminal guanine residue of the primer to offer such stacking interactions to the incoming purine nucleotides.

Other than the primer, the sequence of the template could also play a role in inducing effective stacking. This is especially relevant in our reaction as the templating base is followed by three pyrimidine residues (U, C, U), all of which can base pair with purine co-solutes and this allows for further stabilization via stacking interactions (Kanavarioti et al. 1998). Since purine–purine

stacking is stronger than purine–pyrimidine stacking, AMP and GMP potentially stacked better with the 3'-terminal guanine residue of the primer, resulting in the ability to successfully compete with the incoming ImpU, thereby reducing this reaction rate in our study. This further emphasizes the potential of near-neighbour interactions in determining nonenzymatic reaction rates, resulting in adverse effects especially in the presence of readily competing co-solutes.

As for why the potential stacking effect was not seen to be prominent in the case of C_G reaction, this could result from the efficient base pairing capability of ImpC (three hydrogen bonds) with the template base G, which possibly could be compensating for the competition coming from the spent purine monomers. The exact role of template sequence in inhibiting the reaction rate, especially in the presence of spent purine nucleotides, can be confirmed by undertaking a detailed study to characterize the effect of mutations downstream of the templating base, or by having short sequence elements occupying those positions (Vogel et al. 2005).

In all, observations from our study suggest the following about spent nucleotides as co-solutes: (i) The co-solute's concentration and affinity towards the templating base determines the extent to which the rate would be affected. (ii) Contribution from G-U wobble pairing in inhibiting the reaction is substantial. (iii) Sequence of the primer and template, and consequently the near-neighbour interactions that can be facilitated, can determine how fast the reaction would proceed in the presence of co-solutes. This is significant as it indicates that the dependence of a spent monomer's inhibitory action on a sequence of RNA would have affected the replication of some sequences more readily than that of others. This would have had a direct implication for the evolution of the prebiotic RNA sequence space in the absence of enzymatic machinery.

Specifically, in the absence of an enzymatic translation machinery, 'single nucleotide translation' is proposed to have happened, for which base-pairing of the aminoacylated nucleotide with the template is an essential requirement (Jash et al. 2021). Therefore, spent nucleotides available in the vicinity could have had an inhibitory or regulatory role on these reactions as they would have directly competed for base-pairing with the templating base in these scenarios. Furthermore, replication happening inside phase-separated systems containing nucleoside triphosphates (NTPs) as anionic moieties (Nakashima et al. 2021; Liu et al. 2022) could also get affected, as the NTPs in these systems could potentially interact with the template and hinder the access of the activated nucleotides to the templating base.

Nevertheless, having a prebiotically plausible 'scrutinizer' may have saved such crucial reactions from 'parasitic' co-solutes. In this context, overcoming inhibition by removing the

spent nucleotides from the reaction mixture has been studied (Deck et al. 2011; Adamala and Szostak 2013). Here, we propose that replication of RNA inside fatty acid-based vesicles could have acted as a putative mechanism to overcome inhibition of spent nucleotides (Mansy et al. 2008; Jin et al. 2018). The inherent characteristic of prebiotically relevant protocellular membranes could have, in principle, allowed for the selective diffusion of imidazole activated nucleotides over the spent monomers (Mansy et al. 2008). This is because spent nucleotides are charged molecules while imidazole activated nucleotides are not charged at neutral pH. This would have directly impinged on the permeability of the activated nucleotides across the bilayer, as the charge difference could have resulted in pertinent monomers being selectively favoured for replication over inhibition. This possibility is currently being investigated systematically by us. Significantly, this would have also depended on the nature of the protocellular membrane, thereby providing another selection pressure that could have also helped in potentially shaping the prebiotic amphiphilic landscape on the early Earth.

Discerning the aforementioned aspects could shed light on whether the lipid boundary (and the type thereof) could have also saved replication reactions from spent monomers present in the vicinity, in addition to protecting them from parasitic sequences and metabolites. Taken together, our study comprehensively exemplifies how chemical diversity of the prebiotic soup, especially in the context of the concentration and affinity of its constituents towards templating bases, could have directly affected the error rates of nonenzymatic template-directed replication reactions.

3.5. Summary of the work:

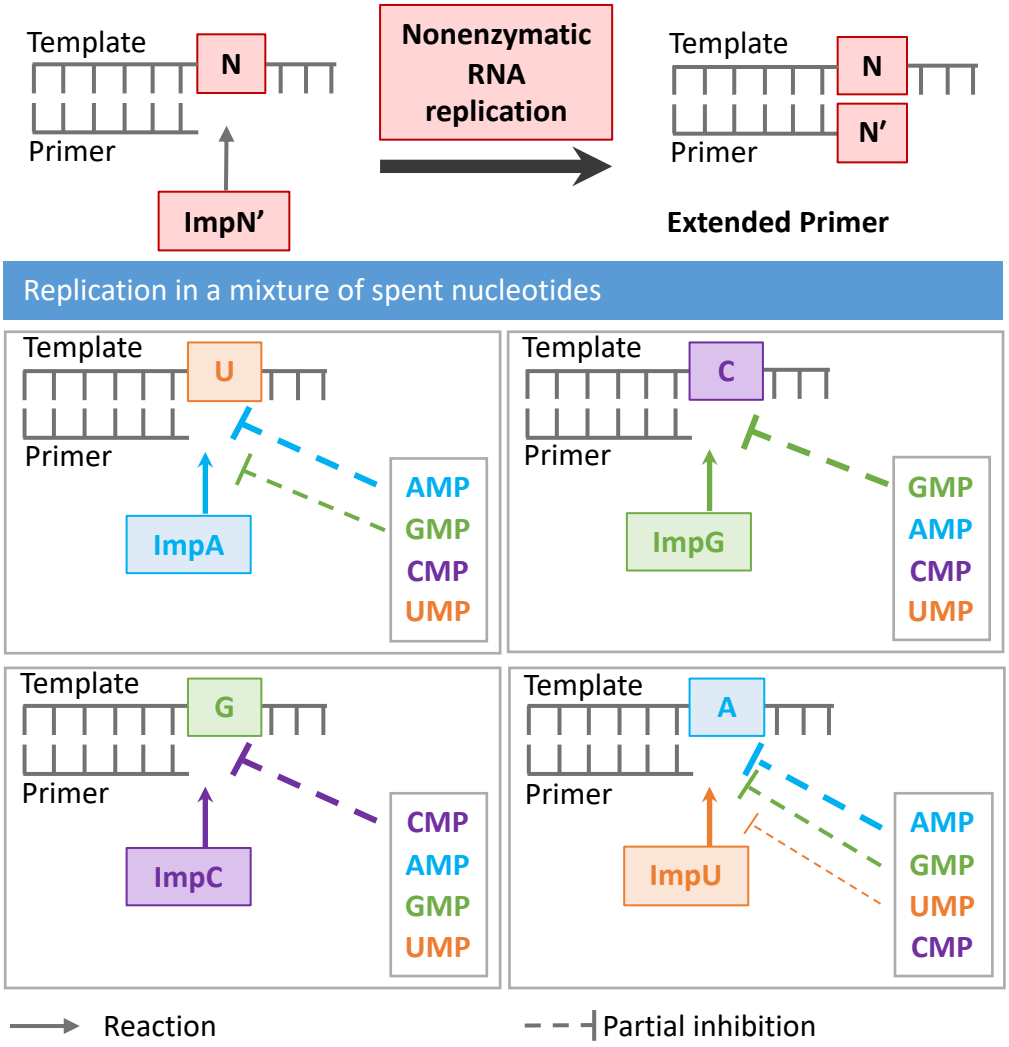

3.6. References:

1. Adamala K, Szostak JW (2013) Non-enzymatic template-directed RNA synthesis inside model protocells. Science 342:1098–1100. https://doi.org/10.1126/science.1241888

2. Bapat NV, Rajamani S (2018) Templated replication (or lack thereof) under prebiotically pertinent conditions. Sci Rep 8:15032. https://doi.org/10.1038/s41598-018-33157-9

3. Bapat NV, Rajamani S (2015) Effect of Co-solutes on Template-Directed Nonenzymatic Replication of Nucleic Acids. J Mol Evol 81:72–80. https://doi.org/10.1007/s00239-015-9700-1

4. Blain JC, Szostak JW (2014) Progress Toward Synthetic Cells. Annu Rev Biochem 83:615–640. https://doi.org/10.1146/annurev-biochem-080411-124036

5. Dagar S, Sarkar S, Rajamani S (2023) Nonenzymatic Template-Directed Primer Extension Using 2′-3′ Cyclic Nucleotides Under Wet-Dry Cycles. Orig Life Evol Biosph. https://doi.org/10.1007/s11084-023-09636-z

6. Dagar S, Sarkar S, Rajamani S (2020) Geochemical influences on nonenzymatic oligomerization of prebiotically relevant cyclic nucleotides. RNA 26:756–769. https://doi.org/10.1261/rna.074302.119

7. Deck C, Jauker M, Richert C (2011) Efficient enzyme-free copying of all four nucleobases templated by immobilized RNA. Nature Chem 3:603–608. https://doi.org/10.1038/nchem.1086

8. Desai R, Kilburn D, Lee H-T, Woodson SA (2014) Increased Ribozyme Activity in Crowded Solutions*. Journal of Biological Chemistry 289:2972–2977. https://doi.org/10.1074/jbc.M113.527861

9. Ellis RJ (2001) Macromolecular crowding: obvious but underappreciated. Trends in Biochemical Sciences 26:597–604. https://doi.org/10.1016/S0968-0004(01)01938-7

10. Gilbert W (1986) Origin of life: The RNA world. Nature 319:618–618. https://doi.org/10.1038/319618a0

11. Hagenbuch P, Kervio E, Hochgesand A, et al (2005) Chemical Primer Extension: Efficiently Determining Single Nucleotides in DNA. Angew Chem 117:6746–6750. https://doi.org/10.1002/ange.200501794

12. Izgu EC, Fahrenbach AC, Zhang N, et al (2015) Uncovering the Thermodynamics of Monomer Binding for RNA Replication. J Am Chem Soc 137:6373–6382. https://doi.org/10.1021/jacs.5b02707

13. Jash B, Tremmel P, Jovanovic D, Richert C (2021) Single nucleotide translation without ribosomes. Nat Chem 13:751–757. https://doi.org/10.1038/s41557-021-00749-4

14. Jin L, Kamat NP, Jena S, Szostak JW (2018) Fatty Acid/Phospholipid Blended Membranes: A Potential Intermediate State in Protocellular Evolution. Small 14:1704077. https://doi.org/10.1002/smll.201704077

15. Kanavarioti A, Bernasconi CF, Baird EE (1998) Effects of Monomer and Template Concentration on the Kinetics of Nonenzymatic Template-Directed Oligoguanylate Synthesis. J Am Chem Soc 120:8575–8581. https://doi.org/10.1021/ja9807237

16. Kervio E, Claasen B, Steiner UE, Richert C (2014) The strength of the template effect attracting nucleotides to naked DNA. Nucleic Acids Research 42:7409–7420. https://doi.org/10.1093/nar/gku314

17. Kervio E, Sosson M, Richert C (2016) The effect of leaving groups on binding and reactivity in enzyme-free copying of DNA and RNA. Nucleic Acids Res 44:5504–5514. https://doi.org/10.1093/nar/gkw476

18. Kilburn D, Roh JH, Behrouzi R, et al (2013) Crowders Perturb the Entropy of RNA Energy Landscapes to Favor Folding. J Am Chem Soc 135:10055–10063. https://doi.org/10.1021/ja4030098

19. Leslie E. O (2004) Prebiotic Chemistry and the Origin of the RNA World. Critical Reviews in Biochemistry and Molecular Biology 39:99–123. https://doi.org/10.1080/10409230490460765

20. Leu K, Kervio E, Obermayer B, et al (2013) Cascade of Reduced Speed and Accuracy after Errors in Enzyme-Free Copying of Nucleic Acid Sequences. J Am Chem Soc 135:354–366. https://doi.org/10.1021/ja3095558

21. Liu Z, Chen J, Bai Q, et al (2022) Coacervate Formed by an ATP-Binding Aptamer and Its Dynamic Behavior under Nonequilibrium Conditions. Langmuir 38:6425–6434. https://doi.org/10.1021/acs.langmuir.2c00580

22. Loeb LA, Kunkel TA (1982) Fidelity of DNA Synthesis. Annual Review of Biochemistry 51:429–457. https://doi.org/10.1146/annurev.bi.51.070182.002241

23. Mansy SS, Schrum JP, Krishnamurthy M, et al (2008) Template-directed synthesis of a genetic polymer in a model protocell. Nature 454:122–125. https://doi.org/10.1038/nature07018

24. Nakano S, Miyoshi D, Sugimoto N (2014) Effects of Molecular Crowding on the Structures, Interactions, and Functions of Nucleic Acids. Chem Rev 114:2733–2758. https://doi.org/10.1021/cr400113m

25. Nakashima KK, van Haren MHI, André AAM, et al (2021) Active coacervate droplets are protocells that grow and resist Ostwald ripening. Nat Commun 12:3819. https://doi.org/10.1038/s41467-021-24111-x

26. Prabahar KJ, Ferris JP (1996) Adenine derivatives as phosphate activating groups for prebiotic RNA synthesis. Origins Life Evol Biosphere 26:251–252. https://doi.org/10.1007/BF02459740

27. Rajamani S, Ichida JK, Antal T, et al (2010) Effect of Stalling after Mismatches on the Error Catastrophe in Nonenzymatic Nucleic Acid Replication. J Am Chem Soc 132:5880–5885. https://doi.org/10.1021/ja100780p

28. Robertson MP, Joyce GF (2012) The origins of the RNA world. Cold Spring Harb Perspect Biol 4:a003608. https://doi.org/10.1101/cshperspect.a003608

29. Szostak JW (2012) The eightfold path to non-enzymatic RNA replication. Journal of Systems Chemistry 3:2. https://doi.org/10.1186/1759-2208-3-2

30. Vogel SR, Deck C, Richert C (2005) Accelerating chemical replication steps of RNA involving activated ribonucleotides and downstream-binding elements. Chem Commun 4922–4924. https://doi.org/10.1039/B510775J

31. Walton T, Zhang W, Li L, et al (2019) The Mechanism of Nonenzymatic Template Copying with Imidazole-Activated Nucleotides. Angewandte Chemie International Edition 58:10812–10819. https://doi.org/10.1002/anie.201902050

Chapter 4

CHARACTERIZING MIXED SINGLE-CHAIN AMPHIPHILE-BASED COACERVATES AS A ROBUST PROTOCELL SYSTEM

Adapted from: *ChemBioChem*, 202500437

4.1.Introduction:

Modern living cells are comprised of an enormous framework of biomolecules and biochemical reactions that are spatially concentrated in different regions by a fundamental principle of compartmentalization (Ovádi and Saks 2004; Zhao and Zhang 2020). Although spatially segregated, these compartments perform biochemical reactions in a harmonious and consistent manner so as to produce energy and raw materials that is required for the cell to undergo growth and division. These complex entities are considered a result of evolution from much simpler compartmentalized systems, which are considered to have existed on the prebiotic Earth (Szostak et al. 2001; Blain and Szostak 2014). These primordial compartments known as 'protocells' are hypothesized to have formed in the prebiotic soup. They would have possessed the ability to concentrate monomeric molecules and oligomers like nucleic acids/proteins, while also facilitating prebiotically plausible reactions, and undergoing growth and division (Joyce and Szostak 2018; Schrum et al. 2010; Mansy et al. 2008). In this regard, study of prebiotically plausible protocells has mainly involved the characterization of two types of model systems – membrane bound fatty acid-based vesicles and membraneless compartments that are formed by liquid-liquid phase separation (LLPS).

The reasons why fatty acid vesicles have been extensively studied as model protocells are multifold (Gebicki and Hicks 1973; Hargreaves and Deamer 1978; Morigaki and Walde 2007; Chen and Walde 2010; Sarkar et al. 2020b; Das et al. 2024). First, small chain fatty acids (SCFAs) are thought to have been exogenously delivered on the early Earth (Deamer 1985; Deamer and Pashley 1989; Monnard and Walde 2015; Lai et al. 2019) and their terrestrial synthesis under prebiotically plausible conditions has also been demonstrated (McCollom et al. 1999; Rushdi and Simoneit 2001). Second, they form vesicles spontaneously when the pH of the surrounding environment is close to the pKa of their carboxylic acid head group (Deamer 1985; Morigaki and Walde 2007). Third, they have the potential to encapsulate a range of solutes, including small molecules, nucleic acids, proteins, and the capacity to facilitate related prebiotically pertinent reactions such as nonenzymatic oligomerization/replication and ribozyme catalysis, etc (Chen et al. 2005; Mansy et al. 2008; Maurer and Monnard 2011; Monnard and Walde 2015; Deamer 2016; Saha et al. 2018).

The aforementioned are the properties that also make them resemble today's cellular compartments. However, pure fatty acid vesicles are stable only over a narrow pH range. In order to increase the stability of these vesicles over a wide pH range, mixed amphiphile systems have been characterized extensively (Apel et al. 2002; Sarkar et al. 2020a, b). Specifically,

doping the pure fatty acid system with alcohol and glycerol monoester containing derivatives has been shown to substantially increase the stability of the vesicles across a broad range of pH and salt concentrations (Apel et al. 2002; Sarkar et al. 2020b). Despite these characteristics of fatty acid-based vesicles that make it close-to-ideal as a model protocell, the bilayer membrane acts as a semipermeable barrier to the diffusion of large and polar molecules across the membrane.

Conversely, compartments formed by LLPS, including aqueous two-phase systems (ATPS) or coacervates, act as open systems that allow ready diffusion of solute molecules within the compartment as well as with the bulk solution (Keating 2012; Poudyal et al. 2018; Jia et al. 2019, 2021). Further, LLPS compartments have been shown to sequester biomolecules, and consequently increase their effective concentration within these compartments by several orders of magnitude (Koga et al. 2011; Strulson et al. 2012; Frankel et al. 2016). Additionally, they have also been demonstrated to increase the rate of ribozyme-based as well as metabolic reactions (Koga et al. 2011; Strulson et al. 2012; Poudyal et al. 2018, 2019; Drobot et al. 2018; Smokers et al. 2022, 2024).

With an aim to explore such 'open' systems as protocell models, several LLPS systems have been developed and studied over the last decade (Poudyal et al. 2018). Recently, a myristic acid-guanidinium hydrochloride-based system was described, where the myristic acid was shown to reversibly transition from vesicles (at pH 8.5) to coacervates (at pH 9.5). This was shown to result from the interaction of guanidinium ions with higher order aggregates of micelles, which form at alkaline pH (Garenne et al. 2016a, b). Even though this system seems prebiotically relevant; the resultant coacervates were shown to sequester RNA poorly as a result of the negatively charged interior.

This problem of alkaline pH was partially circumvented by the demonstration of a coacervate system that used decanoic acid vesicles, which were shown to transition into coacervate droplets upon addition of dopamine (Zhou et al. 2022b). However, dopamine is known to form polydopamine as a result of spontaneous oxidation, which led to the collapse of the coacervate upon increasing the pH beyond 7.5 (Zhou et al. 2022b). Moreover, the system was found to be stable for only a short time (~1 hr) after which it started forming crystals (Zhou et al. 2022a). Furthermore, it was shown to sequester hydrophobic and cationic molecules by 1-2 orders of magnitude when compared to anionic molecules, thus rendering the system less efficient for the sequestration of RNA (Zhou et al. 2022b). In this context, the efficient

sequestration of hydrophobic molecules has been ascribed to the disordered 'sponge-like' internal structure of these fatty acid coacervates having hydrophobic domains and hydrophilic interfaces. Notably, lipid sponge droplets composed of mixed non-ionic single-chain amphiphiles have also been shown to be versatile biomimetic systems. They have been shown to demonstrate programmable behaviour, selective molecular sequestration and capacity to enhance biochemical reaction rates (Bhattacharya et al. 2020). Further, DNA functionalized lipid sponge droplets have been shown to facilitate the uptake of complementary strands, and their release by strand displacement reactions, demonstrating intriguing properties of fatty acid-based coacervates (Cho et al. 2022).

In the aforementioned backdrop, we set out to characterize short chain fatty acids that could not only form coacervates but also sequester RNA; an important informational molecule of the RNA World. In addition to being prebiotically relevant when compared to systems comprising of polymer-based coacervates (such as PDDA-spermine), short chain fatty acids are hypothesized to be prebiotically more abundant than the longer chain fatty acids (McCollom et al. 1999; Rushdi and Simoneit 2001; Lai et al. 2019). Nonetheless, they are much less explored than longer chain fatty acids as compartmentalization systems because those that can form vesicles (especially C8-10 chain length SCAs), result in very dynamic and, consequently, leaky membranes.

In this study, we characterized a C9-based mixed amphiphile coacervate system. We demonstrate how these nonanoic acid (NA) and nonanol (NOH) containing vesicles transition into coacervates upon the addition of tyramine (Tyra). The resultant NA-NOH/Tyra coacervates undergo coalescence, a quintessential property of LLPS; while also readily forming droplets upon mixing even after several days, unlike the previously described system (decanoic acid-dopamine). Furthermore, they were found to be stable across pHs (from pH 7 to 9), and temperatures ranging from 5°C to 65°C. Pertinently, they also could sequester biomolecules such as protein and RNA.

To the best of our knowledge, we report for the first time a mixed amphiphile-based coacervate system, which can tolerate various prebiotically pertinent selection pressures as well as sequester biomolecules like RNA, making it a robust protocellular model than the pure fatty acid-based coacervates. In all, these studies underline how the compositional heterogeneity of the prebiotic soup could have enabled the formation of robust SCA-based coacervates; entities that were minimally discussed in the context of vesicle systems. Further, such studies enable

describing amphiphilic moieties that can eventually be used in fabricating multi-compartment cells, setting the stage for characterizing more extant cell-like entities wherein physicochemically distinct LLPS compartments could be used to facilitate different kinds of reactions within the same protocell.

4.2. Materials and methods:

4.2.1. Materials:

Nonanoic acid (N5502-25G), 1-nonanol (131210-100ML), dopamine hydrochloride (PHR1090-1G) and tyramine hydrochloride (T2879-25G) were purchased from Sigma-Aldrich (Bangalore). Tris base was procured from Himedia. $MgCl_2$ hexahydrate was procured from Qualigens. NaCl was purchased from Sigma-Aldrich (Bangalore). Cy3-labelled RNA (for sequestration) was obtained from Sigma (Bangalore). Glass slides and coverslips (18 mm × 18 mm) were obtained from Himedia. Adenoside-5'-phosphorimidazolides (ImpA) was purchased from GLSynthesis Inc. The RNA primer used here was terminated with a 3′-amino-2′,3′-dideoxynucleotide (Amino G primer) and was acquired from Keck laboratory, Yale, USA. It was gel purified before use. The template was purchased from Sigma-Aldrich (Bangalore) and it was used without any further purification. All other reagents (analytical grade) were purchased from Sigma-Aldrich.

Sequences of the RNAs used in the study are as follows:

1. RNA used for sequestration experiments: (Cy3) 5′ GG GAU UAA UAC GAC UCA CUG G
2. Amino G Primer: (Cy3) 5′ GG GAU UAA UAC GAC UCA CUG-NH_2
3. Template: 5′ AGU GAU CU**U** CAG UGA GUC GUA UUA AUC CC
   (The nucleotide mentioned in bold is the templating base.)

4.2.2. Methods:

4.2.2.1.Preparation of Tyramine stock:

A 500 mM Tyramine stock was prepared by dissolving tyramine hydrochloride in 200 mM Tris buffer, pH 8. The solution was filtered through 0.22 μm syringe filter and the stock was stored in -40°C.

4.2.2.2.Preparation of NA-NOH/Tyra coacervate droplets:

Nonanoic acid and nonanol were mixed in 10:1 ratio in a microcentrifuge tube at room temperature, vortexed to ensure proper mixing, and briefly centrifuged using a benchtop centrifuge to avoid sticking of the contents to the walls of the tube. Then 200 mM Tris buffer of pH 8 was added to the above mixture and vortexed vigorously to prepare 150 mM NA-NOH vesicle stock. While preparing NA-NOH/Tyra droplets, NA-NOH vesicles were added at desired concentration to the diluent (200 mM Tris buffer with pH 8) and were mixed, and the desired amount of tyramine was then added. As soon as tyramine was added to the vesicles, the sample turned turbid, indicating the transition into coacervate droplets. It was then thoroughly mixed by gentle pipetting.

4.2.2.3.Slide preparation and microscopy:

Glass slides were first rinsed with water and cleaned thoroughly, and were kept soaked in 1M HCl overnight. They were then rinsed with water extensively to remove any traces of the acid. For imaging, the coacervate sample was applied onto the clean glass slide, a coverslip was placed on it and was immediately sealed with nail polish. Olympus BX63 system was used for acquiring DIC images (using 20X/0.50 NA and 100X/1.4 NA objectives) while Zeiss LSM 710 system was used for acquiring confocal images and for performing FRAP (63X/1.4 objective). All images were analyzed using FIJI (FIJI Is Just ImageJ) software.

4.2.2.4.Optical density (OD) measurements:

To carry out turbidity assays, 100 μL coacervate sample was prepared and was gently mixed by pipetting. 80 μL of the sample was then dispensed in a 96 well plate for measuring the OD at 600 nm. The samples in the plate were read using a Perkin Elmer EnSight plate reader.

4.2.2.5.Selection Pressure experiments:

All these experiments were carried out on 60/100 NA-NOH/Tyra coacervates.

i) Salt tolerance:

$MgCl_2$ or NaCl was added to 100 μL of preformed coacervates at the desired concentration. The sample was mixed well and was imaged using DIC microscopy and checked for OD at 600 nm using plate reader. Addition of $MgCl_2$ above 20 mM concentration resulted in the formation of precipitates in the sample as soon as the sample was mixed.

ii) Temperature tolerance:

100 µL coacervate sample was prepared and was incubated at the desired temperatures for 30 minutes. They were then immediately imaged using DIC microscopy and checked for OD at 600 nm using plate reader.

4.2.2.6.Fluorescence recovery after photobleaching (FRAP):

FRAP experiments were performed by exciting the sequestered GFP within the droplets at 488 nm. The diameter of the droplets that was selected for performing FRAP ranged between 5 to 10 µm. A sequence of 10 images was taken as pre-bleach images. For bleaching, a region of interest (ROI) having an area of 1 μm^2 was placed at the center of the droplet and it was bleached using 100% of 488 nm and 405 nm laser power, and the fluorescence intensity change in the bleached ROI was recorded by checking the emission between 493 to 797 nm. To analyze the FRAP data, ROIs of areas 1μm^2 were used to measure the average florescence intensity of the bleached spot, the reference spot (a site away from the bleached spot on the same droplet), and that of the background (outside the droplet). Average fluorescence intensities of the aforementioned ROIs were also measured for all the pre-bleach images. As reported earlier, double normalization was carried out by using the following equation:

$$\text{I (t)} = \frac{[BL(t) - BG(t)]/[REF(t) - BG(t)]}{[BL(0) - BG(0)]/[REF(0) - BG(0)}$$

… (Equation 2)

Normalized fluorescence intensities were then plotted against time, and the recovery curve was fitted assuming single exponential recovery kinetics, with the following equation:

$$Y = Y_0 + (Plateau - Y_0)(1 - e^{-Kx})$$

… (Equation 3)

Where, Y is the fluorescence intensity at time t, Y0 is the fluorescence intensity at time 0, plateau is the fluorescence intensity at infinite times, and K is the rate constant, expressed as reciprocal of time units on X axis. Analysis was carried out in GraphPad Prism 10, and values for half-time of recovery were obtained for all the thirty droplets analyzed across the three experimental replicates. Furthermore, apparent diffusion coefficient was calculated using the following equation:(Aumiller et al. 2016)

$$\text{Apparent diffusion coefficient} = \frac{0.88r^2}{4\tau_{1/2}}$$

where r is the radius of the bleached area, $\tau_{1/2}$ is the half-time of recovery of fluorescence.

… (Equation 4)

4.2.2.7.Laurdan Generalized Polarization (GP):

Laurdan was added at a final concentration of 5 μM to the coacervate (or vesicle) sample and the sample was incubated at room temperature for 5 mins. Laurdan emission was recorded from 400 nm to 600 nm, and GP value was calculated using the following equation:

$$GP = \frac{I_{430} - I_{500}}{I_{430} + I_{500}}$$

where I_{430} and I_{500} are the fluorescence intensities at 430 and 500 nm, respectively.

… (Equation 5)

4.2.2.8.Confocal microscopy for RNA sequestration:

Cy3 labelled RNA (5 μM) was added to 60 mM NA-NOH vesicles in 200 mM Tris, pH 8 and the sample was mixed properly. This was followed by inducing coacervation by adding tyramine at a final concentration of 100 mM. The sample was incubated for 5 mins before imaging. The sample on the glass slide was excited using 561 nm laser. We observed increased fluorescence in the droplets with the addition of lysine or arginine at the time of standardizing the experiment. Therefore, to stay below saturation in all the cases and be able to quantify images, we first imaged samples that contained arginine and standardized the microscope settings, mainly the digital gain and the laser power.

After confirming that there was no saturation in any image, the rest of the samples containing no amino acid (control) were imaged under exactly identical settings. All the images were analyzed using particle analysis in FIJI. While analyzing the particles, we excluded particles below 3 μm. We recorded the integrated densities of the droplets and the mean intensity of the background. The background intensity was then subtracted from the integrated density values for the droplets and plotted these values on the Y axis. Kruskal-Wallis test for performed on the dataset by using GraphPad Prism 10.

4.2.2.9.Template-directed nonenzymatic replication of RNA in the coacervate phase:

A previously standardized reaction scheme was used to perform the template-directed nonenzymatic replication reaction in the coacervate phase.(Rajamani et al. 2010; Bapat and Rajamani 2015; Patki and Rajamani 2023) Specifically, we first added the primer (0.325 μM)

and template (1.3 μM) in 200 mM Tris at pH 8 and heated the sample to 90 °C for 5 mins. This was followed by flash cooling on ice and centrifuging the sample briefly. Subsequently, NA-NOH vesicles (60 mM), amino acid (25 mM Lys or Arg) and tyramine (100 mM) were added and the sample was incubated for 5 mins. The control reaction had no amino acid added to the reaction. Following this, imidazole activated nucleotide (ImpA) was added at a final concentration of 10 mM and the sample was immediately centrifuged at 14000 rcf for 2.5 mins at 15 °C.

Coacervate phase was then separated from the bulk phase and was incubated at 25 °C for 2 hrs. This was followed by the addition of 7 μL TBE buffer containing 8 M urea and freezing the samples at -40 °C. Before loading the samples on 22 % denaturing urea PAGE, non-labelled RNA having an exactly identical sequence as that of the primer was added in 50 times excess when compared to the primer. The loading dye was added and this was followed by heating the sample at 90 °C for 5 mins and flash cooling on ice.(Rajamani et al. 2010; Bapat and Rajamani 2015; Patki and Rajamani 2023) For zero time point, a control reaction was set up where the coacervate phase was separated and immediately frozen as mentioned earlier albeit without incubating.

4.3. Results

4.3.1. A mixed amphiphile-based coacervate system as a prebiotic model protocell

With an intention to discern short chain fatty acids other than decanoic acid that can form coacervates, we first checked whether dopamine (DPA) could induce vesicle to coacervate transition in pure nonanoic acid (NA) vesicles. We used dopamine, because it was earlier reported to induce vesicle to coacervate transition in decanoic acid (DA) vesicles. When dopamine was added to nonanoic acid vesicles at pH 7, an increase in turbidity as observed in the sample, which upon visualizing under microscope, showed droplets, as reported for DA vesicles (Zhou et al. 2022b). The stability of the droplets was evaluated across different pHs (7, 8, and 9) since prebiotic pools are thought to have had variable pH because of their diverse constituents (Mulkidjanian et al. 2012; Sarkar et al. 2020a).

Droplets were observed only at pH 7 and this can be attributed to the absence of nonanoic acid vesicles at pHs above 7 (Figure 4.1a, upper panel). To increase the pH range across which coacervate droplets could be observed, pure nonanoic acid was doped with nonanol (NOH) in 10:1 ratio to prepare NA-NOH mixed vesicles (Figure 4.2). This is because, ‘vesicle to

coacervate' transition would require vesicles to exist in the first place, and NA-NOH system has been shown to form vesicles across a broad range of pHs (Apel et al. 2002). Relevantly, with the NA-NOH/DPA system, we observed coacervate droplets at all the three pHs (Figure 4.1b, lower panel).

A protocellular system that can tolerate a broad range of pHs would have had higher chances of survival in the environment of changing pH on the early Earth. Thus, the mixed amphiphile-based coacervate system would have been beneficial over the pure system under related selection pressures. In this regard, we wish to highlight that although the importance of compositional heterogeneity in the formation of robust protocells has been established for fatty acid vesicles, it is largely unexplored in the context of coacervate-based systems (Dworkin et al. 2001; Schrum et al. 2010; Rendón et al. 2012; Sarkar et al. 2020a, b).

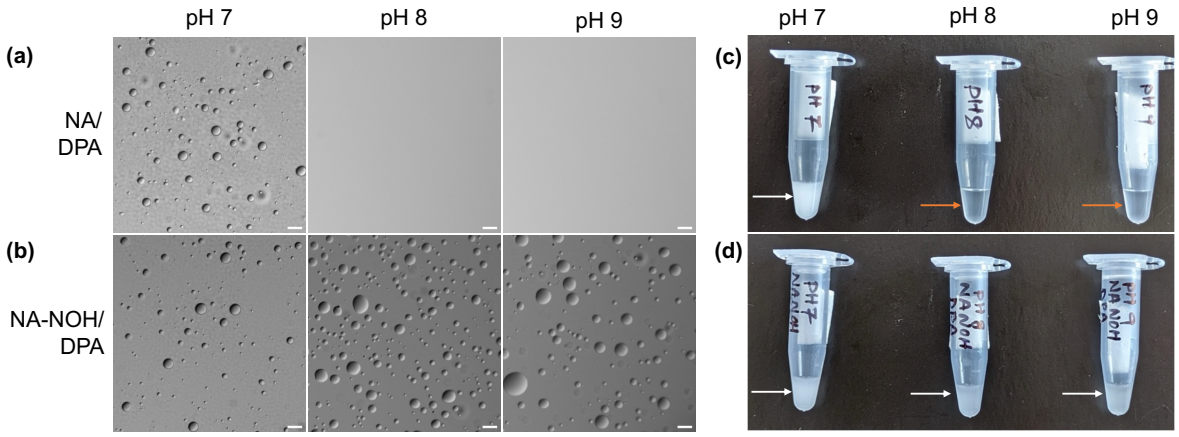

Figure 4.1: Compositional heterogeneity forms robust coacervate droplets. Pure NA/DPA based coacervates forming only at pH 7 **(a)**, and the reflection of their presence on the turbidity of the samples **(c)**. **(b)** Compositionally diverse, mixed NA-NOH/DPA based coacervates forming across a broad pH range (7 to 9), and the reflection of their presence on the turbidity of the samples **(d)**. The white and the orange arrows in **(c)** and **(d)** represent turbid samples and clear samples, respectively. Scale bar: 20 μm. N=3.

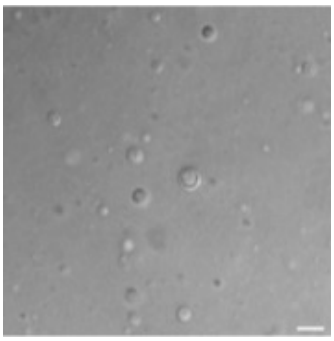

Figure 4.2: 60 mM NA:NOH (10:1) vesicles at pH 8. Differential interference contrast (DIC) image showing the presence of NA-NOH vesicles. Scale bar: 10 μm.

4.3.2. Towards constructing robust NA-NOH-based coacervates: Replacing dopamine with tyramine

Dopamine is known to undergo spontaneous oxidation to form polydopamine. Hence, it could be hypothesized that when dopamine is used for inducing coacervation, it would get consumed over the course of time in the absence of any reducing agent. In order to check whether the NA-NOH/DPA droplets could persist even after the spontaneous oxidation of dopamine, we prepared NA-NOH/DPA droplets in the absence of any reducing agent and observed the presence of droplets over time. We observed that the sample progressively turned brown with time (Figure 4.3).

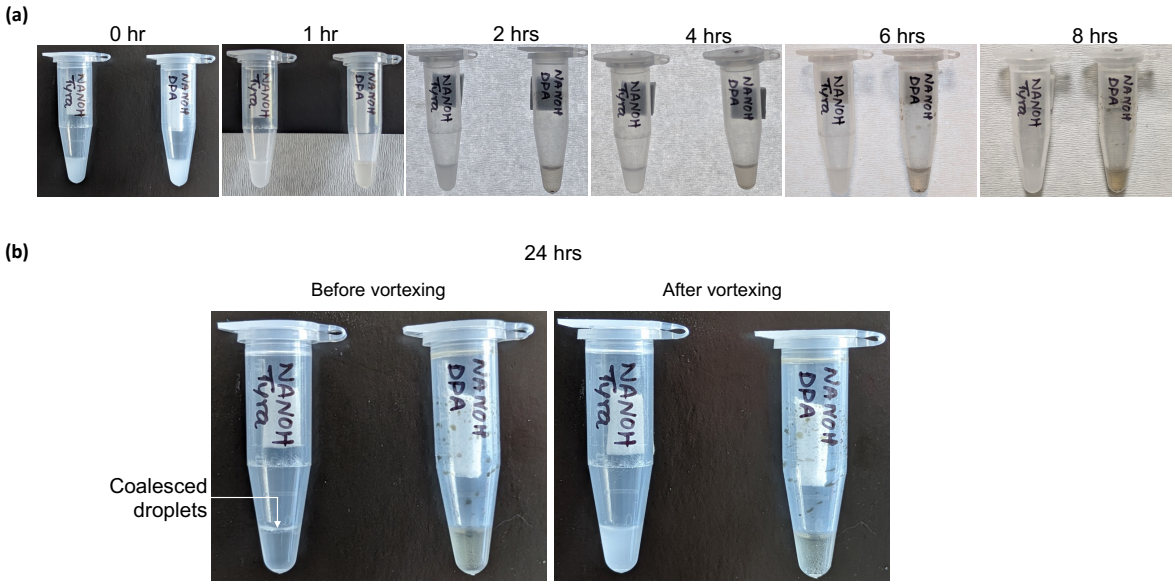

Figure 4.3: NA-NOH/Tyra system is more robust than NA-NOH/DPA system. 100 µL samples of 60/100 NA-NOH/Tyra and NA-NOH/DPA were prepared, which were monitored over time. **(a)** Due to spontaneous oxidation of dopamine (DPA), the NA-NOH/DPA sample started to turn brown in 1 hour itself, and progressively became darker. **(b)** Upon incubating the samples at room temperature for 24 hours, the NA-NOH/Tyra droplets coalesced, which came at the top because of their lesser density than the bulk solution. However, upon vortexing, the solution turned turbid, reforming the droplets. On the other hand, the NA-NOH/DPA system remained brown and clear even after vortexing.

Additionally, on microscopic analysis, it was qualitatively observed that the number of droplets went down with time and no droplets could be observed after 8 hours (Figure 4.4a). This indicated that the consumption of dopamine through its spontaneous oxidation was resulting in the reduction in the number of NA-NOH/DPA droplets with time possibly due to their disruption.

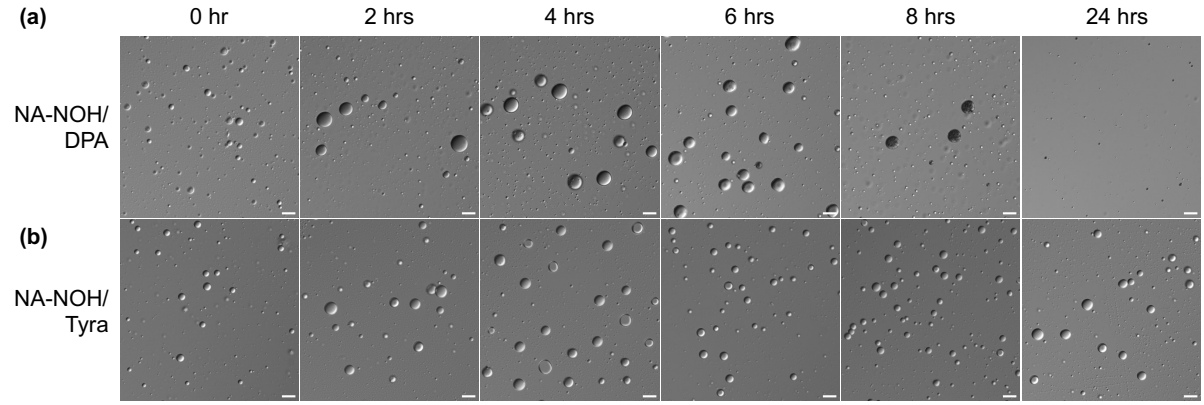

Figure 4.4: Microscopic observation of NA-NOH/Tyra droplets over a period of 24 hours It was observed that the NA-NOH/DPA droplets started to turn darker with time. Furthermore, they could not be observed after 6 hours **(a)**. To increase the stability and the robustness of the system, DPA was replaced with Tyra as it does not undergo spontaneous oxidation like DPA does. Indeed, the NA-NOH/Tyra system continued to form coacervate droplets over a much longer time (24 hours) **(b)** than NA-NOH/DPA system. Scale bar: 20 μm. N=3.

To overcome the issue of spontaneous oxidation and form a more robust and durable coacervate system, dopamine was replaced with tyramine (Tyra) to induce vesicle-to-coacervate transition in NA-NOH vesicles. Dopamine contains a catechol group, which is easily oxidized, leading to polydopamine formation. Tyramine, on the other hand has a phenol group, which is less reactive than catechol and, thus, is more stable under similar conditions. As a result, droplets formed using NA-NOH/tyramine were expected to result in more stable droplets than NA-NOH/DPA. In stark contrast to NA-NOH/DPA droplets, NA-NOH/Tyra droplets could be observed even after days (Figure 4.4b, Figure 4.5). In both the systems, the droplets would coalesce in the tube with time; however, they would reappear upon gentle mixing, making the suspension turbid. This reappearance of droplets after mixing was seen only for the first six hours in NA-NOH/DPA system, whereas, for NA-NOH/Tyra system, the same was observed even after a few days (Figure 4.5).

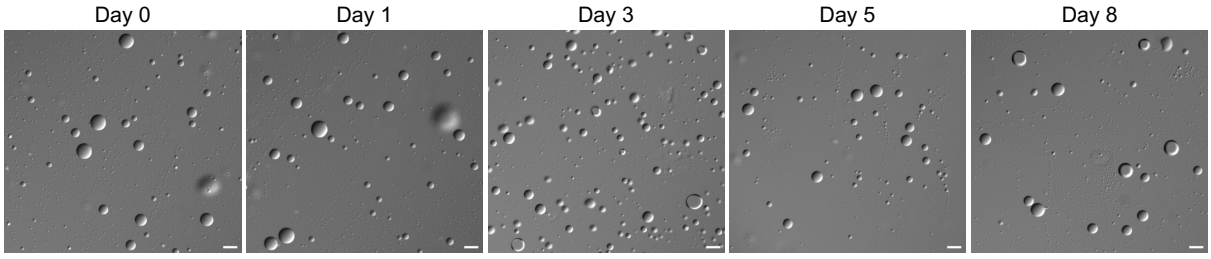

Figure 4.5: Long term stability of NA-NOH/Tyra droplets (DIC microscopy). NA-NOH/Tyra droplets were observed for 8 days, and they were found to form droplets throughout this time frame. 500 μL 60/100 NA-NOH/Tyra droplets were prepared (Day 0). At every time point, the sample was first mixed by gentle tapping followed by pipette mixing, and then 5.5 μL of this mixed sample was observed under 20X objective. Scale bar:

20 μm. The coacervates coalesce over time, and hence, it was necessary to mix the sample well before imaging it. N=3.

Further, at no point did the NA-NOH/Tyra system turn brown, highlighting the robustness of the NA-NOH/Tyra system over the one composed of NA-NOH/DPA. Having established that this new NA-NOH/Tyra system was indeed a more robust coacervate system, we next took a systematic approach to characterize the system for its potential to be acknowledged and used as a model protocell.

Towards this, it was essential to first determine the range of concentrations of NA-NOH and tyramine that resulted in the formation of droplets. It has been reported earlier that the critical vesicle concentration (CVC) of NA-NOH (10:1) system is 20 mM. Since it was established earlier that the presence of NA-NOH vesicles is indeed required for coacervates to form (Figure 4.1 a-d), we chose to stay well above this CVC and worked with total amphiphile concentrations of 40, 50, and 60 mM (Figure 4.6), where the NA-NOH vesicles would surely be present. Next, for every NA-NOH concentration, a range of Tyra concentrations were scanned, beginning with a concentration that was equivalent to that of NA-NOH in the system. A general trend was observed in which the size of the droplets increased upon increasing the concentration of NA-NOH. The spike in the turbidity indicates the transition of the vesicles into droplets (Figure 4.7). In this context, the higher error bars seen in case of 50/80 and 60/70 NA-NOH/Tyra systems (Figure 4.6) may have been because of the different optical properties of these suspensions since they contained a co-existing population of droplets and other higher order aggregates (Figure 4.7). And, at these ratios, there could be transition occurring from vesicles to coacervates. In this study, the notation ‘X/Y’ refers to systems composed of ‘X’ mM NA-NOH and ‘Y’ mM tyramine.

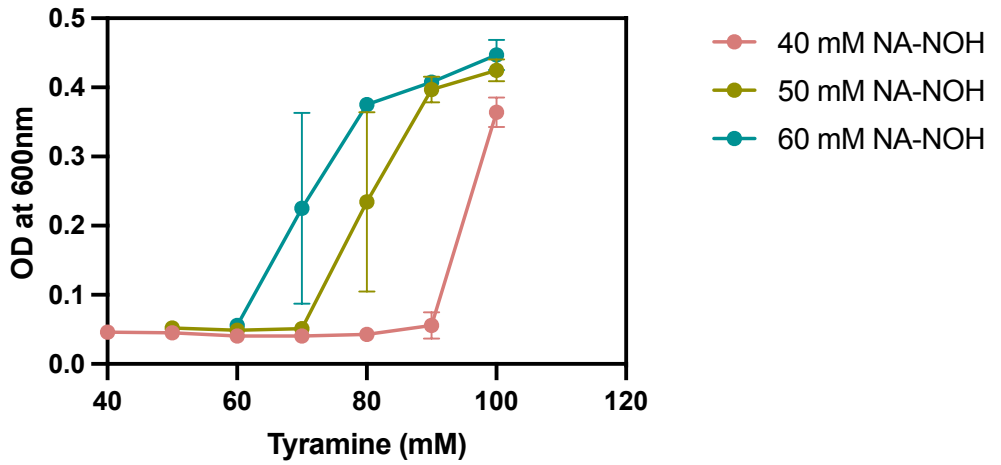

Figure 4.6: Determining the concentration range of NA-NOH and Tyra for droplet formation. 50/80 and 60/70 NA-NOH/Tyra systems are thought to be the transitioning phases, where coexisting populations having different optical properties were observed (Figure 4.7), which may be resulting in the huge error bars in the OD values. Error bars: S.D. N=3.

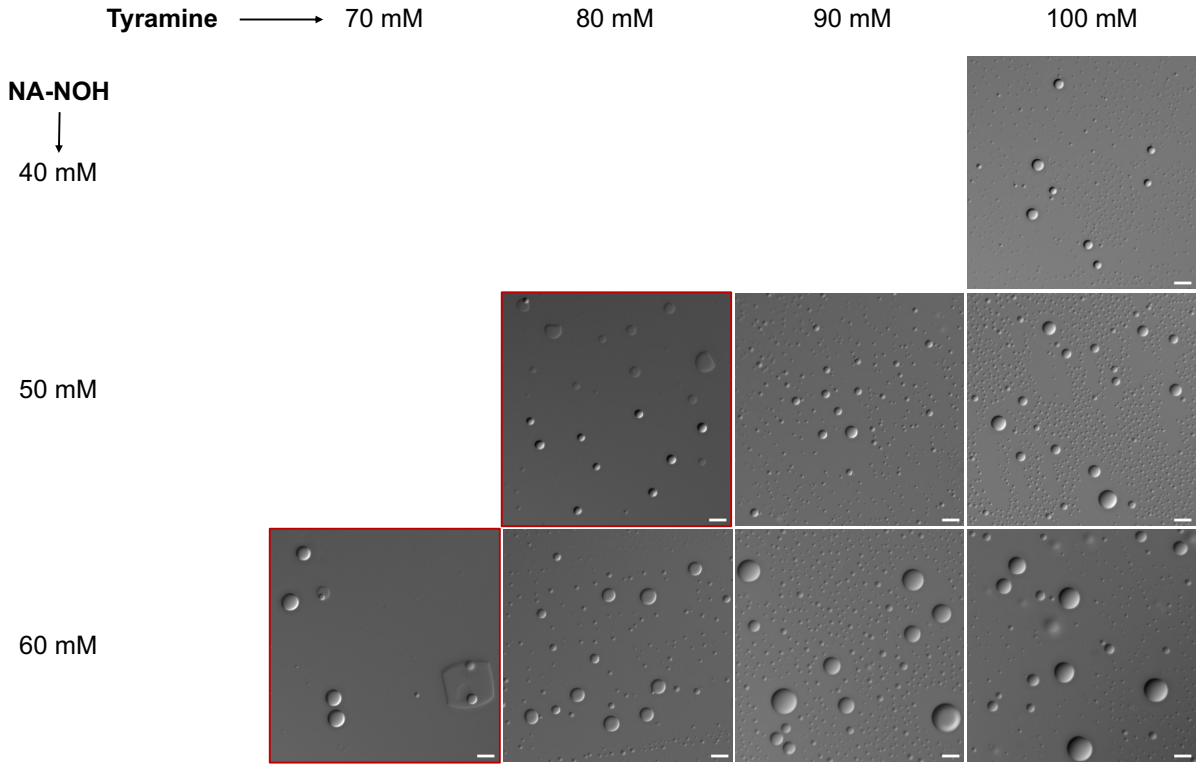

Figure 4.7: DIC Microscopic images of droplets at various NA-NOH and tyramine concentrations. For every concentration of NA-NOH (40, 50, and 60 mM), only those tyramine concentrations are shown where the turbidity readings started to rise in Figure 2a. Images with the red border seemed to represent the concentrations for the transition phase, where droplets can be seen along with other higher order structures. Scale bar: 20 µm. N=3.

Based on microscopic observation, we narrowed down to NA-NOH concentration of 60 mM for all further characterization because it yielded consistent and numerous droplets at and above 80 mM Tyra concentration (Figure 4.7). To further understand the coacervation limit of this system, Tyra concentrations ranging from 60 mM to 350 mM were scanned (Figure 4.8).

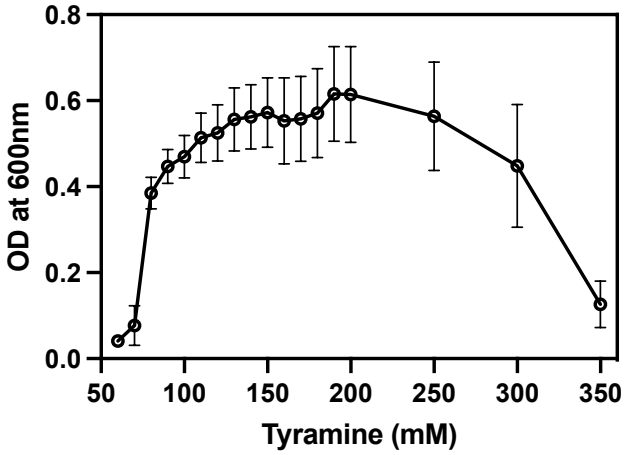

Figure 4.8: Scanning the concentrations of tyramine across which 60 mM NA-NOH forms droplets**.**

It was found that at all the Tyra concentrations that were studied (from 80 mM to 200 mM), droplets were observed (Figures 4.7, 4.9).

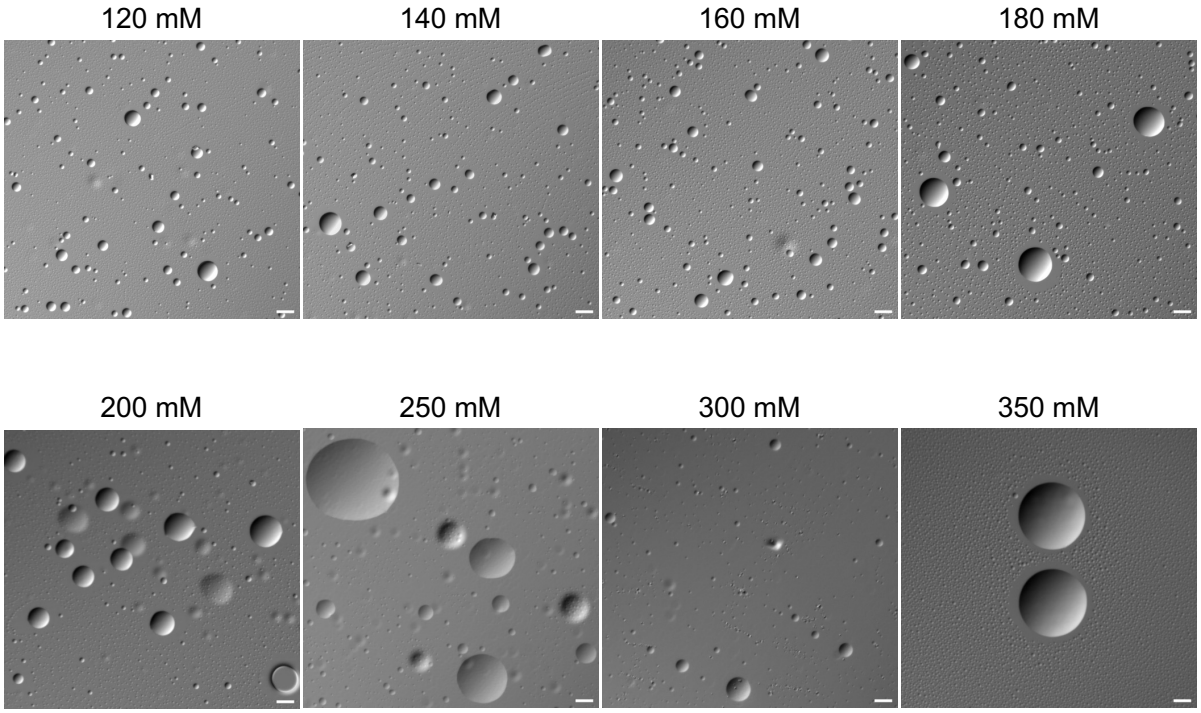

Figure 4.9: Coacervates form across a broad range of tyramine concentrations. For 60 mM NA-NOH concentration, coacervates were observed to be forming across a broad range of tyramine concentrations, from 80

mM (S4) to 200 mM. When the concentration of tyramine was increased beyond 200 mM, huge droplets were observed, which, however, were sticking largely to the glass surface of the slide. Scale bar: 20 μm. N=3.

Furthermore, from visual analysis of microscopy data, it was seen that the size of the droplets was found to increase with increasing Tyra concentration, especially from 140 mM onwards. At 250mM, 300 mM and 350mM Tyra, very few but huge droplets were observed (Figure 4.9). These results suggested that for 60 mM NA-NOH vesicles, coacervates could be observed for a very broad range of Tyra concentrations. Furthermore, we evaluated the micropolarity of the coacervates as a proxy to understand whether the coacervates formed using the different tyramine concentrations, resulted in coacervates with similar internal environment.

Towards this, Laurdan was used as a solvatochromic probe (Klymchenko 2017; Sarkar et al. 2021; Deshpande et al. 2024). and as a first step, the partitioning of Laurdan into the coacervates was checked (Figure 4.10). After ensuring that the emission was being recorded only in the coacervate phase, we went ahead and calculated the generalized polarization (GP) values. Fluorescence emission by Laurdan molecules is sensitive to the polarity (hydration) of its surrounding environment and it emits at 430 nm when the surrounding is hydrophobic. However, if the surrounding environment is hydrophilic, its emission shifts towards 500 nm. Generalized polarization (GP) value quantifies this shift by taking into account the intensities of fluorescence emission at 430 and 500 nm, with a high GP value suggesting a hydrophobic (or nonpolar) environment and a low GP value suggesting a hydrophilic (or polar) environment. The GP value of NA-NOH vesicles increased upon adding tyramine to the vesicles, suggesting that the micropolarity of the coacervates is significantly higher than that of the vesicles (Figure 4.11). Furthermore, statistically non-significant difference was observed across coacervates containing various tyramine concentrations ranging from 80 mM to 350 mM, suggesting that they could have similar microenvironments. The observation that coacervates could be formed at various Tyra concentrations is noteworthy, as there is a plausibility that Tyra or Tyra-like molecules, which can induce vesicle to coacervate transition, may have been available at variable concentrations in the prebiotic soup.

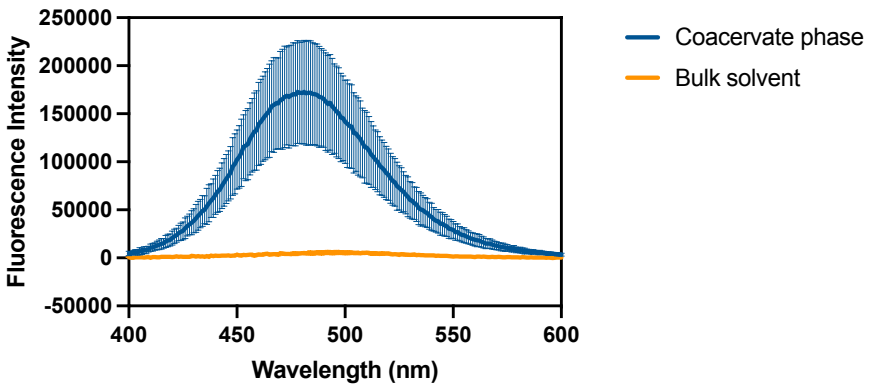

Figure 4.10: Laurdan partitioning into coacervate droplets. In order to determine the Laurdan GP value as a measure of micropolarity inside the coacervate droplets, partitioning of Laurdan in the coacervates was first checked. This was done by adding 5 μM Laurdan into 60/90 droplet preparation, followed by centrifugation and separation of the coacervate phase from bulk solvent. Laurdan emission spectra (from 400 nm to 600 nm.) were then recorded for both the phases. As could be observed, Laurdan emission is seen only in the coacervate phase. This could either be because of the extremely efficient partitioning of Laurdan into the hydrophobic coacervate phase or quenching of Laurdan's fluorescence in the bulk aqueous phase. Error bars: S.D. N=3

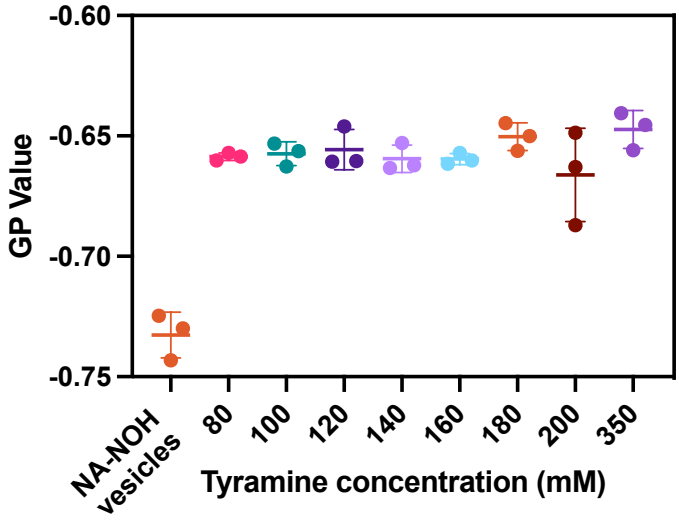

Figure 4.11: Laurdan GP values of coacervates prepared from 60 mM NA-NOH with variable tyramine concentrations. We performed Tuckey's multiple comparisons test on this dataset, where we observed statistically nonsignificant difference between the coacervate samples containing tyramine concentrations ranging from 80 mM to 350 mM ($p > 0.5$). All the populations containing tyramine, however, were found to be statistically significantly different from the corresponding vesicle population ($p < 0.0001$).

4.3.3. NA-NOH/Tyra droplets enable molecular diffusion within the compartments

Life is thought to have emerged in a chemically heterogenous prebiotic soup, where interactions between the reactants would have resulted in the formation of precursors of

biomolecules, including nucleosides, nucleotides, amino acids etc. These, in turn, would have interacted with each other to form more complex biomolecules like nucleic acids, peptides etc. (Leslie E. 2004). However, since the prebiotic soup is thought to have been dilute, mechanisms to concentrate these molecules would have been crucial to facilitate their interactions. In this regard, LLPS compartments have been demonstrated to sequester biomolecules and increase their local concentration by several orders of magnitude than that in the bulk solution, as well as to enhance the rates of the reactions being contained within them (Strulson et al. 2012; Frankel et al. 2016; Poudyal et al. 2018). For molecular reactions to take place inside these compartments, the coacervates should facilitate diffusion of molecules within the interior. Given this, we checked whether the NA-NOH/Tyra droplets can allow molecular diffusion. For this, GFP was sequestered within the droplets and subjected to partial photobleaching, and the fluorescence recovery after photobleaching (FRAP) was monitored.

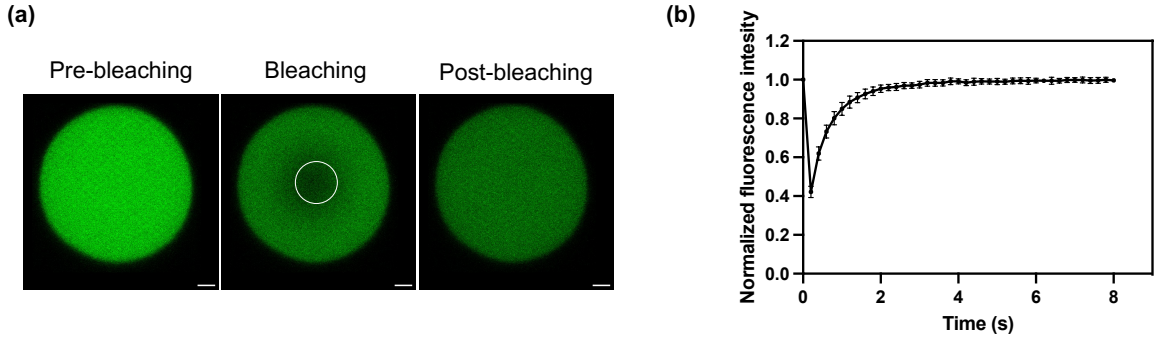

Figure 4.12: FRAP inside the 60/100 NA-NOH/Tyra droplets. To understand whether the NA-NOH/Tyra droplets allow molecular diffusion, 0.5 μM GFP was sequestered within the droplets. Panel **(a)** represents sequestered GFP (pre-bleaching) and partial photobleaching (white circle) of the sequestered GFP followed by fluorescence recovery within the bleached spot (post-bleaching). **(b)** Quantification of FRAP experiments. Error bars: Standard deviation. N=3; n=30. Scale bar: 1μm.

As is evident in Figures 4.12a and 4.12b, the photobleached spot recovered fluorescence, confirming that the droplets allow for molecular diffusion, while also corroborating that the NA-NOH/Tyra droplets are indeed LLPS compartments. The half-time of recovery of fluorescence and the apparent diffusion coefficient of GFP in 60/100 NA-NOH/Tyra system were found to be 0.41 ± 0.07 s and 0.14 ± 0.02 $\mu m^2 s^{-1}$, respectively. Furthermore, this implied that such systems could facilitate prebiotically plausible reactions between the molecules sequestered within the compartments since it allows molecular diffusion. Additionally, it would also support the exchange of molecules with the bulk solution; a process central for taking up fresh nutrients inside these protocells while also allowing for the removal of waste

material out of the system. Thus, fatty acid coacervates provide an advantage over fatty acid vesicles as model protocells, wherein similar kind of ready exchange of molecules is limited by the bilayer of the fatty acid vesicles. In this backdrop, we characterized the tolerance of these systems to various selection pressures to further discern the robustness of NA-NOH/Tyra coacervates as model protocells.

4.3.4. NA-NOH/Tyra system tolerates prebiotically plausible selection pressures

Emergence of early life would have been shaped by ocean tides, hence protocellular assemblies would have required to survive selection pressures such as high salt concentrations, fluctuating pH and temperatures (Saha et al. 2022). Given this, the tolerance of 60/100 NA-NOH/Tyra system towards various concentrations of monovalent (NaCl) and divalent ($MgCl_2$) cations was systematically estimated. As per the RNA World hypothesis, RNAs are thought to have played the dual role of acting as a genetic polymer while also catalyzing chemical reactions (ribozymes) (Gilbert 1986). For the ribozyme to catalyze chemical reactions, the presence of divalent cations, especially Mg^{2+}, is extremely crucial. Such dual-function genetic polymers are thought to have been encapsulated inside protocells to result in functional cellular moieties (Schrum et al. 2010). However, fatty acid vesicles, which have been demonstrated to encapsulate genetic polymers, are known to form precipitates of fatty acid salts at concentrations of divalent cations above 2-4 mM (Chen et al. 2005; Szostak 2012). Therefore, we first checked the stability of NA-NOH/Tyra system towards various $MgCl_2$ concentrations.

Figure 4.13a shows that the NA-NOH/Tyra droplets could be observed till 20 mM $MgCl_2$ concentration, after which crystals were forming. Similarly, the stability of the droplets was checked over a range of NaCl concentrations since early ocean NaCl concentrations are thought to be as high as 600 mM (Saha et al. 2022). Figure 4.13b shows that NA-NOH/Tyra system forms droplets at a wide range of NaCl concentrations, ranging from 10 mM and all the way through 600 mM. However, visual observation suggested that the number of droplets reduced with increasing concentrations of NaCl, which was also corroborated by turbidity measurements (Figure 4.14).

After determining the tolerance of the NA-NOH/Tyra droplets to monovalent and divalent cations, we further subjected the droplets to various temperatures. Checking the stability of the droplets at various temperatures is important since temperatures on the prebiotic Earth are thought to have been variable (Mansy and Szostak 2008; Budin and Szostak 2010; Saha et al.

2022). Notably, droplets were observed at all the temperatures tested, ranging from 5 °C to 65 °C; above this no droplets were present and the solution was clear (Figures 4.13c and 4.15). These results suggested that the NA-NOH/Tyra system has an upper critical solution temperature (UCST) of 65 °C, which is the temperature above which the system does not phase separate to result in droplets.

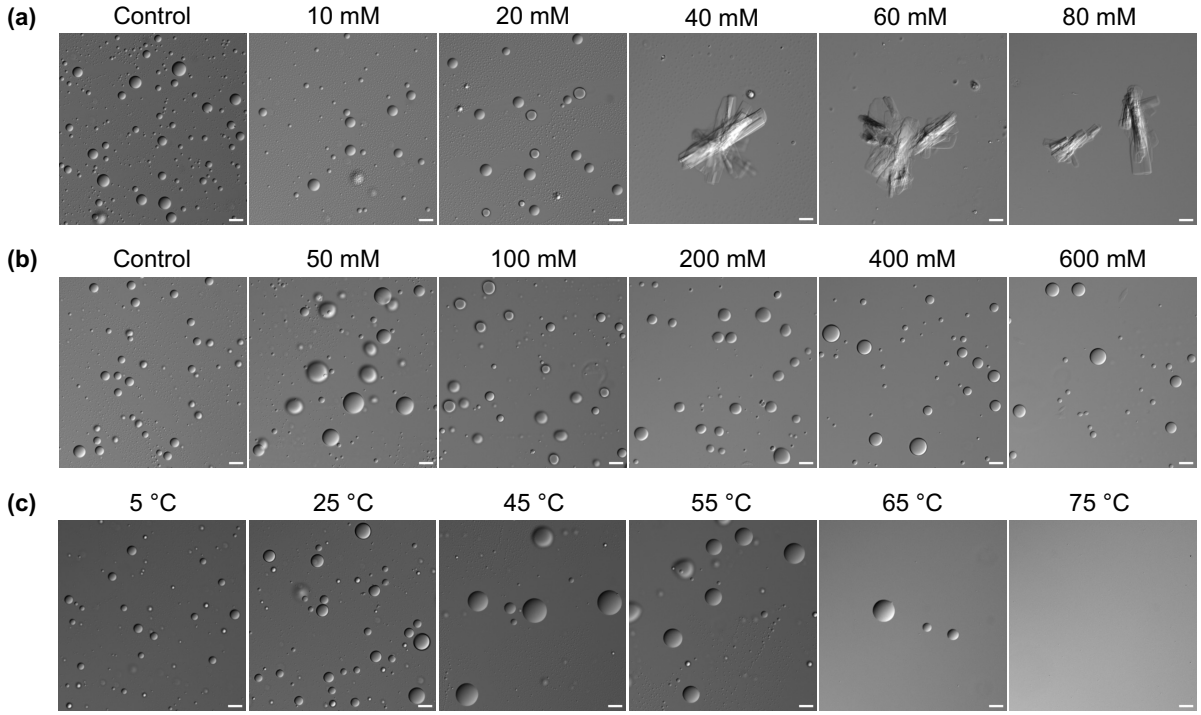

Figure 4.13: Tolerance of NA-NOH/Tyra system towards prebiotically pertinent selection pressures. Salt tolerance of 60/100 NA-NOH/Tyra droplets to various concentrations of $MgCl_2$ **(a)** and NaCl **(b)**. When 60/100 NA-NOH/Tyra samples were incubated at various temperatures for 30 mins, ranging from 5 °C to 75 °C, droplets were observed till 65 °C **(c)**. The density of the droplets, however, reduced substantially at 65 °C. The sample incubated at 75 °C for 30 mins appeared clear, and no droplets were observed. N=3. Scale bar: 20 μm.

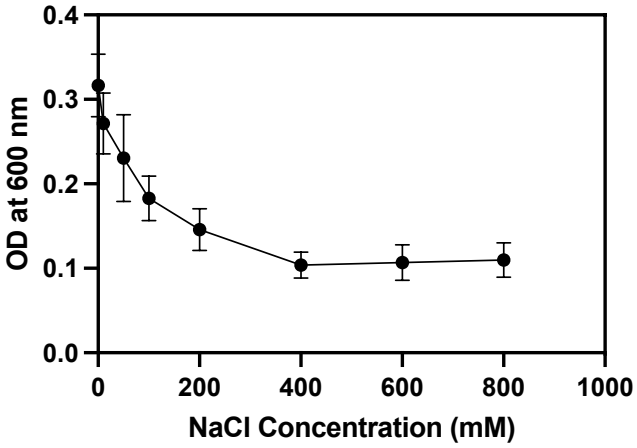

Figure 4.14: Monitoring the turbidity of NA-NOH/Tyra samples containing various concentrations of NaCl. Error bars: S.D. N=3.

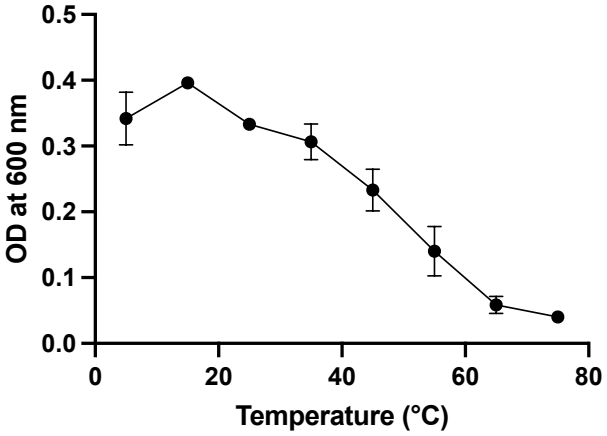

Figure 4.15: Monitoring the turbidity of NA-NOH/Tyra samples at various temperatures. Error bars: S.D. N=3.

Overall, the observations in Figure 4.13 suggest that the NA-NOH/Tyra system is a robust one and shows tolerance to prebiotically relevant temperatures and high salt concentrations. In the context of $MgCl_2$, although the coacervate droplets crashed out at concentrations above 20 mM, they could have still supported chemical reactions crucial to the putative RNA World hypothesis. These include nonenzymatic RNA replication and certain ribozyme-based reactions, which do not necessarily need concentrations of $MgCl_2$ higher than 20 mM. As a first step towards undertaking such reactions within fatty acid coacervates, we asked whether RNA could get sequestered within the NA-NOH/Tyra droplets.

4.3.5. RNA sequestration inside the NA-NOH/Tyra droplets: Implications for nonenzymatic RNA replication

RNA has been shown to get sequestered within complex coacervates (Poudyal et al. 2018; Strulson et al. 2012). Complex coacervates are a type of associative LLPS, wherein the interactions between two oppositely charged polyelectrolyte species results in their phase separation from the bulk solvent (Poudyal et al. 2018). In these cases, one of the two components forming the coacervates is a cationic polyelectrolyte, which can offer interactions with the anionic RNA molecules, and thus, can readily facilitate the sequestration of RNA inside the droplets (Aumiller et al. 2016; Poudyal et al. 2018, 2019; Choi et al. 2022).

On the other hand, the two-fatty acid coacervates studies to date have been reported to be inefficient in sequestering nucleic acid, mainly because of the repulsion between two anionic species, i.e. the fatty acids and the oligonucleotide. In order to circumvent this problem, cationic amphiphiles like cetylpyridinium chloride and cetyltrimethylammonium bromide have been used to make coacervates, which were found to sequester DNA (Douliez et al. 2017). However, the prebiotic relevance of these amphiphiles is unknown and possibly improbable (Douliez et al. 2017). In this backdrop, we wanted to check whether our NA-NOH/Tyra droplets could sequester RNA. Towards this, we incorporated a Cy3 labelled 22-mer RNA and looked for Cy3 fluorescence inside the droplets.

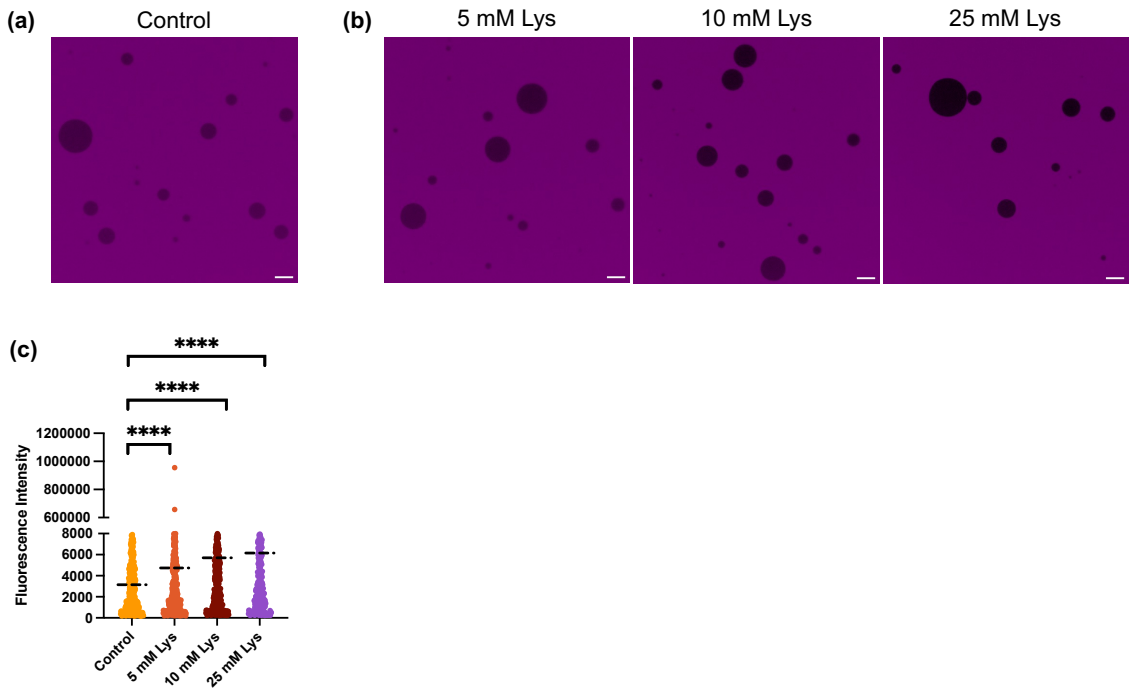

Figure 4.16: Effect of co-solutes in enhancing RNA sequestration. Confocal microscopy images showing the sequestration of Cy3 labelled RNA within 60/100 coacervate droplets **(a)** enhanced upon addition of cationic

amino acid, Lysine, as a co-solute **(b)**. Scale bar: 10 µm. Quantification of the Cy3 fluorescence inside the droplets with varying concentrations of lysine **(c).** Here, Kruskal-Wallis test was performed to statistically compare the fluorescence intensities between the droplets samples without the co-solute (control) and those with different concentrations of the co-solute. $p<0.0001$. N=3; n: at least 300 droplets per sample.

Figure 4.16a shows that the 60/100 NA-NOH/Tyra droplets do indeed show fluorescence, suggesting the sequestration of RNA within the droplets. However, while imaging the droplets, background fluorescence was also being observed suggesting that not all RNA was getting sequestered into the droplets. As reported previously, this could be because of the internal hydrophobic environment and is getting compounded due to repulsion coming from the negatively charged fatty acids constituting the droplets (Zhou et al. 2022b). Therefore, we wondered whether any simple, cationic molecules, which could have been present as co-solutes along with the droplets in the prebiotic soup, could enhance the sequestration of RNA.

Towards this, cationic amino acids and prebiotically relevant co-solutes like lysine and arginine were evaluated for their role in RNA sequestration. Figure 4.16b shows that with the addition of lysine, RNA sequestration was significantly enhanced (Figure 4.16c). A similar effect was observed when arginine was added as a co-solute (Figure 4.17). Additionally, by doing Z stack analysis of the images, we also confirmed the even distribution of RNA across the droplet (Figure 4.18).

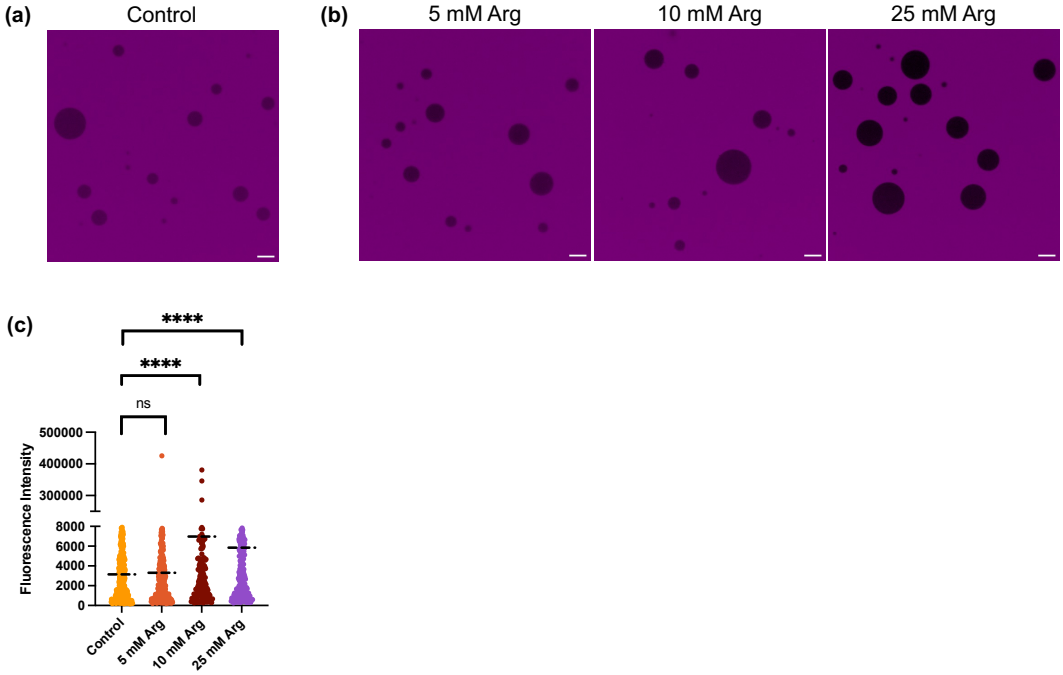

Figure 4.17: Enhanced RNA sequestration in the presence of arginine. Cy3 labelled RNA was sequestered in the absence (control) **(a)** and the presence of various concentrations of Arg **(b).** Kruskal-Wallis test was performed

to statistically compare the fluorescence intensities between the droplets samples without the co-solute (control) and those with different concentrations of arginine as co-solute **(c)**. $p<0.0001$. N=3; n: at least 300 droplets per sample. Scale bar: 10 μm.

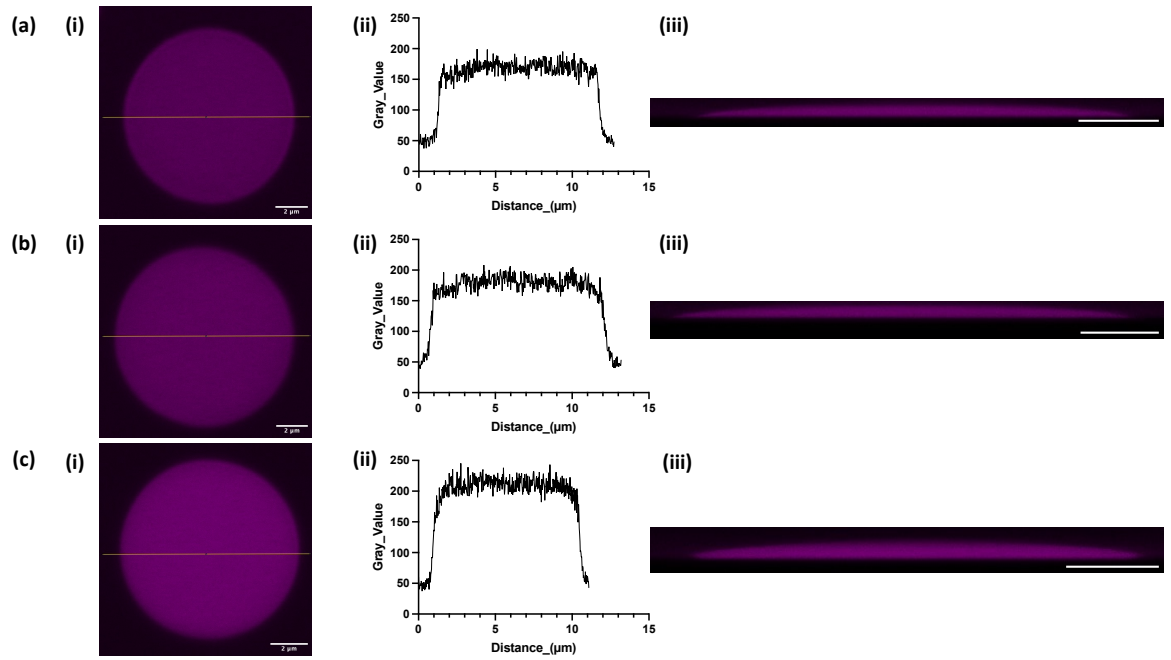

Figure 4.18: Z-stack profile: Left panel shows microscopy images of NA-NOH/Tyra droplets containing Cy3-labelled RNA in the absence of any amino acid **(a)**, in the presence of 25 mM Lys **(b)** and 25 mM Arg **(c)**. Middle and right panels show intensity profiles and Z-stack profiles in XZ plane corresponding to the yellow lines in the left panel. Scale bar: 2 μm. N=3.

Once RNA sequestration by NA-NOH/Tyra droplets was confirmed, we further asked whether they could facilitate nonenzymatic replication reactions. Towards this, an RNA primer-template complex was encapsulated inside the 60/100 NA-NOH/Tyra droplets, and a nonenzymatic replication reaction was initiated by adding imidazole activated nucleotides. Specifically, we studied the incorporation of adenosine monophosphate (AMP) on to the 3′ end of the template-bound primer against the templating base U, by using imidazole activated AMP (ImpA). To the encapsulated RNA primer-template complex, we added ImpA and immediately centrifuged the samples to separate the coacervate phase from the bulk solvent (Figure 4.19a).

The separated coacervate phases from the individual reactions were incubated for 2 hours, which was followed by running them on 22% denaturing urea PAGE (Methods). Upon visualizing the gel, the extension of the primer was observed in all the reactions (Figure 4.19b). These reactions were performed in the presence of 25 mM Lysine and Arginine while control

reactions without amino acids were also simultaneously carried out. To the best of our knowledge, this is the first ever demonstration of nonenzymatic template-directed RNA replication in a fatty acid-based coacervate system. In all, these results highlight the importance of chemical heterogeneity in the prebiotic soup and what it means for making robust and functional protocells of different types (i.e. membraneless and membrane-bound).

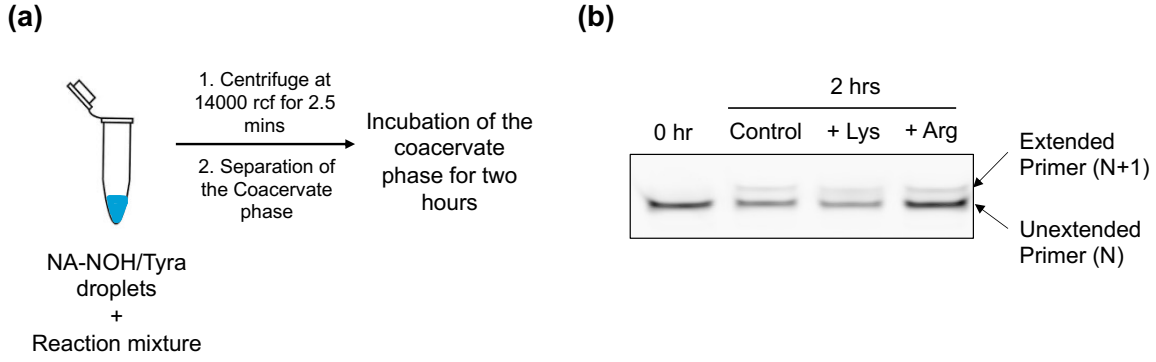

Figure 4.19: Functional significance of NA-NOH/Tyra coacervates towards prebiotically significant processes. Reaction scheme nonenzymatic template-directed replication of RNA in the 60/100 NA-NOH/Tyra coacervate phase **(a)**. Extension of the primer being observed when template-directed nonenzymatic replication reaction was allowed to proceed in the coacervate phase without amino acid (control), and with either lysine or arginine **(b).**

4.4. Discussion

Short chain fatty acids are thought to be prebiotically more abundant than long chain fatty acids (McCollom et al. 1999; Rushdi and Simoneit 2001; Lai et al. 2019). However, since the dynamicity of vesicles that result from short chain fatty acids is very high, their role in forming prebiotic compartments has remained less explored. The earlier report showing the potential of decanoic acid vesicles to transition into coacervate droplets (Martin and Douliez 2021) prompted us to question whether fatty acids having chain lengths shorter than decanoic acid be characterized for their potential to form coacervates. These also are the ones that have been poorly explored as compartment forming entities. In this context, the focus of this study was to come up with a short chain fatty acid-based coacervate system that is more stable than the two previously reported systems, which could withstand prebiotically pertinent selection pressures and that are functionally significant in the context of origins of life. Furthermore, we introduced compositional heterogeneity in our amphiphile-based coacervate system, which has been previously reported only for vesicles (Schrum et al. 2010; Sarkar et al. 2020b).

To the best of our knowledge, we report for the first time a coacervate system composed of a binary mixture of short chain fatty acid and the corresponding alcohol, along with the molecule tyramine (NA-NOH/Tyra). The coacervate droplets were found to be stable from pH 7-9. pH values above 9 were not considered since we intended to demonstrate a system that would support encapsulation of RNA, which gets hydrolyzed quickly in alkaline pHs. Furthermore, replacing dopamine with tyramine substantially increased the stability of the droplets. The presence of tyrosine has been shown to occur in the Inter Stellar Medium (ISM), which is the precursor for the formation of tyramine from pyrolysis-like events hypothesized to have been facilitated in thermal hydrothermal systems (Mast 2024; Iglesias-Groth et al. 2025). This study serves as a proof of principle to illustrate how a prebiotically plausible molecule with similar functional groups and properties as tyramine, could mediate vesicle-to-coacervate transition and influence the properties of the resulting coacervates. While the NA-NOH/DPA droplets could be observed only till 6 hours, the droplets formed using the NA-NOH/Tyra system could be observed for up to 8 days. It is important to note that the NA-NOH/Tyra droplets do coalesce, but readily reform upon mixing.

The increased stability of NA-NOH/Tyra droplets over a long period of time does not refer to the droplets not coalescing (which does happen), but rather alluded to their ability to reform upon mixing after the reported time periods. A previous study showed that the concentration of $MgCl_2$ inside the coacervates was orders of magnitude higher than the bulk solution (Frankel

et al. 2016). Given this, we characterized the system for this and other prebiotically relevant selection pressures. We found that NA-NOH/Tyra droplets could tolerate up to 20 mM of $MgCl_2$ and 600 mM NaCl. Next, the temperature stability of coacervate droplets was evaluated and it was found that the droplets were forming until 60°C.

Finally, we checked whether the system could act as a compartment to sequester biologically relevant molecules. In this context, the sequestration of GFP was found to be much better than that of the short RNA. This effect can be attributed to the potential of the protein to facilitate more interactions with the components of the coacervates than RNA. This would be through hydrophobic and other interactions coming from various functional groups that the protein contains. Moreover, as mentioned earlier, being negatively charged, RNA could experience more repulsion from the negatively charged fatty acids present in the coacervate droplets. However, we observed enhanced sequestration of RNA with the addition of positively charged amino acids, such as lysine and arginine.

Our results show that the RNA sequestration could be brought about inside the coacervates by simple amino acids that would have been present as co-solutes. This implies that even relatively small co-solutes present in the prebiotic soup could have potentially altered the physicochemical properties of the coacervate droplets. This is especially appealing given that most previous coacervate research showed that such RNA sequestration necessarily needed coacervates composed of higher molecular weight cationic peptides or complex polymers.

The FRAP experiments involving the fatty acid coacervates, show that they could facilitate diffusion of molecules in the interior, suggesting the feasibility of carrying out prebiotically pertinent chemical reactions within these compartments. Towards this, when a reaction involving template-directed nonenzymatic replication of RNA was carried out in the coacervate phase, we observed extension of the primer, suggesting the compatibility of the system to prebiotically important reactions. However, it is likely that the sequestered biomolecules could also be getting exchanged with the bulk solution by diffusion as coacervates are an open system unlike membrane-bound vesicles (Jia et al. 2014).

This then poses a question of whether fatty acid-based coacervates could be encapsulated by a semipermeable lipid bilayer to make them relevant in this specific context (Dora Tang et al. 2014). Such an assembly could help with limiting the diffusion of entrapped molecules into the bulk solution while also allowing the ready diffusion within the coacervate interior. Furthermore, this work also shows how the chemical diversity of amphiphiles enhance the

stability of the resultant coacervates. This invokes the importance of systematically characterizing other SCAs, including those that have been recently described as vesicle forming protoamphiphiles (e.g. N-acyl amino acids) to delineate even more robust fatty acid coacervate systems with implications for fabricating compartments with more complex functionalities (Joshi et al. 2021, 2022).

In conclusion, this work just scratches at the surface of delineating coacervate systems using prebiotically available SCA-based systems, especially on the shorter end of the chain length spectrum. Eventually, further studies are required to delve deeper into discovering the role of compositional heterogeneity in prebiotically relevant coacervate systems. This would eventually allow us to characterize SCA-based coacervate forming composite systems, allowing for effectively modulating their physicochemical properties and fabricating complex cell-like entities with multiple kinds of encapsulated compartments.

For instance, compositionally heterogenous coacervates would differ in their microenvironment and this could potentially influence differential partitioning of molecules within their interior. By extension, compositionally diverse protocellular populations could potentially harbor various metabolic reactions within them, setting the stage for evolving into more complex protocells. Lastly, exploring the SCA chemical space will allow for tweaking the constituents of the coacervates that would permit the modulation of their microenvironment in different ways. Notably, this could also pave the way to develop novel delivery systems that can carry chemically distinct cargo molecules, finding relevant use both in basic and applied synthetic biology applications.

4.5. Summary of the work:

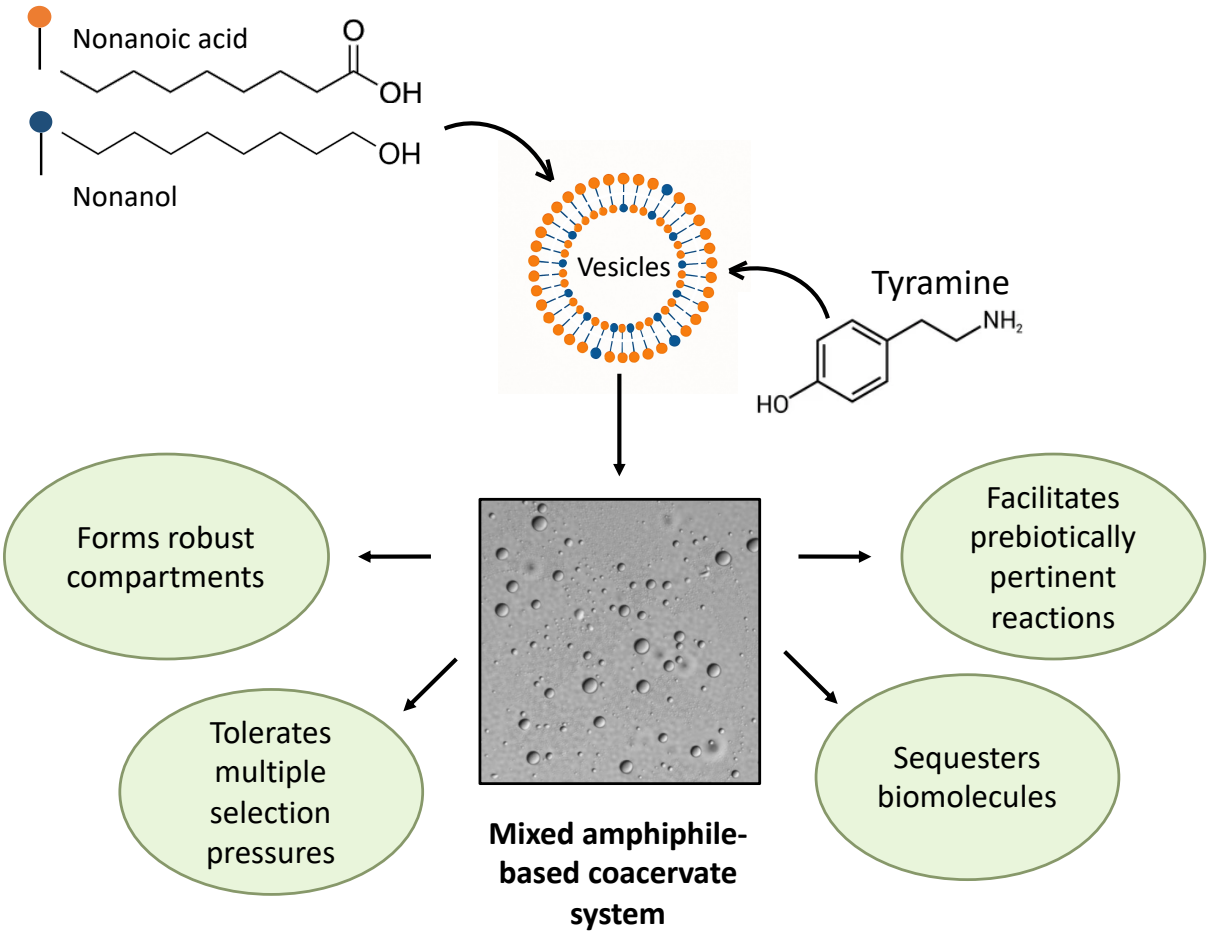

4.6. References

1. Apel CL, Deamer DW, Mautner MN (2002) Self-assembled vesicles of monocarboxylic acids and alcohols: conditions for stability and for the encapsulation of biopolymers. Biochimica et Biophysica Acta (BBA) - Biomembranes 1559:1–9. https://doi.org/10.1016/S0005-2736(01)00400-X

2. Aumiller WM, Pir Cakmak F, Davis BW, Keating CD (2016) RNA-Based Coacervates as a Model for Membraneless Organelles: Formation, Properties, and Interfacial Liposome Assembly. Langmuir 32:10042–10053. https://doi.org/10.1021/acs.langmuir.6b02499

3. Bapat NV, Rajamani S (2015) Effect of Co-solutes on Template-Directed Nonenzymatic Replication of Nucleic Acids. J Mol Evol 81:72–80. https://doi.org/10.1007/s00239-015-9700-1

4. Bhattacharya A, Niederholtmeyer H, Podolsky KA, et al (2020) Lipid sponge droplets as programmable synthetic organelles. Proceedings of the National Academy of Sciences 117:18206–18215. https://doi.org/10.1073/pnas.2004408117

5. Blain JC, Szostak JW (2014) Progress Toward Synthetic Cells. Annu Rev Biochem 83:615–640. https://doi.org/10.1146/annurev-biochem-080411-124036

6. Budin I, Szostak JW (2010) Expanding Roles for Diverse Physical Phenomena During the Origin of Life. Annual Review of Biophysics 39:245–263. https://doi.org/10.1146/annurev.biophys.050708.133753

7. Chen IA, Salehi-Ashtiani K, Szostak JW (2005) RNA Catalysis in Model Protocell Vesicles. J Am Chem Soc 127:13213–13219. https://doi.org/10.1021/ja051784p

8. Chen IA, Walde P (2010) From Self-Assembled Vesicles to Protocells. Cold Spring Harb Perspect Biol 2:a002170. https://doi.org/10.1101/cshperspect.a002170

9. Cho CJ, Niederholtmeyer H, Seo H, et al (2022) Functionalizing Lipid Sponge Droplets with DNA. ChemSystemsChem 4:e202100045. https://doi.org/10.1002/syst.202100045

10. Choi S, Meyer MO, Bevilacqua PC, Keating CD (2022) Phase-specific RNA accumulation and duplex thermodynamics in multiphase coacervate models for membraneless organelles. Nat Chem 14:1110–1117. https://doi.org/10.1038/s41557-022-00980-7

11. Das S, Patki GM, Sridhar V, et al (2024) Compartmentalization as a ubiquitous feature of life: from origins of life to biomimetics. Eur Phys J Spec Top. https://doi.org/10.1140/epjs/s11734-024-01203-5

12. Deamer D (2016) Membranes and the Origin of Life: A Century of Conjecture. J Mol Evol 83:159–168. https://doi.org/10.1007/s00239-016-9770-8

13. Deamer DW (1985) Boundary structures are formed by organic components of the Murchison carbonaceous chondrite. Nature 317:792–794. https://doi.org/10.1038/317792a0

14. Deamer DW, Pashley RM (1989) Amphiphilic components of the murchison carbonaceous chondrite: Surface properties and membrane formation. Origins Life Evol Biosphere 19:21–38. https://doi.org/10.1007/BF01808285

15. Deshpande K, Kulshreshtha NN, Mulewar SS, Rajamani S (2024) Nucleotide-Protocell Interactions: A Reciprocal Relationship in Prebiotically Pertinent Environments. ChemSystemsChem 6:e202300031. https://doi.org/10.1002/syst.202300031

16. Dora Tang T-Y, Rohaida Che Hak C, Thompson AJ, et al (2014) Fatty acid membrane assembly on coacervate microdroplets as a step towards a hybrid protocell model. Nature Chem 6:527–533. https://doi.org/10.1038/nchem.1921

17. Douliez J-P, Martin N, Gaillard C, et al (2017) Catanionic Coacervate Droplets as a Surfactant-Based Membrane-Free Protocell Model. Angewandte Chemie International Edition 56:13689–13693. https://doi.org/10.1002/anie.201707139

18. Drobot B, Iglesias-Artola JM, Le Vay K, et al (2018) Compartmentalised RNA catalysis in membrane-free coacervate protocells. Nat Commun 9:3643. https://doi.org/10.1038/s41467-018-06072-w

19. Dworkin JP, Deamer DW, Sandford SA, Allamandola LJ (2001) Self-assembling amphiphilic molecules: Synthesis in simulated interstellar/precometary ices. Proc Natl Acad Sci U S A 98:815–819

20. Frankel EA, Bevilacqua PC, Keating CD (2016) Polyamine/Nucleotide Coacervates Provide Strong Compartmentalization of Mg^{2+} , Nucleotides, and RNA. Langmuir 32:2041–2049. https://doi.org/10.1021/acs.langmuir.5b04462

21. Garenne D, Beven L, Navailles L, et al (2016a) Sequestration of Proteins by Fatty Acid Coacervates for Their Encapsulation within Vesicles. Angewandte Chemie International Edition 55:13475–13479. https://doi.org/10.1002/anie.201607117

22. Garenne D, Navailles L, Nallet F, et al (2016b) Clouding in fatty acid dispersions for charge-dependent dye extraction. Journal of Colloid and Interface Science 468:95–102. https://doi.org/10.1016/j.jcis.2016.01.049

23. Gebicki JM, Hicks M (1973) Ufasomes are Stable Particles surrounded by Unsaturated Fatty Acid Membranes. Nature 243:232–234. https://doi.org/10.1038/243232a0

24. Gilbert W (1986) Origin of life: The RNA world. Nature 319:618–618. https://doi.org/10.1038/319618a0

25. Hargreaves WR, Deamer DW (1978) Liposomes from ionic, single-chain amphiphiles. Biochemistry 17:3759–3768. https://doi.org/10.1021/bi00611a014

26. Iglesias-Groth S, Marín Dobrincic M, Pérez Garrido A, Gutierrez C (2025) Evidence of the Amino Acids Tyrosine and Phenylalanine in the Interstellar Material of IC348 in Perseus. Life 15:181. https://doi.org/10.3390/life15020181

27. Jia TZ, Chandru K, Hongo Y, et al (2019) Membraneless polyester microdroplets as primordial compartments at the origins of life. Proc Natl Acad Sci USA 116:15830–15835. https://doi.org/10.1073/pnas.1902336116

28. Jia TZ, Hentrich C, Szostak JW (2014) Rapid RNA Exchange in Aqueous Two-Phase System and Coacervate Droplets. Orig Life Evol Biosph 44:1–12. https://doi.org/10.1007/s11084-014-9355-8

29. Jia TZ, Wang P-H, Niwa T, Mamajanov I (2021) Connecting primitive phase separation to biotechnology, synthetic biology, and engineering. J Biosci 46:79. https://doi.org/10.1007/s12038-021-00204-z

30. Joshi MP, Sawant AA, Rajamani S (2021) Spontaneous emergence of membrane-forming protoamphiphiles from a lipid–amino acid mixture under wet–dry cycles. Chem Sci 12:2970–2978. https://doi.org/10.1039/D0SC05650B

31. Joshi MP, Uday A, Rajamani S (2022) Elucidating N-acyl amino acids as a model protoamphiphilic system. Commun Chem 5:147. https://doi.org/10.1038/s42004-022-00762-9

32. Joyce GF, Szostak JW (2018) Protocells and RNA Self-Replication. Cold Spring Harb Perspect Biol 10:a034801. https://doi.org/10.1101/cshperspect.a034801

33. Keating CD (2012) Aqueous Phase Separation as a Possible Route to Compartmentalization of Biological Molecules. Acc Chem Res 45:2114–2124. https://doi.org/10.1021/ar200294y

34. Klymchenko AS (2017) Solvatochromic and Fluorogenic Dyes as Environment-Sensitive Probes: Design and Biological Applications. Acc Chem Res 50:366–375. https://doi.org/10.1021/acs.accounts.6b00517

35. Koga S, Williams DS, Perriman AW, Mann S (2011) Peptide–nucleotide microdroplets as a step towards a membrane-free protocell model. Nature Chem 3:720–724. https://doi.org/10.1038/nchem.1110

36. Lai JC-Y, Pearce BKD, Pudritz RE, Lee D (2019) Meteoritic abundances of fatty acids and potential reaction pathways in planetesimals. Icarus 319:685–700. https://doi.org/10.1016/j.icarus.2018.09.028

37. Leslie E. O (2004) Prebiotic Chemistry and the Origin of the RNA World. Critical Reviews in Biochemistry and Molecular Biology 39:99–123. https://doi.org/10.1080/10409230490460765

38. Mansy SS, Schrum JP, Krishnamurthy M, et al (2008) Template-directed synthesis of a genetic polymer in a model protocell. Nature 454:122–125. https://doi.org/10.1038/nature07018

39. Mansy SS, Szostak JW (2008) Thermostability of model protocell membranes. Proceedings of the National Academy of Sciences 105:13351–13355. https://doi.org/10.1073/pnas.0805086105

40. Martin N, Douliez J-P (2021) Fatty Acid Vesicles and Coacervates as Model Prebiotic Protocells. ChemSystemsChem 3:e2100024. https://doi.org/10.1002/syst.202100024

41. Mast CB (2024) Heat-Flow-Driven Nonequilibria for Prebiotic Chemistry. ChemSystemsChem 6:e202400039. https://doi.org/10.1002/syst.202400039

42. Maurer SE, Monnard P-A (2011) Primitive Membrane Formation, Characteristics and Roles in the Emergent Properties of a Protocell. Entropy 13:466–484. https://doi.org/10.3390/e13020466

43. McCollom TM, Ritter G, Simoneit BRT (1999) Lipid Synthesis Under Hydrothermal Conditions by Fischer- Tropsch-Type Reactions. Orig Life Evol Biosph 29:153–166. https://doi.org/10.1023/A:1006592502746

44. Monnard P-A, Walde P (2015) Current Ideas about Prebiological Compartmentalization. Life 5:1239–1263. https://doi.org/10.3390/life5021239

45. Morigaki K, Walde P (2007) Fatty acid vesicles. Current Opinion in Colloid & Interface Science 12:75–80. https://doi.org/10.1016/j.cocis.2007.05.005

46. Mulkidjanian AY, Bychkov AYu, Dibrova DV, et al (2012) Origin of first cells at terrestrial, anoxic geothermal fields. Proc Natl Acad Sci U S A 109:E821–E830. https://doi.org/10.1073/pnas.1117774109

47. Ovádi J, Saks V (2004) On the origin of intracellular compartmentation and organized metabolic systems. Mol Cell Biochem 256:5–12. https://doi.org/10.1023/B:MCBI.0000009855.14648.2c

48. Patki GM, Rajamani S (2023) Nonenzymatic RNA replication in a mixture of "spent" nucleotides. FEBS Lett 597:3125–3134. https://doi.org/10.1002/1873-3468.14785

49. Poudyal RR, Guth-Metzler RM, Veenis AJ, et al (2019) Template-directed RNA polymerization and enhanced ribozyme catalysis inside membraneless compartments formed by coacervates. Nat Commun 10:490. https://doi.org/10.1038/s41467-019-08353-4

50. Poudyal RR, Pir Cakmak F, Keating CD, Bevilacqua PC (2018) Physical Principles and Extant Biology Reveal Roles for RNA-Containing Membraneless Compartments in Origins of Life Chemistry. Biochemistry 57:2509–2519. https://doi.org/10.1021/acs.biochem.8b00081

51. Rajamani S, Ichida JK, Antal T, et al (2010) Effect of Stalling after Mismatches on the Error Catastrophe in Nonenzymatic Nucleic Acid Replication. J Am Chem Soc 132:5880–5885. https://doi.org/10.1021/ja100780p

52. Rendón A, Carton DG, Sot J, et al (2012) Model Systems of Precursor Cellular Membranes: Long-Chain Alcohols Stabilize Spontaneously Formed Oleic Acid Vesicles. Biophysical Journal 102:278–286. https://doi.org/10.1016/j.bpj.2011.12.026

53. Rushdi AI, Simoneit BRT (2001) Lipid Formation by Aqueous Fischer-Tropsch-Type Synthesis over a Temperature Range of 100 to 400 °C. Orig Life Evol Biosph 31:103–118. https://doi.org/10.1023/A:1006702503954

54. Saha A, Yi R, Fahrenbach AC, et al (2022) A Physicochemical Consideration of Prebiotic Microenvironments for Self-Assembly and Prebiotic Chemistry. Life 12:1595. https://doi.org/10.3390/life12101595

55. Saha R, Verbanic S, Chen IA (2018) Lipid vesicles chaperone an encapsulated RNA aptamer. Nat Commun 9:2313. https://doi.org/10.1038/s41467-018-04783-8

56. Sarkar S, Dagar S, Rajamani S (2021) Influence of Wet–Dry Cycling on the Self-Assembly and Physicochemical Properties of Model Protocellular Membrane Systems. ChemSystemsChem 3:e2100014. https://doi.org/10.1002/syst.202100014

57. Sarkar S, Dagar S, Verma A, Rajamani S (2020a) Compositional heterogeneity confers selective advantage to model protocellular membranes during the origins of cellular life. Sci Rep 10:4483. https://doi.org/10.1038/s41598-020-61372-w

58. Sarkar S, Das S, Dagar S, et al (2020b) Prebiological Membranes and Their Role in the Emergence of Early Cellular Life. J Membrane Biol 253:589–608. https://doi.org/10.1007/s00232-020-00155-w

59. Schrum JP, Zhu TF, Szostak JW (2010) The origins of cellular life. Cold Spring Harb Perspect Biol 2:a002212. https://doi.org/10.1101/cshperspect.a002212

60. Smokers IBA, Van Haren MHI, Lu T, Spruijt E (2022) Complex Coacervation and Compartmentalized Conversion of Prebiotically Relevant Metabolites**. ChemSystemsChem 4:e202200004. https://doi.org/10.1002/syst.202200004

61. Smokers IBA, Visser BS, Slootbeek AD, et al (2024) How Droplets Can Accelerate Reactions─Coacervate Protocells as Catalytic Microcompartments. Acc Chem Res 57:1885–1895. https://doi.org/10.1021/acs.accounts.4c00114

62. Strulson CA, Molden RC, Keating CD, Bevilacqua PC (2012) RNA catalysis through compartmentalization. Nature Chem 4:941–946. https://doi.org/10.1038/nchem.1466

63. Szostak JW (2012) The eightfold path to non-enzymatic RNA replication. Journal of Systems Chemistry 3:2. https://doi.org/10.1186/1759-2208-3-2

64. Szostak JW, Bartel DP, Luisi PL (2001) Synthesizing life. Nature 409:387–390. https://doi.org/10.1038/35053176

65. Zhao YG, Zhang H (2020) Phase Separation in Membrane Biology: The Interplay between Membrane-Bound Organelles and Membraneless Condensates. Developmental Cell 55:30–44. https://doi.org/10.1016/j.devcel.2020.06.033

66. Zhou L, Justin Koh J, Hou X, et al (2022a) The crystallization of decanoic acid/dopamine supramolecular self-assemblies in the presence of coacervates. Journal of Colloid and Interface Science 615:759–767. https://doi.org/10.1016/j.jcis.2022.02.016

67. Zhou L, Koh JJ, Wu J, et al (2022b) Fatty Acid-Based Coacervates as a Membrane-free Protocell Model. Bioconjugate Chem 33:444–451. https://doi.org/10.1021/acs.bioconjchem.1c00559

Chapter 5

SUMMARY AND FUTURE PROSPECTS

Life is hypothesized to have emerged on the prebiotic Earth in a primordial soup comprising a complex mix of chemicals. These chemicals are thought to have reacted with each other in order to abiotically form biologically relevant precursors, including nucleotides, amino acids and single chain amphiphiles. In the context of nucleotides, it is considered that they would have undergone nonenzymatic oligomerization and replication under prebiotically plausible conditions to form a pool of RNA oligomers. Furthermore, functional RNA oligomers, such as ribozymes, are proposed to have undergone compartmentalization to give rise to a 'protocell'. Since these processes would have happened in the prebiotic soup, they could potentially have been influenced by the dynamic interplay between the reactant molecules and the chemicals (co-solutes) present in the vicinity. In this context, we looked at the effect of prebiotic soup's heterogeneity on nonenzymatic RNA replication and LLPS-based protocell formation.

Towards systematically understanding the effect of chemical heterogeneity on nonenzymatic RNA replication, we looked at the rates of template-directed nonenzymatic RNA replication in the presence of a mixture of all four spent nucleotides as co-solutes. It was observed that the spent nucleotide mixture significantly reduces the rate of the nonenzymatic replication, underscoring the influence of the interactions between the reactant molecules and the co-solutes on prebiotically relevant processes. Amongst the four spent nucleotides, the nucleotide that was the Watson-Crick base-pairing partner of the templating base, was observed to be affecting the reaction to the greatest extent, indicating the specificity of the co-solute interaction with the templating base. Additionally, wobble-base pairing and near neighbour interactions were also observed to be having a significant contribution in reducing the rates of specific reactions.

These results suggest that the co-solutes would have played a crucial role in determining the rates of nonenzymatic RNA replication, and may have appreciably contributed to the evolution of the RNA sequence space. Furthermore, the results emphasize the necessity of compartmentalization of RNA molecules inside a protocell. Towards this, it is required to look for prebiotically plausible protocellular systems that can sequester RNA molecules within, while allowing the diffusion of activated nucleotides and restricting the diffusion of spent monomers into the protocell from the surrounding environment. Future studies in this regard can shed light on the effect of compartmentalization in rescuing nonenzymatic replication over inhibition by co-solutes.

In the context of prebiotically plausible protocells, LLPS-based protocellular systems are intriguing because of their characteristic properties, including their ability to sequester and concentrate biomolecules, while facilitating molecular diffusion and reactions. Towards this, we characterized a mixed amphiphile-based LLPS system composed of single chain amphiphiles (nonanoic acid (NA) and nonanol (NOH)) and tyramine (Tyra), wherein the vesicles composed of NA-NOH transition into coacervates upon the addition of tyramine. Single chain amphiphiles have predominantly been explored as vesicle forming entities; however, their role in the formation of LLPS-based protocells has only recently gained attention. In this backdrop, the characterization of the NA-NOH/ Tyra coacervates is very exciting as they were also found to thrive under multiple prebiotically plausible selection pressures. Remarkably, they were observed to remain stable for several days. Notably, the compartments formed by these coacervates were observed to be compatible with RNA sequestration in the presence of cationic amino acids.

Thus, prebiotic soup's chemical heterogeneity seems to influence the protocell behaviour in the following ways; (i) compositional heterogeneity of the coacervates make them stable across a broad pH range, (ii) co-solutes present in the prebiotic soup, such as cationic amino acid monomers, benefit these coacervate protocells by enhancing RNA sequestration within them. Furthermore, prebiotically plausible reactions, such as nonenzymatic primer extension was also observed in the coacervate phase. To the best of our knowledge, such a mixed SCA-based coacervate system has not been reported till date. With that in mind, it is imperative us to ask whether short chain amphiphiles other than NA could also have formed LLPS-based protocellular compartments. Towards this, we explored the potential of C-8 and C11 systems to form coacervates. Because, like NA, they are also underexplored as vesicle forming entities when compared to the long chain fatty acid counterparts. As can be seen in Figure 5.1 below, both the systems could be observed to form coacervates.

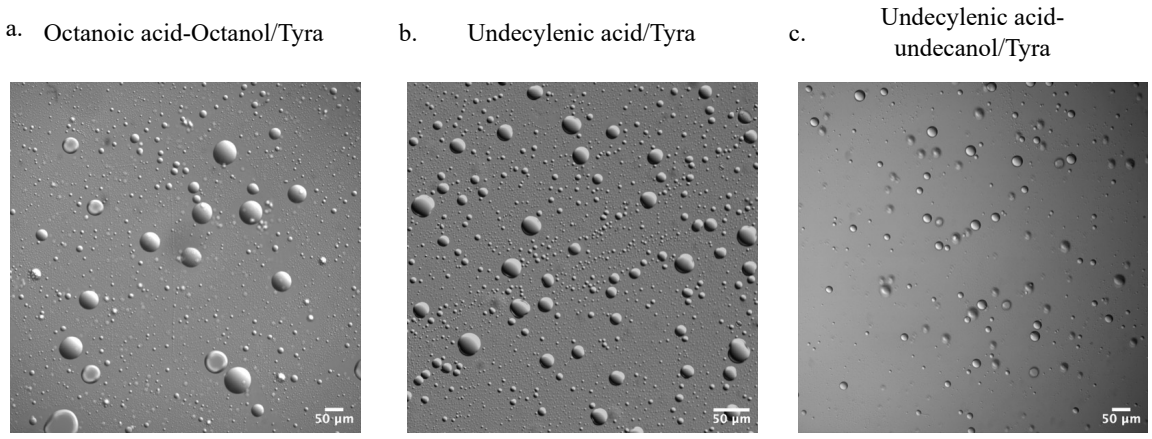

Figure 5.1: Coacervates resulting from 150 mM octanoic acid-octanol and 160 mM Tyra (a), 60 mM undecylenic acid and 100 mM Tyra (b), and 60 mM undecylenic acid-undecanol and 100 mM Tyra (c). Experiment performed with the help from Daksh Barad, IISER Pune. Scale bar: 50 µm.

Towards exploring these and other related systems in the future, it is required to first systematically characterize them to understand their physicochemical properties. In this context, a comprehensive comparison between various parameters, such as stability, micropolarity, sequestration efficiency etc. of the different systems, could help understand the role of chain length in modulating the physicochemical properties of such SCA-based coacervates. Furthermore, determining the catalytic activity of self-replicating ribozymes within these compartments could shed more light on the functional significance of these compartments as robust protocellular entities. In all, the investigations detailed in the thesis highlight the significance of chemical heterogeneity of the prebiotic soup in shaping prebiotically relevant processes, such as nonenzymatic RNA replication and protocell formation, during the origin of life on our planet.

PUBLICATIONS

1. Patki, G. M., Sridhar, V., & Rajamani, S. (2025). Characterizing Mixed Single-Chain Amphiphile-Based Coacervates as a Robust Protocell System. *ChemBioChem*, 202500437.

2. Das, S., Patki, G.M., Sridhar, V., Mulewar, S.S., Roy, R., Bandyopadhyay, U., Kulshreshtha, N.N. and Rajamani, S., 2024. Compartmentalization as a ubiquitous feature of life: from origins of life to biomimetics. *The European Physical Journal Special Topics*, pp.1-20.

3. Patki, G.M. and Rajamani, S., 2023. Nonenzymatic RNA replication in a mixture of 'spent'nucleotides. *FEBS letters*, *597*(24), pp.3125-3134.

4. Sarkar, S., Das, S., Dagar, S., Joshi, M.P., Mungi, C.V., Sawant, A.A., Patki, G.M. and Rajamani, S., 2020. Prebiological membranes and their role in the emergence of early cellular life. *The Journal of Membrane Biology*, *253*, pp.589-608.

COPYRIGHT LICENCE PERMISSIONS

1. Permission for reuse of –

Patki, G.M. and Rajamani, S., 2023. Nonenzymatic RNA replication in a mixture of 'spent'nucleotides. *FEBS letters*, *597*(24), pp.3125-3134.

Nonenzymatic RNA replication in a mixture of 'spent' nucleotides

Author: Gauri M. Patki, Sudha Rajamani
Publication: FEBS Letters
Publisher: John Wiley and Sons
Date: Dec 13, 2023

JOHN WILEY AND SONS LICENSE
TERMS AND CONDITIONS
Apr 11, 2025

This Agreement between Gauri M. Patki ("You") and John Wiley and Sons ("John Wiley and Sons") consists of your license details and the terms and conditions provided by John Wiley and Sons and Copyright Clearance Center.

License Number	6006260124680
License date	Apr 11, 2025
Licensed Content Publisher	John Wiley and Sons
Licensed Content Publication	FEBS Letters
Licensed Content Title	Nonenzymatic RNA replication in a mixture of 'spent' nucleotides
Licensed Content Author	Gauri M. Patki, Sudha Rajamani
Licensed Content Date	Dec 13, 2023
Licensed Content Volume	597
Licensed Content Issue	24
Licensed Content Pages	3134
Type of use	Dissertation/Thesis
Requestor type	Author of this Wiley article
Format	Electronic
Portion	Full article
Will you be translating?	No

Title of new work	Implications of prebiotic soup heterogeneity for nonenzymatic RNA replication and formation of primordial protocells
Institution name	Indian Institute of Science Education and Research, Pune
Expected presentation date	Apr 2025
The Requesting Person / Organization to Appear on the License	Gauri M. Patki
Requestor Location	Ms. Gauri Patki Hostel 3, IISER Pune Pune, 411008 India
Order reference number	1
Publisher Tax ID	EU826007151
Total	0.00 USD

Terms and Conditions

TERMS AND CONDITIONS

This copyrighted material is owned by or exclusively licensed to John Wiley & Sons, Inc. or one of its group companies (each a"Wiley Company") or handled on behalf of a society with which a Wiley Company has exclusive publishing rights in relation to a particular work (collectively "WILEY"). By clicking "accept" in connection with completing this licensing transaction, you agree that the following terms and conditions apply to this transaction (along with the billing and payment terms and conditions established by the Copyright Clearance Center Inc., ("CCC's Billing and Payment terms and conditions"), at the time that you opened your RightsLink account (these are available at any time at http://myaccount.copyright.com).

Terms and Conditions

- The materials you have requested permission to reproduce or reuse (the "Wiley Materials") are protected by copyright.
- **You are hereby granted a personal, non-exclusive, non-sub licensable (on a stand-alone basis), non-transferable, worldwide, limited license to reproduce the Wiley Materials for the purpose specified in the licensing process.** This license, **and any CONTENT (PDF or image file) purchased as part of your order,** is for a one-time use only and limited to any maximum distribution number specified in the license. The first instance of republication or reuse granted by this license must be completed within two years of the date of the grant of this license (although copies prepared before the end date may be distributed thereafter). The Wiley Materials shall not be used in any other manner or for any other purpose, beyond what is granted in the license. Permission is granted subject to an appropriate acknowledgement given to the author, title of the

material/book/journal and the publisher. You shall also duplicate the copyright notice that appears in the Wiley publication in your use of the Wiley Material. Permission is also granted on the understanding that nowhere in the text is a previously published source acknowledged for all or part of this Wiley Material. Any third party content is expressly excluded from this permission.

- With respect to the Wiley Materials, all rights are reserved. Except as expressly granted by the terms of the license, no part of the Wiley Materials may be copied, modified, adapted (except for minor reformatting required by the new Publication), translated, reproduced, transferred or distributed, in any form or by any means, and no derivative works may be made based on the Wiley Materials without the prior permission of the respective copyright owner.**For STM Signatory Publishers clearing permission under the terms of the STM Permissions Guidelines only, the terms of the license are extended to include subsequent editions and for editions in other languages, provided such editions are for the work as a whole in situ and does not involve the separate exploitation of the permitted figures or extracts,** You may not alter, remove or suppress in any manner any copyright, trademark or other notices displayed by the Wiley Materials. You may not license, rent, sell, loan, lease, pledge, offer as security, transfer or assign the Wiley Materials on a stand-alone basis, or any of the rights granted to you hereunder to any other person.

- The Wiley Materials and all of the intellectual property rights therein shall at all times remain the exclusive property of John Wiley & Sons Inc, the Wiley Companies, or their respective licensors, and your interest therein is only that of having possession of and the right to reproduce the Wiley Materials pursuant to Section 2 herein during the continuance of this Agreement. You agree that you own no right, title or interest in or to the Wiley Materials or any of the intellectual property rights therein. You shall have no rights hereunder other than the license as provided for above in Section 2. No right, license or interest to any trademark, trade name, service mark or other branding ("Marks") of WILEY or its licensors is granted hereunder, and you agree that you shall not assert any such right, license or interest with respect thereto

- NEITHER WILEY NOR ITS LICENSORS MAKES ANY WARRANTY OR REPRESENTATION OF ANY KIND TO YOU OR ANY THIRD PARTY, EXPRESS, IMPLIED OR STATUTORY, WITH RESPECT TO THE MATERIALS OR THE ACCURACY OF ANY INFORMATION CONTAINED IN THE MATERIALS, INCLUDING, WITHOUT LIMITATION, ANY IMPLIED WARRANTY OF MERCHANTABILITY, ACCURACY, SATISFACTORY QUALITY, FITNESS FOR A PARTICULAR PURPOSE, USABILITY, INTEGRATION OR NON-INFRINGEMENT AND ALL SUCH WARRANTIES ARE HEREBY EXCLUDED BY WILEY AND ITS LICENSORS AND WAIVED BY YOU.

- WILEY shall have the right to terminate this Agreement immediately upon breach of this Agreement by you.

- You shall indemnify, defend and hold harmless WILEY, its Licensors and their respective directors, officers, agents and employees, from and against any actual or threatened claims, demands, causes of action or proceedings arising from any breach of this Agreement by you.

- IN NO EVENT SHALL WILEY OR ITS LICENSORS BE LIABLE TO YOU OR ANY OTHER PARTY OR ANY OTHER PERSON OR ENTITY FOR ANY SPECIAL, CONSEQUENTIAL, INCIDENTAL, INDIRECT, EXEMPLARY OR PUNITIVE DAMAGES, HOWEVER CAUSED, ARISING OUT OF OR IN CONNECTION WITH THE DOWNLOADING, PROVISIONING, VIEWING OR USE OF THE MATERIALS

REGARDLESS OF THE FORM OF ACTION, WHETHER FOR BREACH OF CONTRACT, BREACH OF WARRANTY, TORT, NEGLIGENCE, INFRINGEMENT OR OTHERWISE (INCLUDING, WITHOUT LIMITATION, DAMAGES BASED ON LOSS OF PROFITS, DATA, FILES, USE, BUSINESS OPPORTUNITY OR CLAIMS OF THIRD PARTIES), AND WHETHER OR NOT THE PARTY HAS BEEN ADVISED OF THE POSSIBILITY OF SUCH DAMAGES. THIS LIMITATION SHALL APPLY NOTWITHSTANDING ANY FAILURE OF ESSENTIAL PURPOSE OF ANY LIMITED REMEDY PROVIDED HEREIN.

- Should any provision of this Agreement be held by a court of competent jurisdiction to be illegal, invalid, or unenforceable, that provision shall be deemed amended to achieve as nearly as possible the same economic effect as the original provision, and the legality, validity and enforceability of the remaining provisions of this Agreement shall not be affected or impaired thereby.

- The failure of either party to enforce any term or condition of this Agreement shall not constitute a waiver of either party's right to enforce each and every term and condition of this Agreement. No breach under this agreement shall be deemed waived or excused by either party unless such waiver or consent is in writing signed by the party granting such waiver or consent. The waiver by or consent of a party to a breach of any provision of this Agreement shall not operate or be construed as a waiver of or consent to any other or subsequent breach by such other party.

- This Agreement may not be assigned (including by operation of law or otherwise) by you without WILEY's prior written consent.

- Any fee required for this permission shall be non-refundable after thirty (30) days from receipt by the CCC.

- These terms and conditions together with CCC's Billing and Payment terms and conditions (which are incorporated herein) form the entire agreement between you and WILEY concerning this licensing transaction and (in the absence of fraud) supersedes all prior agreements and representations of the parties, oral or written. This Agreement may not be amended except in writing signed by both parties. This Agreement shall be binding upon and inure to the benefit of the parties' successors, legal representatives, and authorized assigns.

- In the event of any conflict between your obligations established by these terms and conditions and those established by CCC's Billing and Payment terms and conditions, these terms and conditions shall prevail.

- WILEY expressly reserves all rights not specifically granted in the combination of (i) the license details provided by you and accepted in the course of this licensing transaction, (ii) these terms and conditions and (iii) CCC's Billing and Payment terms and conditions.

- This Agreement will be void if the Type of Use, Format, Circulation, or Requestor Type was misrepresented during the licensing process.

- This Agreement shall be governed by and construed in accordance with the laws of the State of New York, USA, without regards to such state's conflict of law rules. Any legal action, suit or proceeding arising out of or relating to these Terms and Conditions or the breach thereof shall be instituted in a court of competent jurisdiction in New York County in the State of New York in the United States of America and each party hereby consents and submits to the personal jurisdiction of such court, waives any objection to

venue in such court and consents to service of process by registered or certified mail, return receipt requested, at the last known address of such party.

WILEY OPEN ACCESS TERMS AND CONDITIONS

Wiley Publishes Open Access Articles in fully Open Access Journals and in Subscription journals offering Online Open. Although most of the fully Open Access journals publish open access articles under the terms of the Creative Commons Attribution (CC BY) License only, the subscription journals and a few of the Open Access Journals offer a choice of Creative Commons Licenses. The license type is clearly identified on the article.

The Creative Commons Attribution License

The Creative Commons Attribution License (CC-BY) allows users to copy, distribute and transmit an article, adapt the article and make commercial use of the article. The CC-BY license permits commercial and non-

Creative Commons Attribution Non-Commercial License

The Creative Commons Attribution Non-Commercial (CC-BY-NC)License permits use, distribution and reproduction in any medium, provided the original work is properly cited and is not used for commercial purposes.(see below)

Creative Commons Attribution-Non-Commercial-NoDerivs License

The Creative Commons Attribution Non-Commercial-NoDerivs License (CC-BY-NC-ND) permits use, distribution and reproduction in any medium, provided the original work is properly cited, is not used for commercial purposes and no modifications or adaptations are made. (see below)

Use by commercial "for-profit" organizations

Use of Wiley Open Access articles for commercial, promotional, or marketing purposes requires further explicit permission from Wiley and will be subject to a fee.

Further details can be found on Wiley Online Library http://olabout.wiley.com/WileyCDA/Section/id-410895.html

2. Permission for reuse of –

Patki, G. M., Sridhar, V., & Rajamani, S. (2025). Characterizing Mixed Single-Chain Amphiphile-Based Coacervates as a Robust Protocell System. *ChemBioChem*, 202500437.

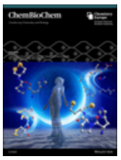

Characterizing Mixed Single-Chain Amphiphile-Based Coacervates as a Robust Protocell System

Author: Gauri M. Patki, Vanthanaa Sridhar, Sudha Rajamani
Publication: ChemBioChem
Publisher: John Wiley and Sons
Date: Aug 26, 2025

JOHN WILEY AND SONS LICENSE
TERMS AND CONDITIONS

Sep 08, 2025

This Agreement between Gauri M. Patki ("You") and John Wiley and Sons ("John Wiley and Sons") consists of your license details and the terms and conditions provided by John Wiley and Sons and Copyright Clearance Center.

License Number	6104141343528
License date	Sep 08, 2025
Licensed Content Publisher	John Wiley and Sons
Licensed Content Publication	ChemBioChem
Licensed Content Title	Characterizing Mixed Single-Chain Amphiphile-Based Coacervates as a Robust Protocell System
Licensed Content Author	Sudha Rajamani, Vanthanaa Sridhar, Gauri M. Patki
Licensed Content Date	Aug 26, 2025
Licensed Content Volume	0
Licensed Content Issue	0
Licensed Content Pages	11
Type of use	Dissertation/Thesis
Requestor type	Author of this Wiley article

Format	Electronic
Portion	Full article
Will you be translating?	No
Title of new work	Implications of prebiotic soup heterogeneity for nonenzymatic RNA replication and formation of primordial protocells
Institution name	Indian Institute of Science Education and Research, Pune
Expected presentation date	Oct 2025
The Requesting Person / Organization to Appear on the License	Gauri M. Patki
Requestor Location	Ms. Gauri Patki Hostel 3, IISER Pune Pune, 411008 India
Order reference number	2
Publisher Tax ID	EU826007151
Total	0.00 USD

Terms and Conditions

TERMS AND CONDITIONS

This copyrighted material is owned by or exclusively licensed to John Wiley & Sons, Inc. or one of its group companies (each a"Wiley Company") or handled on behalf of a society

with which a Wiley Company has exclusive publishing rights in relation to a particular work (collectively "WILEY"). By clicking "accept" in connection with completing this licensing transaction, you agree that the following terms and conditions apply to this transaction (along with the billing and payment terms and conditions established by the Copyright Clearance Center Inc., ("CCC's Billing and Payment terms and conditions"), at the time that you opened your RightsLink account (these are available at any time at http://myaccount.copyright.com).

Terms and Conditions

- The materials you have requested permission to reproduce or reuse (the "Wiley Materials") are protected by copyright.

- You are hereby granted a personal, non-exclusive, non-sub licensable (on a stand-alone basis), non-transferable, worldwide, limited license to reproduce the Wiley Materials for the purpose specified in the licensing process. This license, **and any CONTENT (PDF or image file) purchased as part of your order,** is for a one-time use only and limited to any maximum distribution number specified in the license. The first instance of republication or reuse granted by this license must be completed within two years of the date of the grant of this license (although copies prepared before the end date may be distributed thereafter). The Wiley Materials shall not be used in any other manner or for any other purpose, beyond what is granted in the license. Permission is granted subject to an appropriate acknowledgement given to the author, title of the material/book/journal and the publisher. You shall also duplicate the copyright notice that appears in the Wiley publication in your use of the Wiley Material. Permission is also granted on the understanding that nowhere in the text is a previously published source acknowledged for all or part of this Wiley Material. Any third party content is expressly excluded from this permission.

- With respect to the Wiley Materials, all rights are reserved. Except as expressly granted by the terms of the license, no part of the Wiley Materials may be copied, modified, adapted (except for minor reformatting required by the new Publication), translated, reproduced, transferred or distributed, in any form or by any means, and no derivative works may be made based on the Wiley Materials without the prior permission of the respective copyright owner.**For STM Signatory Publishers clearing permission under the terms of the STM Permissions Guidelines only, the terms of the license are extended to include subsequent editions and for editions in other languages, provided such editions are for the work as a whole in situ and does not involve the separate exploitation of the permitted figures or extracts,** You may not alter, remove or suppress in any manner any copyright, trademark or other notices displayed by the Wiley Materials. You may not license, rent, sell, loan, lease, pledge, offer as security, transfer or assign the Wiley Materials on a stand-alone basis, or any of the rights granted to you hereunder to any other person.

- The Wiley Materials and all of the intellectual property rights therein shall at all times remain the exclusive property of John Wiley & Sons Inc, the Wiley Companies, or their respective licensors, and your interest therein is only that of having possession of and the right to reproduce the Wiley Materials pursuant to

Section 2 herein during the continuance of this Agreement. You agree that you own no right, title or interest in or to the Wiley Materials or any of the intellectual property rights therein. You shall have no rights hereunder other than the license as provided for above in Section 2. No right, license or interest to any trademark, trade name, service mark or other branding ("Marks") of WILEY or its licensors is granted hereunder, and you agree that you shall not assert any such right, license or interest with respect thereto

- NEITHER WILEY NOR ITS LICENSORS MAKES ANY WARRANTY OR REPRESENTATION OF ANY KIND TO YOU OR ANY THIRD PARTY, EXPRESS, IMPLIED OR STATUTORY, WITH RESPECT TO THE MATERIALS OR THE ACCURACY OF ANY INFORMATION CONTAINED IN THE MATERIALS, INCLUDING, WITHOUT LIMITATION, ANY IMPLIED WARRANTY OF MERCHANTABILITY, ACCURACY, SATISFACTORY QUALITY, FITNESS FOR A PARTICULAR PURPOSE, USABILITY, INTEGRATION OR NON-INFRINGEMENT AND ALL SUCH WARRANTIES ARE HEREBY EXCLUDED BY WILEY AND ITS LICENSORS AND WAIVED BY YOU.

- WILEY shall have the right to terminate this Agreement immediately upon breach of this Agreement by you.

- You shall indemnify, defend and hold harmless WILEY, its Licensors and their respective directors, officers, agents and employees, from and against any actual or threatened claims, demands, causes of action or proceedings arising from any breach of this Agreement by you.

- IN NO EVENT SHALL WILEY OR ITS LICENSORS BE LIABLE TO YOU OR ANY OTHER PARTY OR ANY OTHER PERSON OR ENTITY FOR ANY SPECIAL, CONSEQUENTIAL, INCIDENTAL, INDIRECT, EXEMPLARY OR PUNITIVE DAMAGES, HOWEVER CAUSED, ARISING OUT OF OR IN CONNECTION WITH THE DOWNLOADING, PROVISIONING, VIEWING OR USE OF THE MATERIALS REGARDLESS OF THE FORM OF ACTION, WHETHER FOR BREACH OF CONTRACT, BREACH OF WARRANTY, TORT, NEGLIGENCE, INFRINGEMENT OR OTHERWISE (INCLUDING, WITHOUT LIMITATION, DAMAGES BASED ON LOSS OF PROFITS, DATA, FILES, USE, BUSINESS OPPORTUNITY OR CLAIMS OF THIRD PARTIES), AND WHETHER OR NOT THE PARTY HAS BEEN ADVISED OF THE POSSIBILITY OF SUCH DAMAGES. THIS LIMITATION SHALL APPLY NOTWITHSTANDING ANY FAILURE OF ESSENTIAL PURPOSE OF ANY LIMITED REMEDY PROVIDED HEREIN.

- Should any provision of this Agreement be held by a court of competent jurisdiction to be illegal, invalid, or unenforceable, that provision shall be deemed amended to achieve as nearly as possible the same economic effect as the original provision, and the legality, validity and enforceability of the remaining provisions of this Agreement shall not be affected or impaired thereby.

- The failure of either party to enforce any term or condition of this Agreement shall not constitute a waiver of either party's right to enforce each and every term and condition of this Agreement. No breach under this agreement shall be deemed

waived or excused by either party unless such waiver or consent is in writing signed by the party granting such waiver or consent. The waiver by or consent of a party to a breach of any provision of this Agreement shall not operate or be construed as a waiver of or consent to any other or subsequent breach by such other party.

- This Agreement may not be assigned (including by operation of law or otherwise) by you without WILEY's prior written consent.
- Any fee required for this permission shall be non-refundable after thirty (30) days from receipt by the CCC.
- These terms and conditions together with CCC's Billing and Payment terms and conditions (which are incorporated herein) form the entire agreement between you and WILEY concerning this licensing transaction and (in the absence of fraud) supersedes all prior agreements and representations of the parties, oral or written. This Agreement may not be amended except in writing signed by both parties. This Agreement shall be binding upon and inure to the benefit of the parties' successors, legal representatives, and authorized assigns.
- In the event of any conflict between your obligations established by these terms and conditions and those established by CCC's Billing and Payment terms and conditions, these terms and conditions shall prevail.
- WILEY expressly reserves all rights not specifically granted in the combination of (i) the license details provided by you and accepted in the course of this licensing transaction, (ii) these terms and conditions and (iii) CCC's Billing and Payment terms and conditions.
- This Agreement will be void if the Type of Use, Format, Circulation, or Requestor Type was misrepresented during the licensing process.
- This Agreement shall be governed by and construed in accordance with the laws of the State of New York, USA, without regards to such state's conflict of law rules. Any legal action, suit or proceeding arising out of or relating to these Terms and Conditions or the breach thereof shall be instituted in a court of competent jurisdiction in New York County in the State of New York in the United States of America and each party hereby consents and submits to the personal jurisdiction of such court, waives any objection to venue in such court and consents to service of process by registered or certified mail, return receipt requested, at the last known address of such party.

WILEY OPEN ACCESS TERMS AND CONDITIONS

Wiley Publishes Open Access Articles in fully Open Access Journals and in Subscription journals offering Online Open. Although most of the fully Open Access journals publish open access articles under the terms of the Creative Commons Attribution (CC BY) License only, the subscription journals and a few of the Open Access Journals offer a choice of Creative Commons Licenses. The license type is clearly identified on the article.

The Creative Commons Attribution License